UNIVERSITÉ DU QUÉBEC EN ABITIBI-TÉMISCAMINGUE

A RESEARCH ON THREE-DIMENSIONAL RESPONSE FEATURES OF BOREHOLE ELECTROMAGNETIC METHOD

MÉMOIRE PRÉSENTÉ À
L'UNIVERSITÉ DU QUÉBEC À ROUYN-NORANDA
COMME EXIGENCE PARTIELLE
DE LA MAÎTRISE EN INGÉNIERIE

By
Xueping DAI

December 2013

UNIVERSITÉ DU QUÉBEC EN ABITIBI-TÉMISCAMINGUE

UNE ÉTUDE SUR LA CARACTÉRISATION TRIDIMENSIONNELLE DE LA RÉPONSE EM EN FORAGE

MÉMOIRE PRÉSENTÉ À
L'UNIVERSITÉ DU QUÉBEC À ROUYN-NORANDA
COMME EXIGENCE PARTIELLE
DE LA MAÎTRISE EN INGÉNIERIE

Par
Xueping DAI

Décembre 2013

CE MÉMOIRE A ÉTÉ RÉALISÉ

À L'UNIVERSITÉ DU QUÉBEC EN ABITIBI-TÉMISCAMINGUE

DANS LE CADRE DU PROGRAMME

DE MAÎTRISE EN INGÉNIERIE

DE L'ÉCOLE DE GÉNIE

ACKNOWLEDGEMENTS

During the course of this program, I have received the suggestion and assistance of numerical people. I hereby would like to give my acknowledgements to them.

Foremost, I would like to give my deepest gratitude to my supervisor professor Lizhen Cheng who encouraged and guided me all through the master study period and offered lots of invaluable suggestions since the program started. She also carefully reviewed the manuscript and helped me to revise it. Without her assistances the thesis could not be its present level.

I wish to thank Mr. Brakni Mahdi who taught me how to use the software Maxwell and he also gave me several examples. Furthermore, I referred his master dissertation that illuminated me how I can carry out my own research. I also wish to give Mr. Chong Liu my honest acknowledgements, he helped me a lot. We often discussed together and he gave me many useful suggestions.

I greatly acknowledge Abitibi Geophysics Inc. for providing this opportunity to me.

Last but not least, I wish to give my special thanks to my family. I cannot carry through it without their comprehension, support and encouragement.

TABLE OF CONTENTS

LIST OF FIGURES AND TABLES

LIST OF ACRONYMS

$\boldsymbol{emf}$	Electromotive Force
$\boldsymbol{E}$	Vector of electric field intensity in voltage per meter(V/m)
$\boldsymbol{B}$	Vector of magnetic flux density in Tesla(T)
$\boldsymbol{H}$	Vector of magnetic field intensity in ampere per meter$(A\ /\ m)$
$\boldsymbol{D}$	Electric displacement vector in coulombs per square meter(C/m^2)
$\boldsymbol{J}$	Vector of current density in ampere per square meter(A/m^2)
r	Distance from the source to the measurement point in meter(m)
μ	Magnetic permeability in Henry per meter(H/m)
π	Mathematic constant Pi
σ	Electric conductivity in Siemen per meter(S/m)
ω	Angular frequency in radian per second(rad/s)
i	The imaginary unit
t	Time in second(s)
$\boldsymbol{A}$	Secondary currents vector in each ribbon loop in ampere(A)
$\boldsymbol{X}$	Matrix of mutual inductance between any two ribbon loops of conductor
$\boldsymbol{T}$	Vector of mutual inductances between transmitter antenna and ribbon loop
C	Transmitter current in ampere(A)
λ	Eigenvalue of a vector
$\boldsymbol{S}$	Vector of conductance of each ribbon loop
Y	The emf response at receiver sensor in voltage(V)

ABSTRACT

The borehole transient electromagnetic (BHTEM) is a promising exploration tool for searching deep deposits. To increase the effectiveness of fieldwork, we studied the main features of responses BHTEM and quantified the change in BHTEM responses according to changes of parameters of the conductor. By setting a conductor in various situations we have systematically investigated the variations in BHTEM response with different occurrences of the conductor. We observed that the intensity of the secondary magnetic field is proportional to the effective surface. When this surface is perpendicular to the primary magnetic field line, we have the largest effective surface therefore we get a strong BHTEM response. On the contrary, when the effective surface is parallel to the line of primary magnetic field, there is no secondary magnetic field induced due to the absence of coupling between the primary electromagnetic field and the conductor. The results of these simulations are completely consistent with airborne and ground electromagnetic data interpretations that are all based on the same principle of electromagnetic field. The results of this study will be useful for making quick interpretations on the field to select the optimal configuration of the measurement system as interpreted in real time. This will improve the efficiency of fieldwork thus reduce exploration costs.

Keywords: borehole transient electromagnetic, three-dimensional numerical simulations, *Maxwell*

RÉSUMÉ

La méthode électromagnétique transitoire dans le trou de forage (EMTF) est un outil d'exploration prometteur pour la recherche des dépôts profonds. Pour augmenter l'efficacité du travail sur le terrain, l'objectif de cette recherche est d'étudier les principales caractéristiques de réponses EMTF et de quantifier la variation dans les réponses EMTF en fonction de la variation des paramètres du conducteur. En définissant un conducteur dans diverses situations, nous avons systématiquement étudié les variations de réponse EMTF avec différentes occurrences du conducteur. Nous avons observé que l'intensité du champ magnétique secondaire est proportionnelle à la surface effective. Lorsque cette surface est perpendiculaire à la ligne du champ magnétique primaire, nous avons la plus grande surface effective donc nous obtenons une réponse de EMTF forte. Au contraire, lorsque la surface effective est parallèle à la ligne du champ magnétique primaire, il n'y a pas de champ magnétique secondaire induit en raison de l'absence de couplage entre le champ primaire et le conducteur. Les résultats de ces simulations sont entièrement compatibles avec les interprétations de données électromagnétiques aéroportés et au sol qui sont toutes basées sur le même principe du champ électromagnétique. Les résultats de cette étude seront utiles pour faire des interprétations rapides sur le terrain pour sélectionner la configuration optimale du système de mesure selon l'interprétation en temps réel. Cela permettra d'améliorer l'efficacité du travail de terrain ainsi réduire les coûts d'exploration.

Mots-clés : électromagnétique transitoire en forage, simulation numérique en 3D, *Maxwell*

CHAPTER I

INTRODUCTION

Mineral resources play a very important role in the development of our society. The vast exploration in the last decades results in the shallow resources rarer and rarer; therefore we are facing the challenge to find new resources at the depth. Geophysical methods are widely used in mineral exploration due to the advantage of deep penetration and tomography ability for the interior structure of the Earth. Among number of geophysical methods, the electromagnetic methods are especially useful in base metals exploration. The Abitibi greenstone belt is well known rich in gold and base metals. In order to increase the deep exploration capability of electromagnetic methods, we can either increase the power of the transmitter and the sensitivity of the receiver; or go closer to our target. Nowadays, we got two electromagnetic methods in which the receiver is placed closer to the target, they can explore deeper, acquire higher accuracy field data and they also have higher sensitivity, and they are now widely used in massive sulphide deposits exploration. They are cross-borehole electromagnetic and borehole electromagnetic (BHEM) methods. The sensitivity study analysis shows that the cross-hole EM data from boreholes separated by 100 meters can detect subsurface layers as thin as one meter (Wilt *et al.*, 1991); the sensitivity of BHEM is less than that of cross-borehole electromagnetic. Both methods acquire the signal directly in borehole. It is very effective in exploring the blind ore which locates besides or under the drill-hole.

As we know, the transient electromagnetic method (TEM) owns relatively high space resolution compared with frequency electromagnetic methods. This

outstanding feature makes TEM possesses an obvious superiority in prospecting ore deposit, especially when the difference of conductivity between the host rock and the ore body is distinct. For a surface TEM system, in which the transmitter and the receiver are placed on the earth's surface, the topography, the landform and the low resistivity overburden will make the primary field decay very fast and at the same time disturb the measurement of the secondary field. The borehole transient electromagnetic method (BHTEM) may overcome part of those problems by placing the receiver in a borehole which makes it nearer to the target. The physical principle of this method is the same as the surface TEM method; it also makes use of the interaction between a transient electromagnetic field and the target. The concept of a BHTEM is illustrated in Figure 1.1. We can see that the very difference between an surface TEM configuration and the BHTEM configuration is that in the BHTEM configuration the transmitter loop is located near the collar of the drill-hole and in which the receiver is moving, as the measurement carried through, the volume of the rock between the transmitting loop and the path of the drill-hole is prospected. And then, the transmitting loop is moved to a new location and log again. Typically, transmitting loop locations may be in the east, north, south or west of the drill-hole, and also may have one centred on the collar of the drill-hole. From the features of the configuration shown in Figure 1.1, compared with the surface TEM it is obvious that the method can largely overcome the effect of the overburden and the noise, and we can get a stronger response because the receiver is placed nearer to the target.

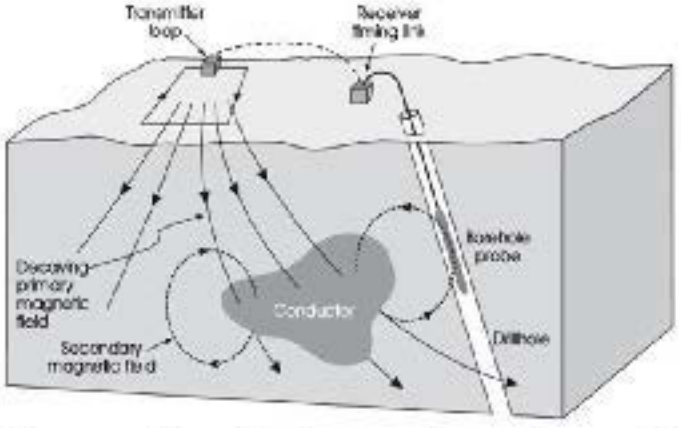

Figure 1.1 The concept of a borehole electromagnetic system (source : Killeen, 1997)

In the past, many theoretical researches have been done for simulating electromagnetic field; and lots of useful results are achieved. Lajoie and West (1976) has determined the three-dimensional electromagnetic field in the vicinity of a finite, thin, conductive plate buried in horizontally stratified, conductive environment by taking advantage of integral equation method. Hanneson and West (1984) employed the method of point collocation and expansion of the scattering current components in global polynomials obtained the frequency-domain electromagnetic response of a thin vertical tabular conductor situated in a two-layer earth. Walker and West (1991) developed an integral equation solution for electromagnetic scattering by a thin plate, scattering in relative resistive, very resistive, or conductive host media. Wang, He and Wei (2007) presented a 3D approach to numerical modeling of the borehole-surface electromagnetic (BSEM) method and conducted 3D inversion of BSEM data help reservoir delineation. Lv, Ruan and Peng (2012) carried out a study on anomaly of surface-borehole direction induced polarization survey.

The importance of borehole electromagnetic stems from its ability to distinguish conductivity variations in the vicinity of a borehole, and then opens the possibilities to determine the conductive materials distribution in three dimensions. The method has, among other capabilities, the ability to detect massive sulphide deposits such as VMS deposits in three dimensions. If there are more than one hole around a VMS deposit, based on measurements from hole to hole we will be able to estimate its tonnage more precisely. Recently, Abitibi Geophysics Inc. is developing a new borehole transient electromagnetic system. In order to help in this new BHTEM system's development, we use numerical simulation method to study some key features of the system by considering multiple parameters which may impact the BHTEM observation. We aim at the following objectives:

1. Learn the difference between a BHTEM and surface TEM system and the basics of numerical simulation for borehole EM data;
2. Build models to figure out the influence some significant parameters have on the BHTEM response;

3. Find out the optical measurement system configuration to assist in planning borehole BHTEM survey.

The modelling works in this dissertation used the software named Maxwell that was developed by EMIT (ElectroMagnetic Imaging Technology Pty Ltd., Australia). Forward modelling allow us to better understand how changes in the conductor (azimuth and dipping direction, location in the space etc.), also changes in the measurement system's configuration (current, waveform, time window, loop position so on) make impact to BHTEM response. We studied the measurement threshold of the BHTEM system by changing multiple factors such as the distance from observation point to the target, and several typical location of the target relative to the drill hole or to the transmitter and so on. Based on the results of 100 models, we concluded some BHTEM response features..

This dissertation contains five chapters including introduction. Main content of each chapter is:

Chapter 1 started from a brief introduction of the study problem and objectives; followed by lecture reviews of previous researches. At the end, a brief description about the methodology of present study.

In Chapter 2 we describe how a BHTEM system works in the field, the basic theory of electromagnetic field and the theoretical basis of numerical simulation for BHTEM data.

Chapter 3 presents three-dimensional numerical simulation of BHTEM responses. This chapter is one of the main parts of this dissertation, in which we study how the BHTEM field varies with changes of parameters.

In Chapter 4 we analysed the numerical simulation results come from Chapter 3; and resumed some regularity of BHTEM responses.

Chapter 5 is Discussion and Conclusion. We highlighted the important results of this study in order to assist the development of the BHTEM system at Abitibi Geophysics Inc.; and we proposed some suggestions to further work.

CHAPTER II

BOREHOLE MEASUREMENT AND THE BASIC THEORY OF BOREHOLE ELECTROMAGNETIC METHOD

2.1 Borehole measurement configurations

Geophysical borehole measurements are made by probes. Accessories of a typical system of geophysical logging are shown in Figure 2.1. They were used for rock's physical properties (density, electric conductivity, thermal conductivity so on) as well as for mineral exploration. Killeen (1997) summarized several types of systems (Figure 2.2) as follows:

1. The sensors can measure the physical properties just with passive sensors in the probe.
2. Some measures require an active source or transmitter except the sensor in the probe, such as measures of acoustic speed with energy source or density measurements with a radioactive source in the probe. Usually kinds of configurations (1) and (2) measure the physical properties near the hole; prospecting radius varies from a few centimetres to a few meters.
3. In the third type of measurement, the signal from a source at the surface is detected by the sensor in a probe.
4. One can measure the properties of the fluid in the hole, as the temperature is measured that binds to the thermal conductivity of the rock.
5. One can also use an electric optical device or a sound in the borehole.

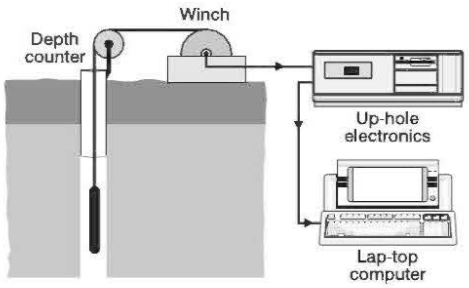

Figure 2.1 Accessories of a typical system for borehole measurements

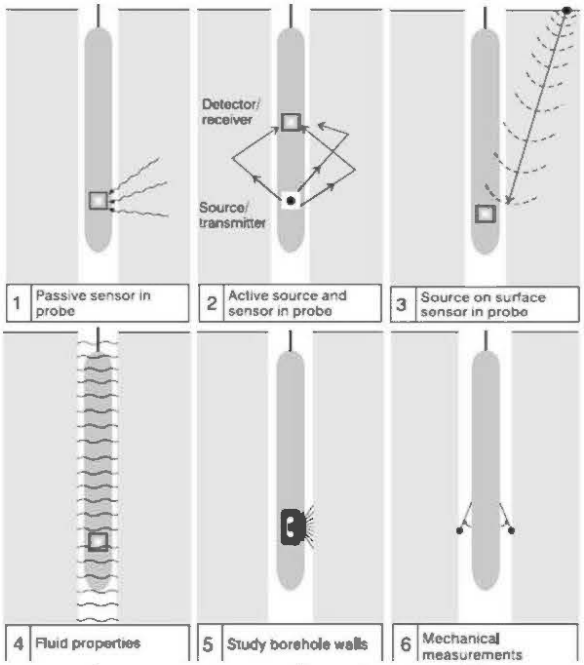

Figure 2.2 The six types of measurement configurations possible for geophysical borehole measurements

In order to increase the space resolution, measurement can be also made in two holes which is the hole-to-hole configuration with transmitter in one hole and the receiver probe in another as shown in Figure 2.3.

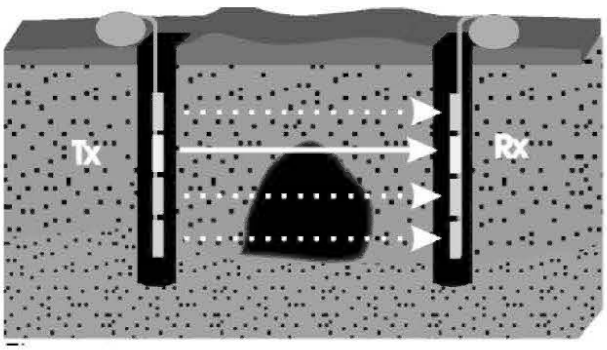

Figure 2.3 The configuration of hole to hole

There are several time-domain borehole electromagnetic systems, such as Geonics system, the UTEM system Lamontagne Geophysics and SIROTEM system of Australia, as well as the frequency domain electromagnetic systems such as BORIS. Virtually any geophysical measurement made with a system of surface or airborne system can potentially be made in a borehole.

Since the receiving probe is in the drill hole and moving toward the depth, the BHTEM response come from the whole space (modelling of airborne or ground data are in a half-space), therefore compared with ground or airborne measurements it is more difficult to interpret BHTEM anomalies. This is why we are looking the main features of BHTEM responses using modelling tools.

2.2 Methodology of work

In borehole electromagnetic measurements, a surface transmitting loop emits electromagnetic field near the collar of the hole in which the receiver probe is moving. If the recording is in function of the amplitude and phase shift related to the primary electromagnetic field (emitted by the transmitter), it is measurement in frequency domain. While the time domain measurements record the variation of the secondary electromagnetic field with time in the absence of the primary electromagnetic field. We concentrate in borehole electromagnetic transient measurement of time domain (BHTEM) in this thesis.

The advanced measuring instruments can record simultaneously three components, which are axial component, and two transverse axial components. Compared with the traditional electromagnetic methods, it is not necessary for BHTEM to do correction with the decay of primary field and the tilt of drill hole, because any anomaly observed in hole is attributed to the geometry and conductivity change of the conductor. But, because of the complicate coupling relationship between the transmitting loop, conductor and receiver, the data interpretation is still very difficult.

In order to better characterize borehole electromagnetic signals' variations with

multiple variables, we firstly design five typical transmitter loop locations such as north, south, east and west around the hole, and one centred over the hole (Figure 2.5). When the receiver probe moves in the hole, the rocks between the transmitting loop and the path of the receiver are investigated for anomalous conductors. Then, we use a thin plate model to simulate the conductor and simulate its electromagnetic response by varying its buried depth, its position with respect to the drill-hole, and its dip angle.

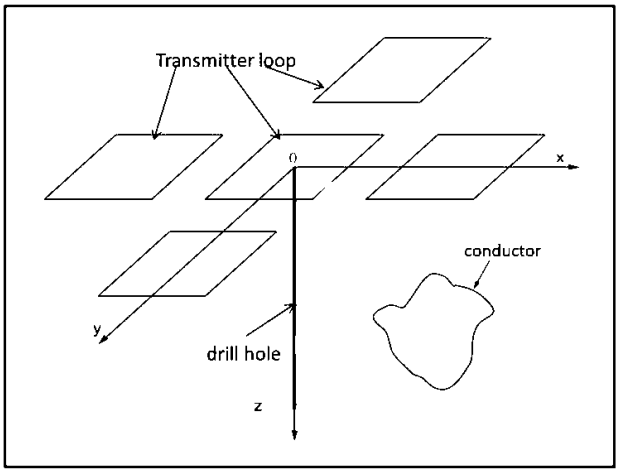

Figure 2.4 Five typical transmitting loop locations in BHTEM measurement

2.3 Calculation of EM field of thin, rectangular plate

The principle of the BHTEM is: an alternative or transient current is provided by the transmitter loop on the surface; a primary electric field is formed around the loop and a decaying primary magnetic field instantaneously setting up in the direction perpendicular to the loop plan. According to the Maxwell theory, decaying primary magnetic field induces a changing secondary electric field (eddy current) in the conductor; since this secondary electric field varies in time it generates a secondary magnetic field whose derivative to time and is recorded by receiver in the drill hole.

We suppose that the conductor is a thin plate and placed in free space; and the electromagnetic field is assumed to be quasi-stationary, i.e., to involve only induction effects. Thin plate means the thickness of the plate is negligible

compared either with the lateral dimensions of the plate or with the distance to the points where the magnetic field of the secondary field is calculated. (LAMONTAGNE, 1971)

From Maxwell's equations:

$$\nabla \times \mathbf{H} = \mathbf{J} + \frac{\partial \mathbf{D}}{\partial t} \tag{2. 1}$$

$$\nabla \times \mathbf{E} = -\frac{\partial \mathbf{B}}{\partial t} \tag{2. 2}$$

For induction problems, the displacement current is far smaller than the conduction current. Thereby, the term $\partial \mathbf{D}/\partial t$ in (2. 1) can be neglected, so

$$\nabla \times \mathbf{H} = \mathbf{J} \tag{2. 3}$$

There are empirical relations,

$$\mathbf{B} = \mu \mathbf{H} \tag{2. 4}$$

$$\mathbf{J} = \sigma \mathbf{E} \tag{2. 5}$$

Using an identity: $\nabla \bullet (\nabla \times) = = 0$, i.e., the divergence of the curl is identically zero, equation (2. 3) yields

$$\nabla \bullet \mathbf{J} = 0 \tag{2. 6}$$

Substitute **B** from equation (2. 4) and **E** from equation (2. 5) into equation (2. 2). For a sinusoidally varying source of angular frequency ω and assuming a uniform medium

$$\nabla \times \mathbf{J} = -i\sigma\mu\omega\mathbf{H} \tag{2. 7}$$

The expression of **H** can be obtained by using Biot-Savart equation and integrating equation (2. 3) and substitute **H** into (2. 7)

$$\nabla \times \mathbf{J}(\mathbf{r}_0) = -i\sigma\mu\omega \int_V \frac{\mathbf{J}(\mathbf{r}) \times (\mathbf{r} - \mathbf{r}_0)}{4\pi |\mathbf{r} - \mathbf{r}_0|^3} d^3\mathbf{r} \tag{2. 8}$$

Where V indicates all regions where the current flows.

The integral term in the equation above can be divided into two parts: one is the transmitting current; the other is the induced current. The transmitting current can be replaced by a known function $\mathbf{P}(\mathbf{r}_0)$

$$\nabla\times\mathbf{J}(\mathbf{r}_0)=-i\sigma\mu\omega\bullet\left\{\mathbf{P}(\mathbf{r}_0)+\int_C\frac{\mathbf{J}(\mathbf{r})\times(\mathbf{r}-\mathbf{r}_0)}{4\pi|\mathbf{r}-\mathbf{r}_0|^3}d^3\mathbf{r}\right\} \tag{2. 9}$$

Where C indicates the space occupied by the conductor.

On condition that the plate is thin enough, the current density can be considered as constant across the thickness. Therefore, the volume density can be replaced by surface density which is defined as:

$$\mathbf{K}=\int_{-t/2}^{t/2}\mathbf{J}dx=\mathbf{J}t$$

Substitute the surface density into (2. 9)

$$\nabla\times\mathbf{K}(\mathbf{r}_0)=-i\sigma\mu\omega t\bullet\left\{\mathbf{P}(\mathbf{r}_0)+\int_S\frac{\mathbf{K}(\mathbf{r})\times(\mathbf{r}-\mathbf{r}_0)}{4\pi|\mathbf{r}-\mathbf{r}_0|^3}d^2\mathbf{r}\right\} \tag{2. 10}$$

where S represents the thin plate's surface. This equation is obtained by assuming that t is geometrically small so that $\left\{(\mathbf{r}-\mathbf{r}_0)/|\mathbf{r}-\mathbf{r}_0|^3\right\}$ does not vary appreciably across the thickness.

In order to solve the equation above, one defined a vector potential $\mathbf{U}$ which satisfies $\nabla\times\mathbf{U}=\mathbf{K}$ and $\nabla\bullet\mathbf{U}=0$ to simply the equation. Use $\nabla\times\mathbf{U}$ to replace $\mathbf{K}$ and the identity $\nabla\times\nabla\times\equiv(\nabla\nabla\bullet)-(\nabla^2)$, equation (2. 10) becomes

$$\nabla^2\mathbf{U}(\mathbf{r}_0)=i\sigma\mu\omega t\bullet\left\{\mathbf{P}(\mathbf{r}_0)+\int_S\frac{[\nabla\times\mathbf{U}(\mathbf{r})]\times(\mathbf{r}-\mathbf{r}_0)}{4\pi|\mathbf{r}-\mathbf{r}_0|^3}d^2\mathbf{r}\right\} \tag{2. 11}$$

In the coordinate system showed in Figure 2.6, the only nonzero component of U is in x-direction. And for that the induced eddy current circulates in the plan which is parallel to the plate, the equation (2. 11) becomes:

$$\nabla^2 U(y,z) = i\sigma\mu\omega t \bullet \left\{ P(y,z) + \int_S \frac{\nabla U(y,z) \bullet (\mathbf{r} - \mathbf{r}_0)}{4\pi |\mathbf{r} - \mathbf{r}_0|^3} d^2 r \right\} \qquad (2.12)$$

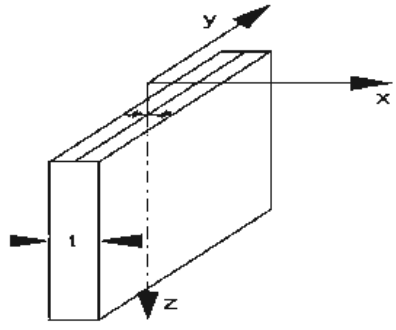

Figure 2.5 The coordinate system which is attached to conductor (Source: Lamontagne and West, 1971)

To solve equation (2. 12), boundary conditions or initial conditions are needed. Since only the derivatives of U be involved in equation (2. 12), the boundary condition can be taken as U=constant everywhere on the edge of the plate, can be simply assigned $U = 0$.

$$\begin{cases} \nabla^2 U(y,z) = i\sigma\mu\omega t \bullet \left\{ P(y,z) + \int_S \frac{\nabla U(y,z) \bullet (\mathbf{r} - \mathbf{r}_0)}{4\pi |\mathbf{r} - \mathbf{r}_0|^3} d^2 r \right\} \\ U|_\Gamma = 0 \end{cases} \qquad (2.13)$$

where Γ represents the boundary of the plate. Now, we get a boundary value problem. We can use numerical methods, such as finite element method or finite difference method, to solve this differential equation (2. 13).

2.4 Theoretical basis of numerical simulation

For simulating a thin plate's electromagnetic response, we use commercial software named *Maxwell* (EMIT), which is based on circuit theory. The problem is posed in terms of mutual inductances of the conductive ribbon elements into which the plate is divided. Consequently, the current is forced to flow within the path assigned by the ribbon. This is similar to assuming a reasonably uniform primary field excitation. The simulation of different plates can be realized by using ribbon elements with different width; and every ribbon element is simulated

as an equivalent circuit. The equivalent mutual inductances include:

1. Between any two ribbon elements.
2. Between any ribbon element and the transmitter or receiver.
3. The mutual inductance between the transmitter and receiver.

For any element j, when the angular frequency is ω, the voltage equation is:

$$i\omega\sum_{l=1}^{n}\mathbf{X}_{jl}\mathbf{A}_l+\frac{\mathbf{A}_j}{\mathbf{S}_j}=i\omega\mathbf{T}_jC \tag{2. 14}$$

Where A_j denotes the current flowing within element j. If this equation system can be solved for A_j, the response can be expressed as:

$$Y=i\omega\mathbf{R}\bullet\mathbf{A} \tag{2. 15}$$

The method used to solve equation (2. 14) is similar to that used by Annan (1974). Since the matrix X can be decomposed by using eigenvector and eigenvalue, we can get another form of (2. 14):

$$i\omega\lambda_k a_k+a_k=i\omega t_k c \tag{2. 16}$$

Where $t_k=\mathbf{T}\bullet\mathbf{V}_k$ and $\mathbf{A}=\sum_k d_k a_k\mathbf{V}_k$; d_k is a damping factor almost equal to one for well determined eigenvectors; smaller than one for poorly determined eigenvectors. The equation 2.15 becomes:

$$y_k=i\omega a_k r_k \tag{2. 17}$$

And the complete solution is:

$$Y=\sum_k d_k r_k t_k\left(\frac{(i\omega)^2 C}{1+i\omega\lambda_k}\right) \tag{2. 18}$$

In time domain it is:

$$y(t)=\sum_k d_k r_k t_k E_k(t) \tag{2. 19}$$

Where $E_k(t)=\left(\frac{d}{dt}e^{t/\lambda_k}\right)*\left(\frac{d}{dt}C(t)\right)$. For a simple pulse excitation, $\frac{d}{dt}C(t)$ is a $\delta(t)$ function. Thus, $E_k(t)=\delta(t)-\frac{e^{t/\lambda_k}}{\lambda_k}$. The time domain response can be normalized by the normalization factor Q: $y_n(t)=\frac{y(t)}{Q}$. The normalization factor Q can be computed in one of three ways:

1. Using the absolute peak primary emf: $Q=|C(t)|_{\max}|\mathbf{P}|$
2. Using the primary root mean square (RMS) emf: $Q=\sqrt{\frac{1}{T}\int_0^T[C(t)]^2\,dt}\,|\mathbf{P}|$
3. Using the average absolute value of emf: $Q=\frac{1}{T}\int_0^T|C(t)|\,dt\,|\mathbf{P}|$

CHAPTER III

NUMERICAL SIMULATION OF BOREHOLE ELECTROMAGNETIC SIGNALS

3.1 An introduction to the software *Maxwell*

The software *Maxwell* is developed by Electromagnetic Imaging Technology Corporation (EMIT) in Australia. It is widely used in electromagnetic data visualization, processing and modelling. It is very useful with friendly interface and straightforward model design and can make direct comparison between simulation result and observation. We can use it to process time domain and frequency domain data and to do forward modelling and inversion calculation of the electromagnetic data collected either on the earth's surface, or in the air (airborne), or in the borehole. Furthermore, it also can be used to process the induced polarization data both in time domain and frequency domain. In this thesis, we used the *Maxwell* to do numerical simulation of BHTEM data with a thin plate for conductor model which is placed in a half-free space.

3.1.1 Model parameters

With the *Maxwell*, we can easily set up the survey line's parameters (line length, orientation and observation points) through the window showed below. We suppose the drill hole has a dip angle of 60°, an azimuth angle of 90°, and the number of survey station along the drill hole is 21, with a spacing of 25m between stations.

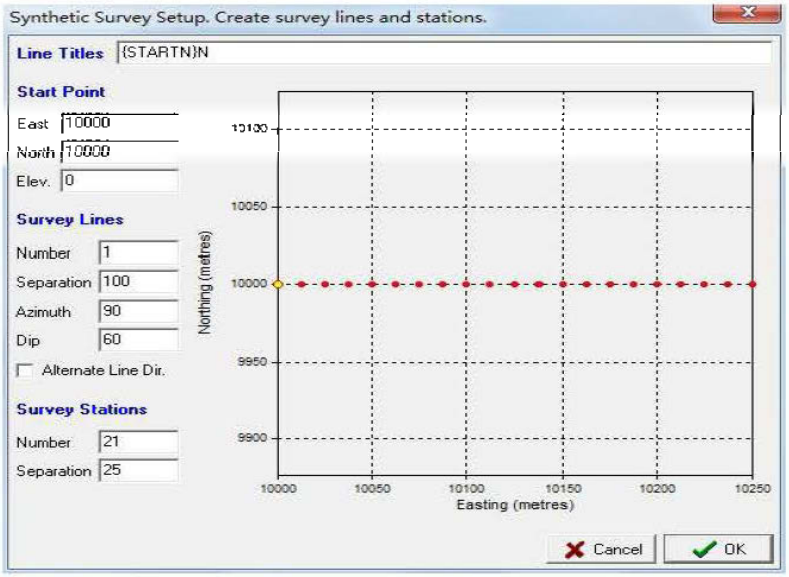

Figure 3.1 Parameter values setup window for survey line

The window below (Figure 3.2(a)) shows how to set up the parameter values of the measurement system. We considered a Geonic system (Protem 25Hz) with the component effective area of three components of 100, transmitting frequency is determined as 30Hz. The component effective area is calculated by: area of a single turn × number of turns × amplification coefficient. A represents axial component, i.e., along the drill hole, pointing upward. U is a component transverse to axial and in the vertical plane containing the drill hole, at 12 o'clock when looking down the hole. V also is a component transverse to axial and in the vertical plane containing the drill hole, at 12 o'clock when looking down the hole. Components A, U and V are corresponding to Z, X and Y, respectively. See Figure 3.2(b).

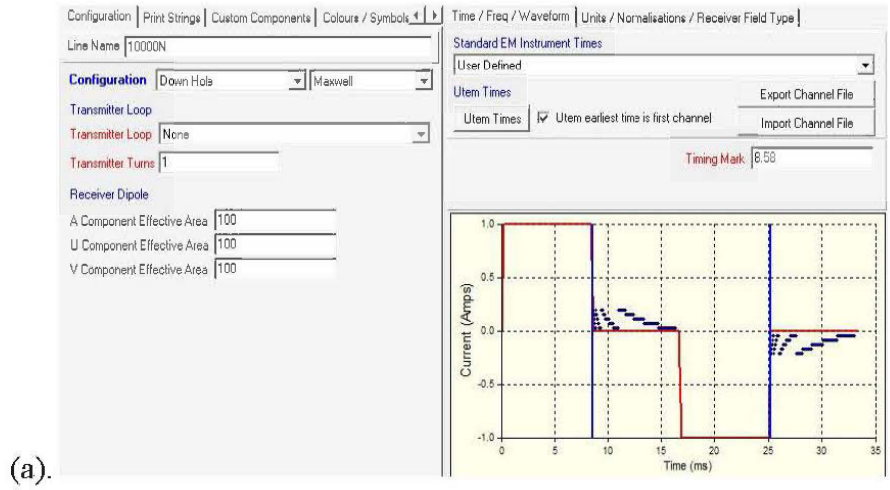

(a).

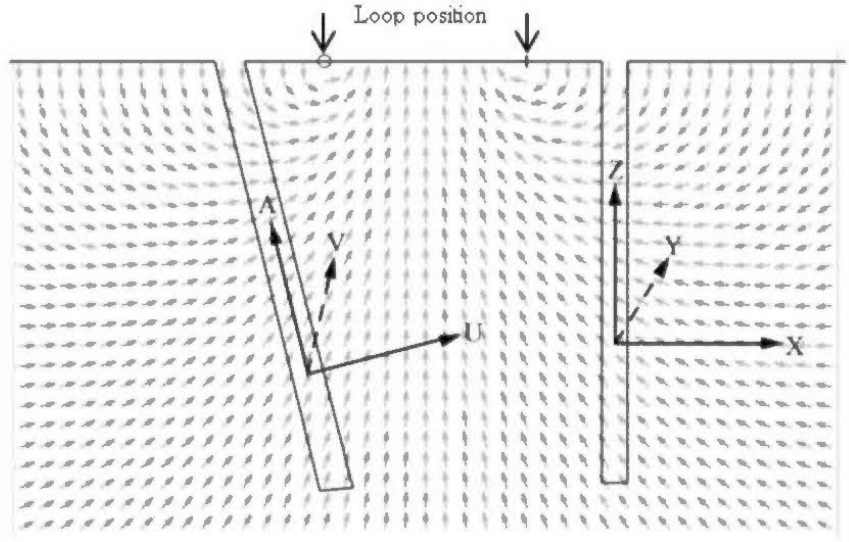

(b).

Figure 3.2 (a) Parameter values setup window for measurement system; (b) Components sketch map and the corresponding relationship between A, U, V and X, Y, Z.

Figure 3.3 shows positions and size of the transmitter loop and the plate. For the space of the figure, we just give out three loops: centre, east and north. There are other two loops which situate on the west and south side, respectively.

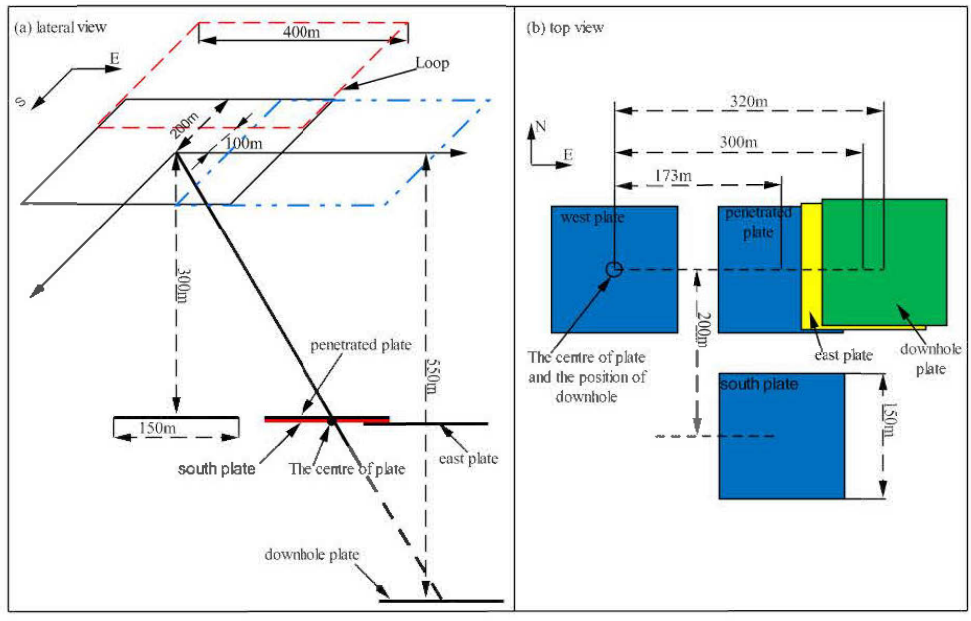

Figure 3.3 A sketch of loop's and plate's size and positions

The thin plate's parameters are set in the window below (Figure 3.4). Common values for each model used in this research are: size of plate is 150m×150m, azimuth is 270°, conductivity of the plate is $100S \cdot m^{-1}$. The simulation results can be visualized very quickly in the window at the right side.

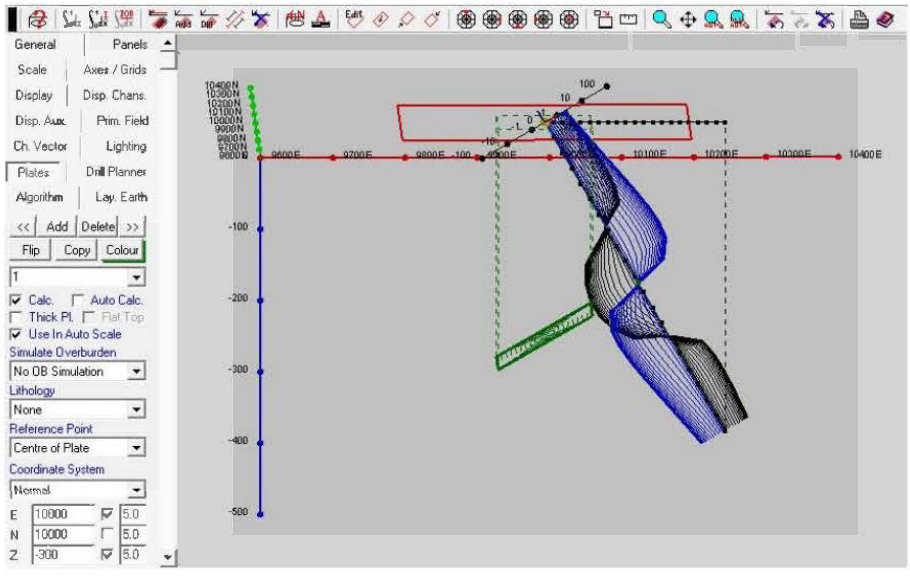

Figure 3.4 Model window

3.2 Three-dimensional numerical simulation

In order to look at the impact on BHTEM signal variations from different geological occurrences of the conductor, combining with the variations of measurement system's configuration, we determined a series of situations for 3-D modeling as stated in Table 3.1.

Table 3.1 Values of parameters involved in numerical simulation

Occurrence of the conductor	Location of the conductor	Loop location related to the drill-hole
Horizontal	In the East of the hole	Centre
Dip 45° to west	In the West of the hole	East
Vertical	In the South of the hole	South
Dip 45° to west	Penetrated by hole	West
	Below the hole	North

The first column contains the different dip angles of the thin plate that are typical occurrences in space. The second column indicates the location of the thin plate related to the drill-hole. The third column is the transmitter loop's location related to the drill-hole. The simulation results are divided into five model series according to the location of the thin plate (the second column). Each model series is then divided into four sub-series, reflecting changes in the inclination of the conductor (first column). In addition, each subseries also contain five possible transmitter loop positions for the measurement system related to the conductor. Therefore, there are $5 \times 4 \times 5 = 100$ models for a given drill-hole. We describe simulation results by series.

3.2.1 Model Series 1

The plate situates on west side of the drill hole; the depth of its centre point is 300m. The distance from the centre point of the plate to the intersection point of drill hole and the horizontal plan which contains the centre point of the plate is 173m. See Figure 3.5.

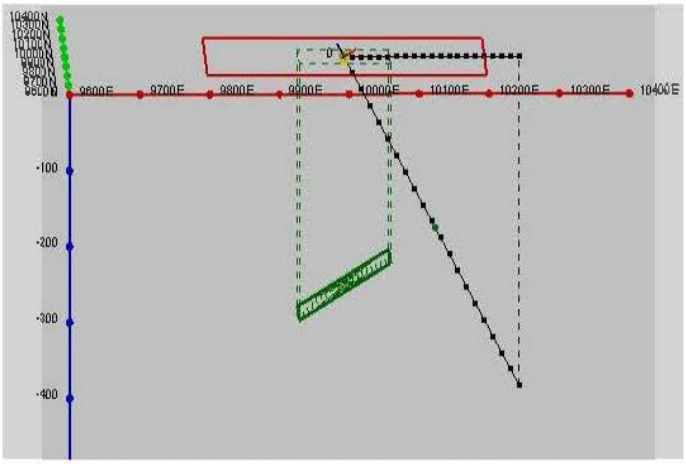

Figure 3.5 The model sketch of Model Series 1

The component V in this model series is zero; we only have components A and U that are presented in following figures.

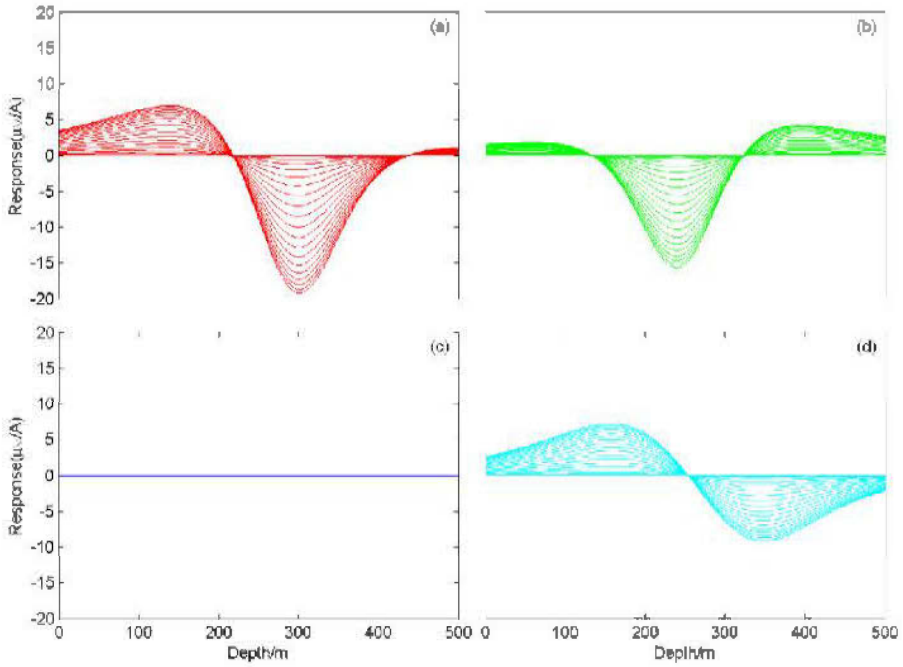

Figure 3.6 The results of component A of Model Series 1 when loop location is in the centre (a) horizontal, (b) dip 45° to west, (c) vertical, (d) dip 45° to east

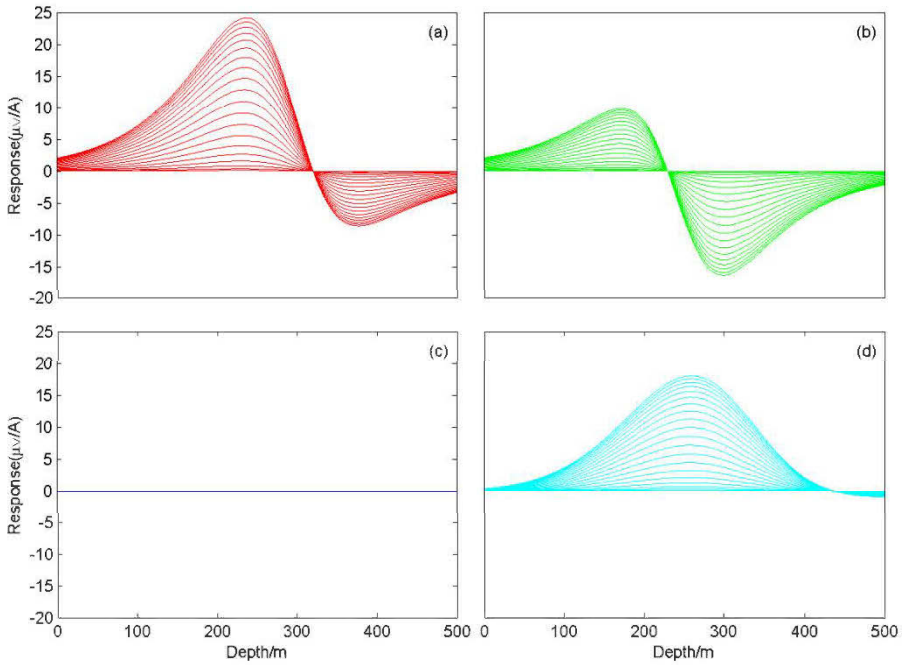

Figure 3.7 The results of component U of Model Series 1 when loop location is in the centre
(a) horizontal, (b) dip 45° to west, (c) vertical, (d) dip 45° to east

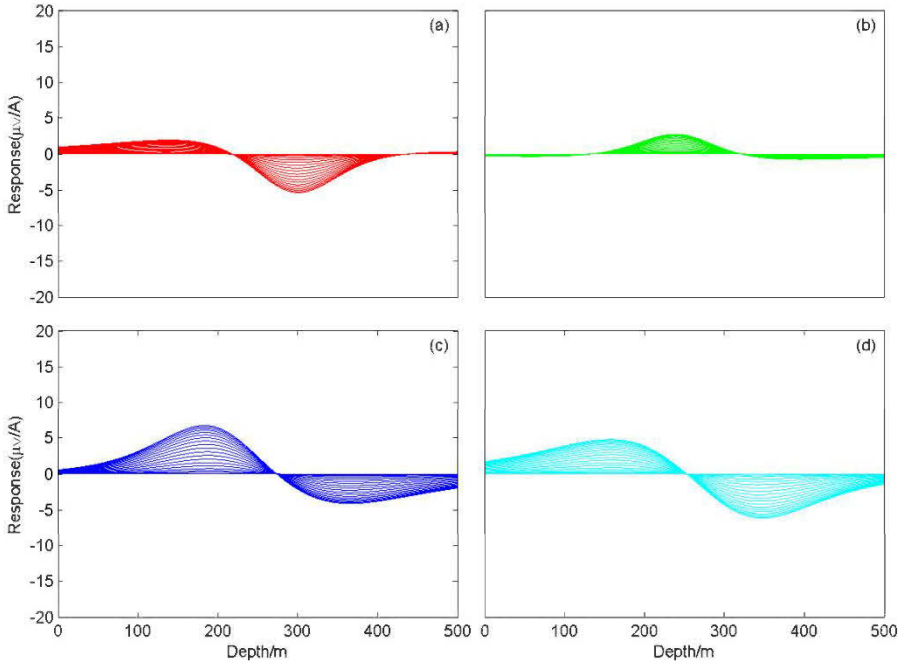

Figure 3.8 The results of component A of Model Series 1 when loop location is in the east of drill hole
(a) horizontal, (b) dip 45° to west, (c) vertical, (d) dip 45° to east

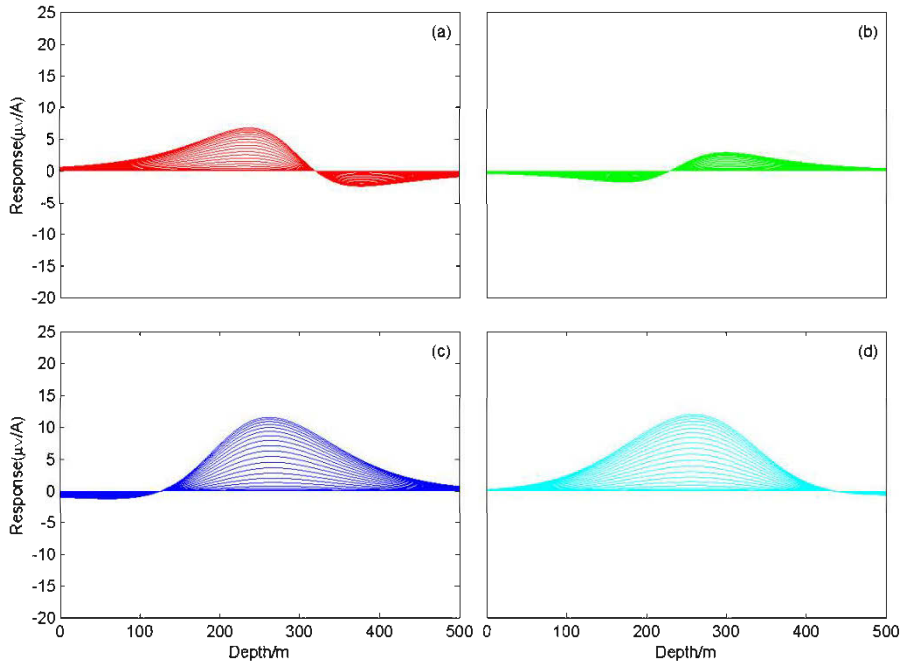

Figure 3.9 The results of component U of Model Series 1 when loop location is in the east of drill hole
(a) horizontal, (b) dip 45° to west, (c) vertical, (d) dip 45° to east

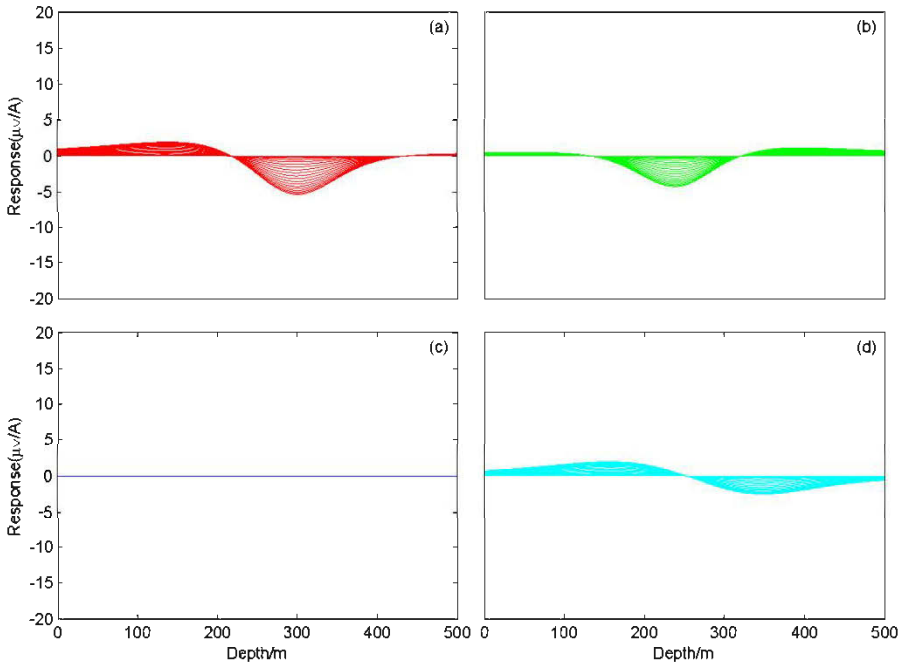

Figure 3.10 The results of component A of Model Series 1 when loop location is the north of drill hole
(a) horizontal, (b) dip 45° to west, (c) vertical, (d) dip 45° to east

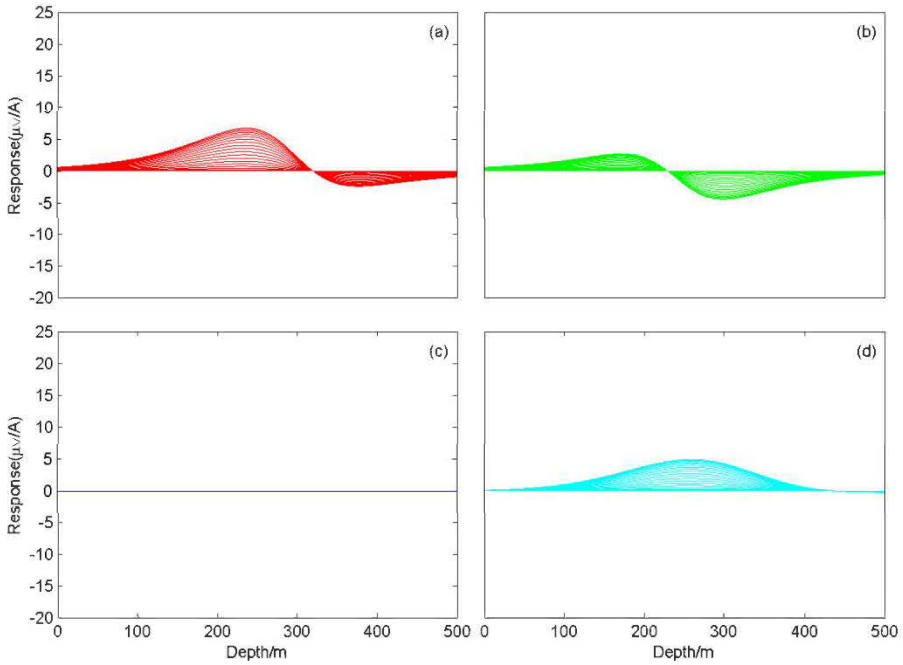

Figure 3.11 The results of component U of Model Series 1 when loop location is the north of drill hole
(a) horizontal, (b) dip 45° to west, (c) vertical, (d) dip 45° to east

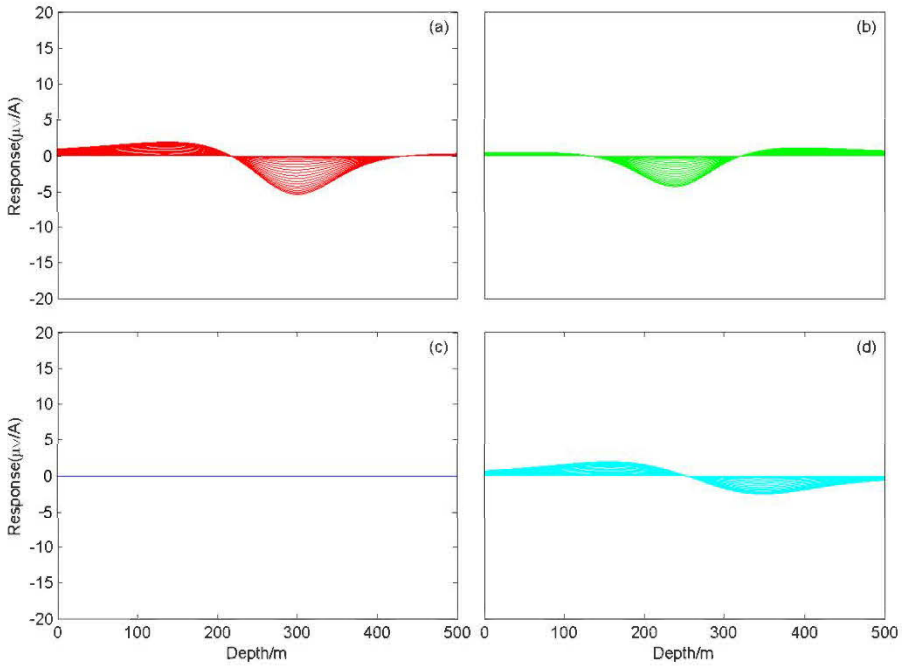

Figure 3.12 The results of component A of Model Series 1 when loop location is in the south of drill hole
(a) horizontal, (b) dip 45° to west, (c) vertical, (d) dip 45° to east

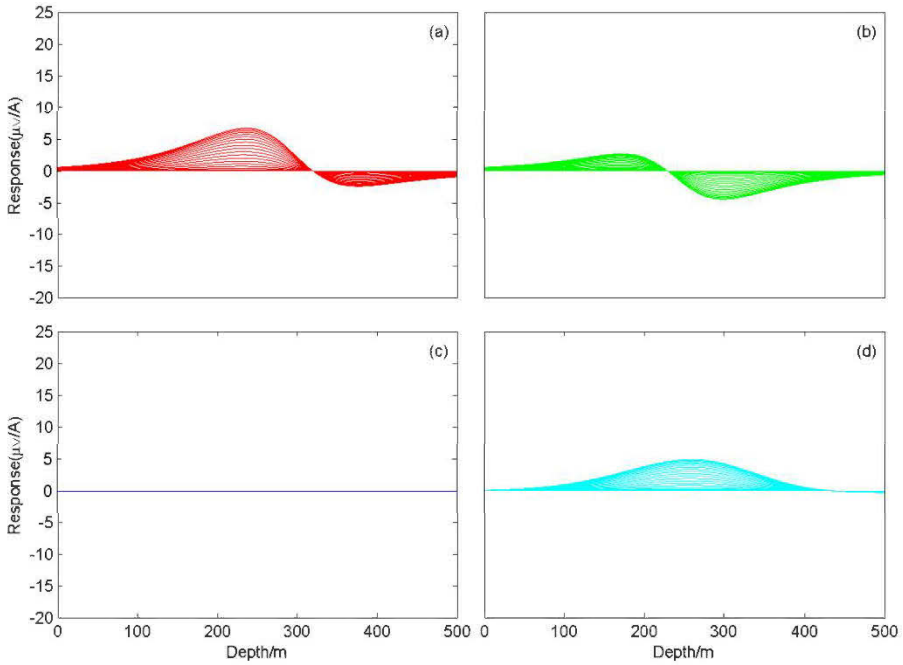

Figure 3.13 The results of component U of Model Series 1 when loop location is in the south of drill hole
(a) horizontal, (b) dip 45° to west, (c) vertical, (d) dip 45° to east

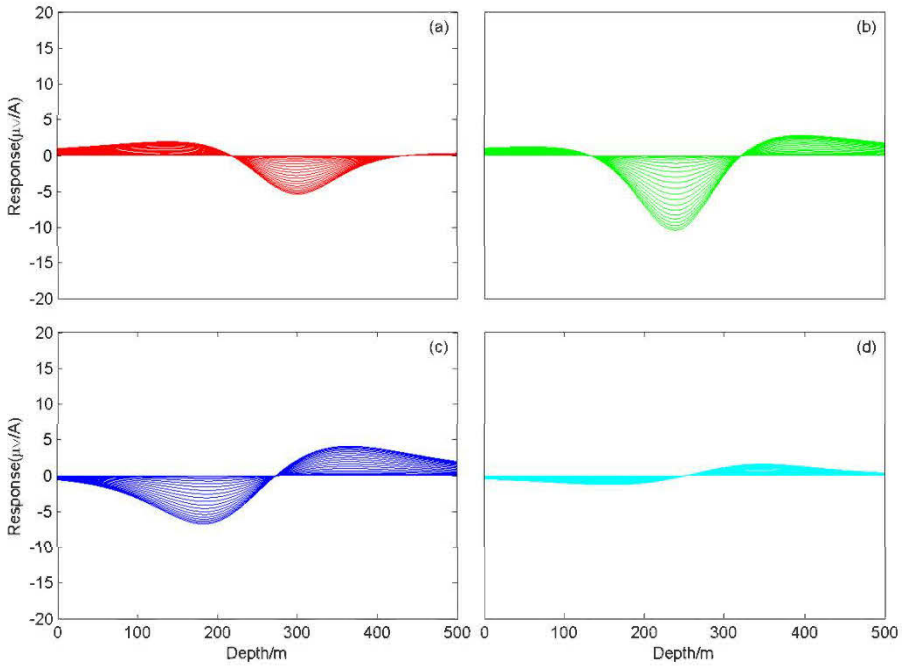

Figure 3.14 The results of component A of Model Series 1 when loop location is in the west of drill hole
(a) horizontal, (b) dip 45° to west, (c) vertical, (d) dip 45° to east

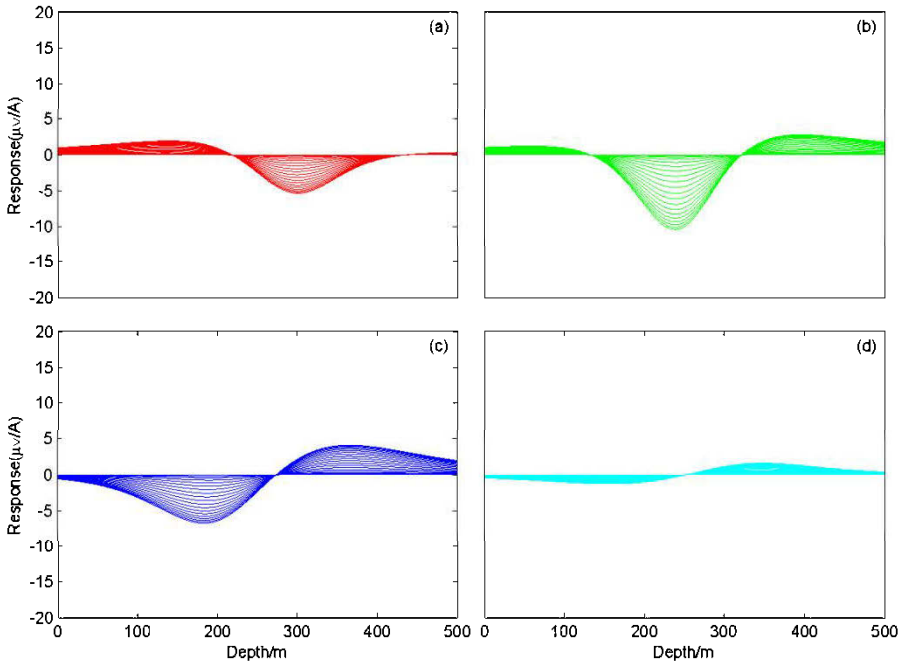

Figure 3.15 The results of component U of Model Series 1 when loop location is in the west of drill hole
(a) horizontal, (b) dip 45° to west, (c) vertical, (d) dip 45° to east

A brief summary for numerical simulation results of Model Series 1:

1. For the vertical plate, if we use east and west loop locations we can get obvious response and the response curves obtained by using these two transmitter loop locations are symmetric (see and compare Figure 3.8c, Figure 3.9c and Figure 3.14c, Figure 3.15c). For other loop locations the BHTEM signal of the plate is null (Figure 3.6c, Figure3.7c, and figures Figure 3.10c to Figure 3.13c).
2. For non-vertical plates (horizontal and inclined plates), we got the largest abnormal amplitude when the transmitter loop is centred over the hole (Figure 3.6 and Figure 3.7).
3. For the horizontal plate, we got same abnormal curves for east, north, south and west loop locations (figures Figure 3.8a to Figure 3.15a). And the centre loop location is the optimal loop location.

Thus for field measurements, we propose: when the target is vertical, the loop should locate on the east or west side of the hole. For other occasions the centred loop should be used.

3.2.2 Model Series 2

The plate situates on east side of the drill hole; the depth of its centre point is 300m. The distance from the centre point of the plate to the intersection point of the drill hole and the horizontal plan which contains the centre point of the plate is 147m. See Figure 3.16.

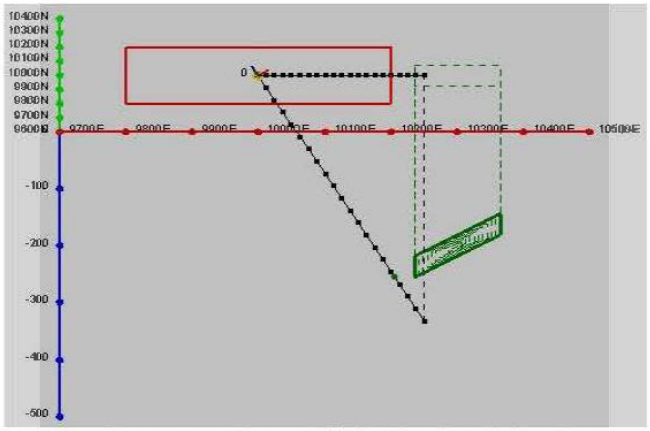

Figure 3.16 The model sketch of Model Series 2

Values of component V in this model series are zero, so only components A and U are presented in following figures.

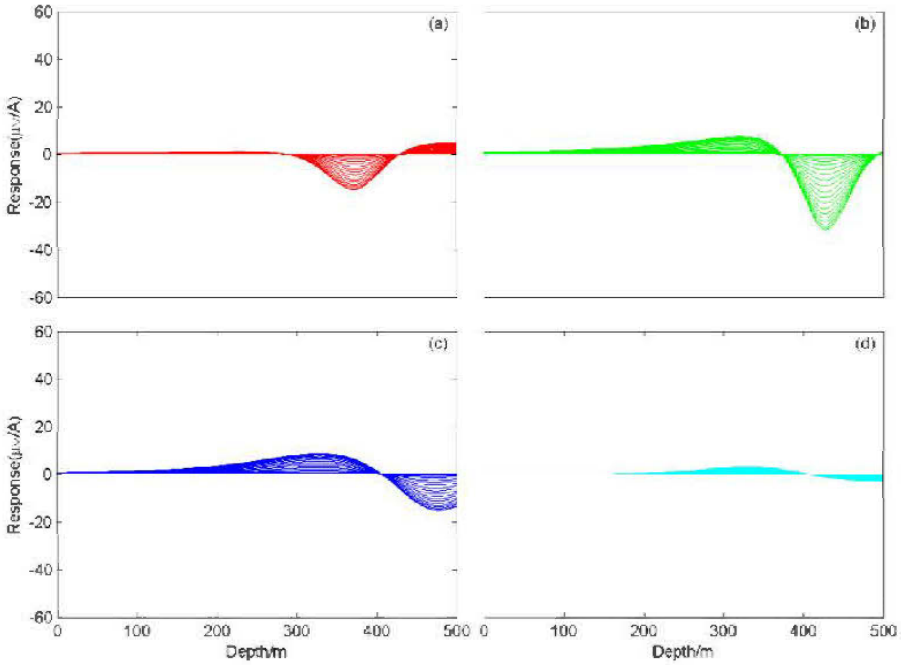

Figure 3.17 The results of componeut A of Model Series 2 when loop location is in the centre (a) horizontal, (b) dip 45° to west, (c) vertical, (d) dip 45° to east

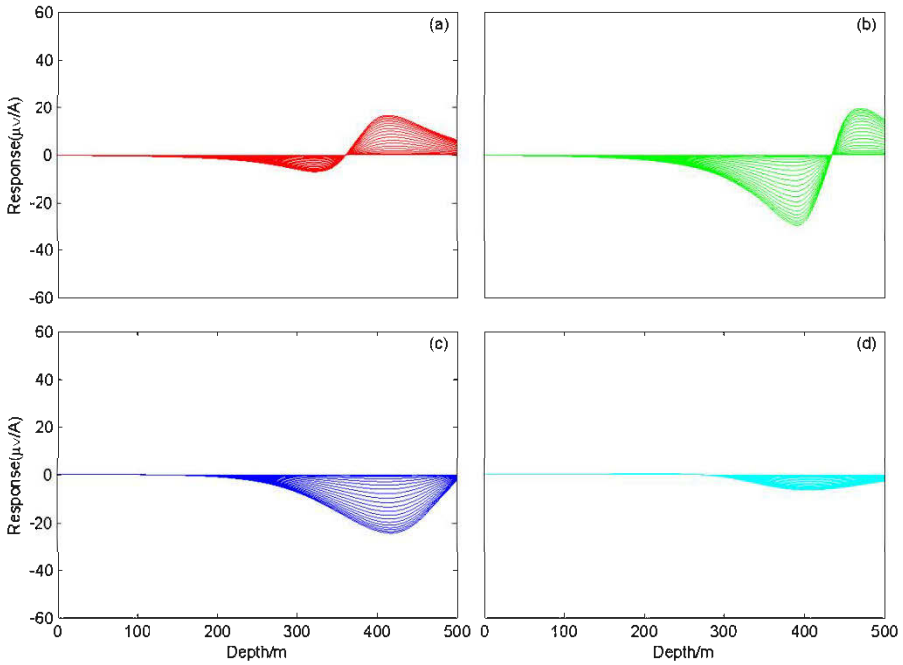

Figure 3.18 The results of component U of Model Series 2 when loop location is in the centre
(a) horizontal, (b) dip 45° to west, (c) vertical, (d) dip 45° to east

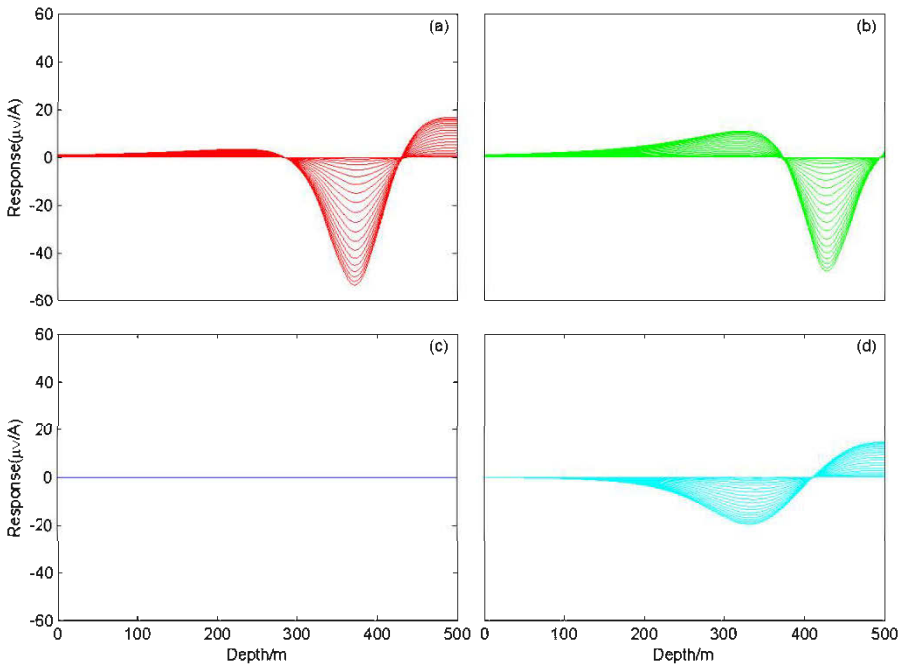

Figure 3.19 The results of component A of Model Series 2 when loop location is in the east of drill hole
(a) horizontal, (b) dip 45° to west, (c) vertical, (d) dip 45° to east

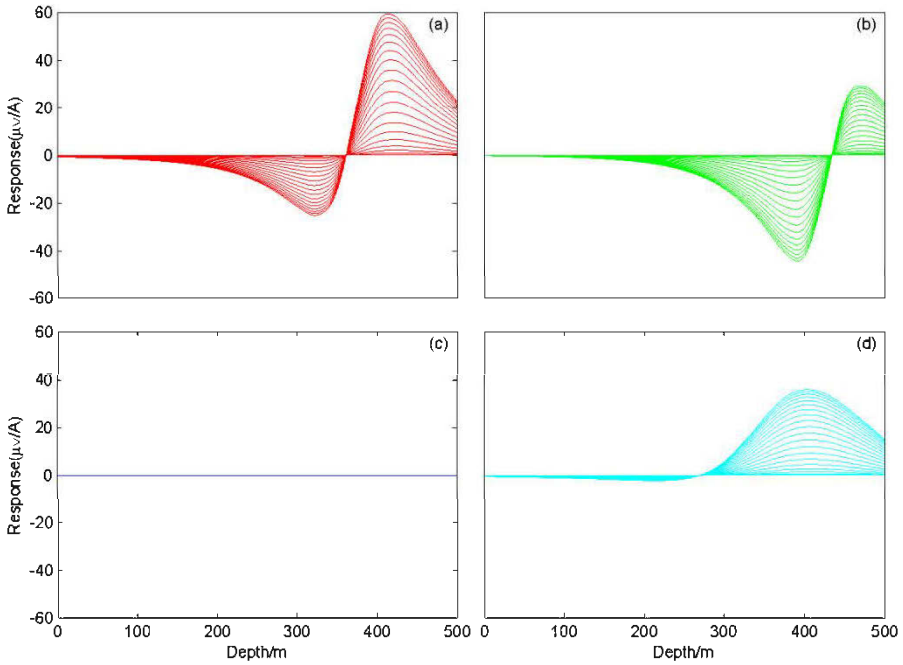

Figure 3.20 The results of component U of Model Series 2 when loop location is in the east of drill hole
(a) horizontal, (b) dip 45° to west, (c) vertical, (d) dip 45° to east

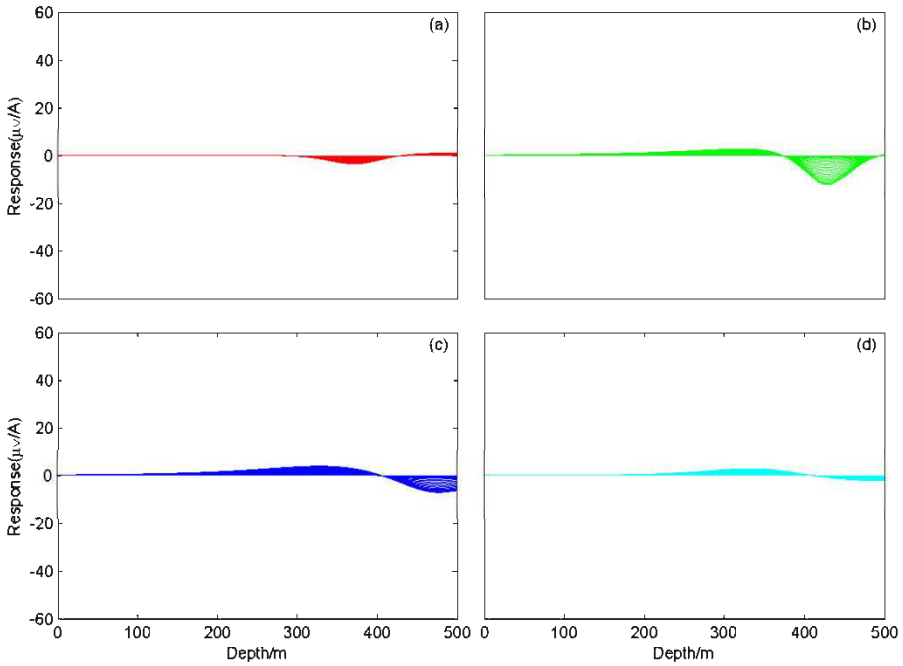

Figure 3.21 The results of component A of Model Series 2 when loop location is in the north of drill hole
(a) horizontal, (b) dip 45° to west, (c) vertical, (d) dip 45° to east

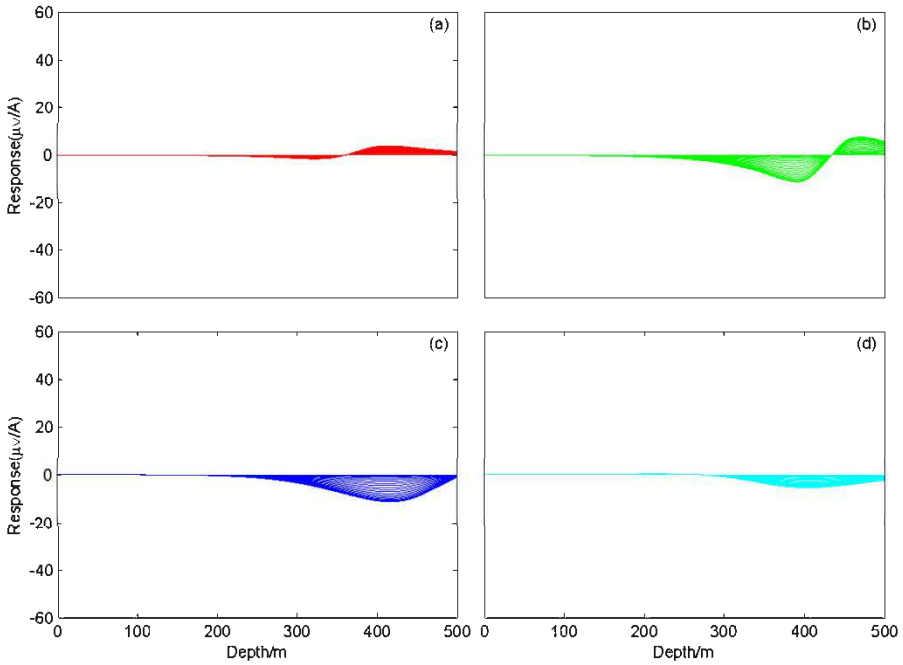

Figure 3.22 The results of component U of Model Series 2 when loop location is in the north of drill hole
(a) horizontal, (b) dip 45° to west, (c) vertical, (d) dip 45° to east

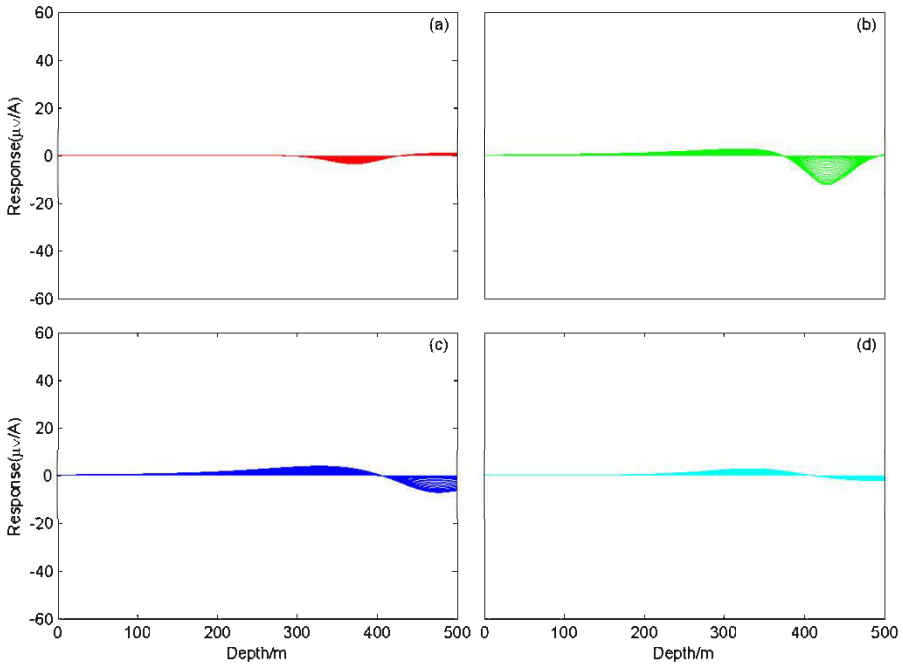

Figure 3.23 The results of component A of Model Series 2 when loop location is in the south of drill hole
(a) horizontal, (b) dip 45° to west, (c) vertical, (d) dip 45° to east

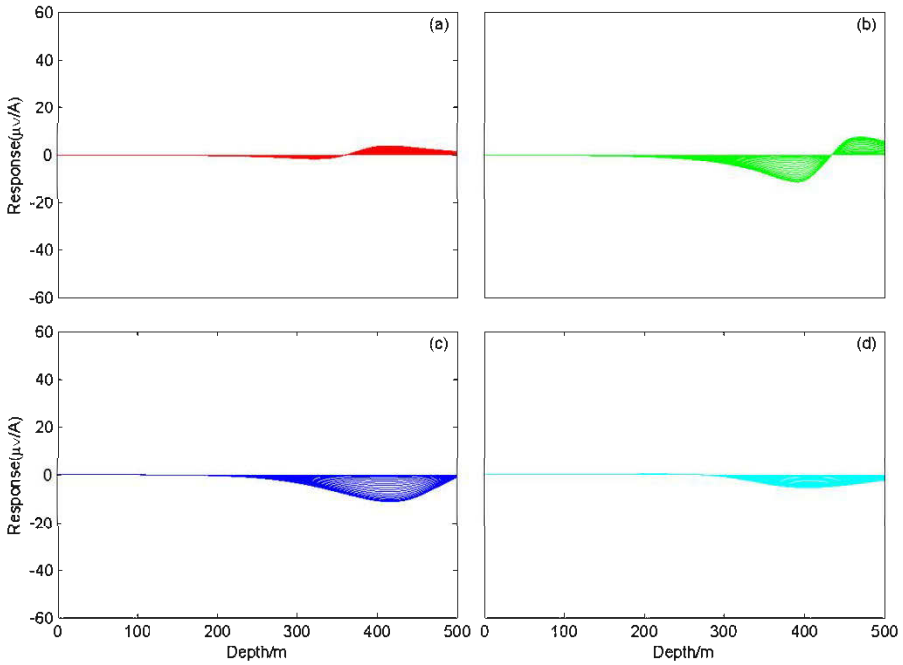

Figure 3.24 The results of component U of Model Series 2 when loop location is in the south of drill hole
(a) horizontal, (b) dip 45° to west, (c) vertical, (d) dip 45° to east

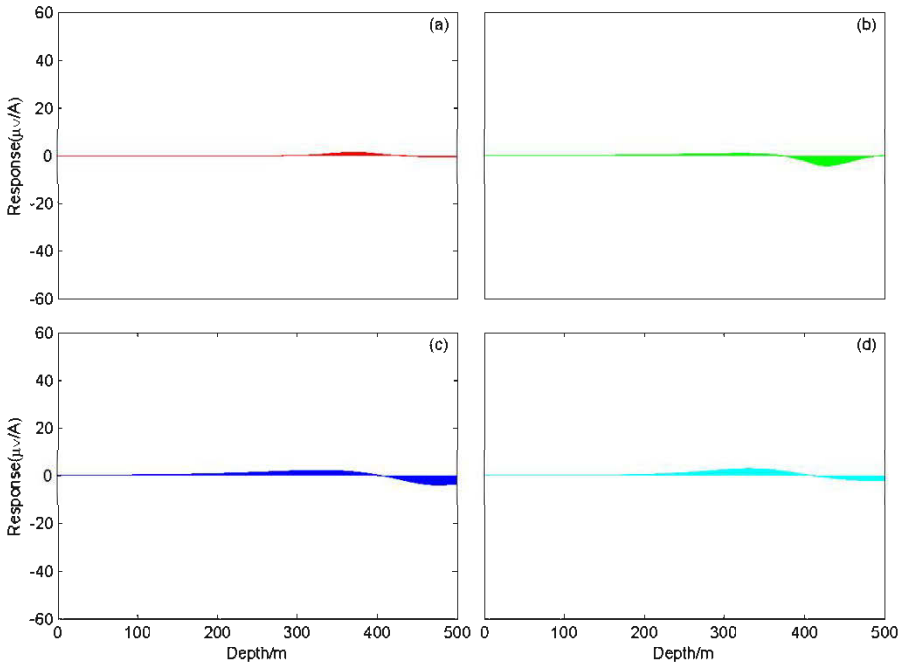

Figure 3.25 The results of component A of Model Series 2 when loop location is in the west of drill hole
(a) horizontal, (b) dip 45° to west, (c) vertical, (d) dip 45° to east

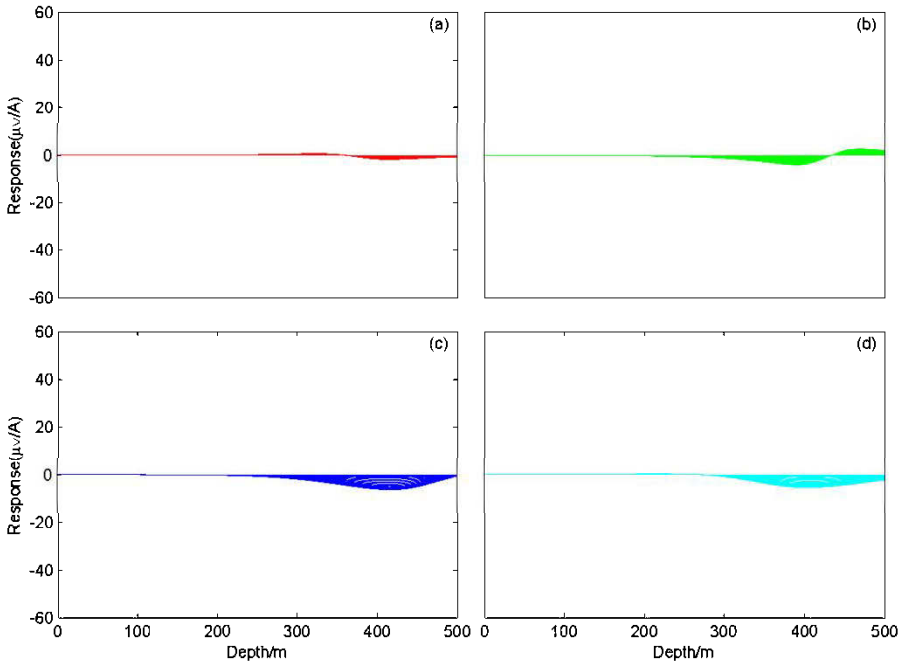

Figure 3.26 The results of component U of Model Series 2 when loop location is in the west of drill hole
(a) horizontal, (b) dip 45° to west, (c) vertical, (d) dip 45° to east

A brief summary for numerical simulation results of Model Series 2:

1. When the loop locates on east side of the hole, we can get largest amplitude of BHTEM signal, except for vertical plate of which amplitude is zero (Figure 3.19 and Figure 3.20).
2. The response curves obtained when the loop locates on south side of the drill-hole are the same as those obtained when the loop locates on north side of the drill-hole (see and compare Figure 3.21, Figure 3.22 and Figure 3.23, Figure 3.24).
3. Abnormal signal is very weak when the loop locates on the west side of the hole, especially, for horizontal plate the abnormal signal is virtually zero (Figure 3.25 and Figure 3.26).
4. For vertical plate, the abnormal amplitude is largest when the loop is centred on the drill-hole (Figure 3.17c and Figure 3.18c).

Thus in field working for Model Series 2 cases, following suggestions should be taken in consideration:

When the target is vertical, the loop should be centred over the hole. Other occasions the loop should be located on the east side of the hole in order to get strongest signal.

3.2.3 Model Series 3

The plate situates under the drill hole and the depth of its centre point through which the extension line of the drill hole penetrates is 550m. See Figure 3.27.

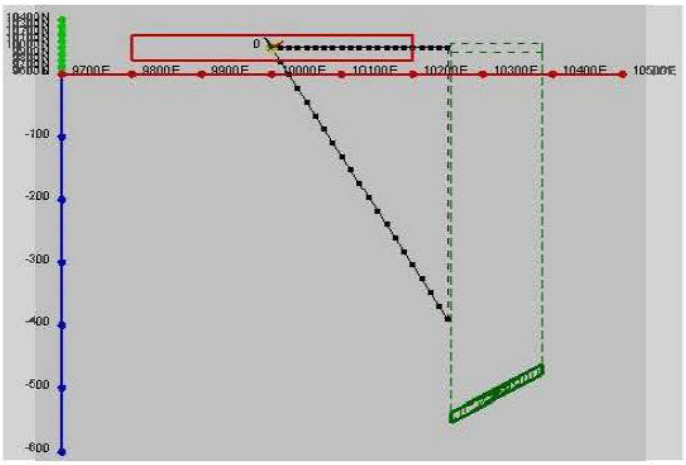

Figure 3.27 The model sketch of Model Series 3

As Model Series 1 and 2, values of component V in this model series are zero, so only components A and U are presented in following figures.

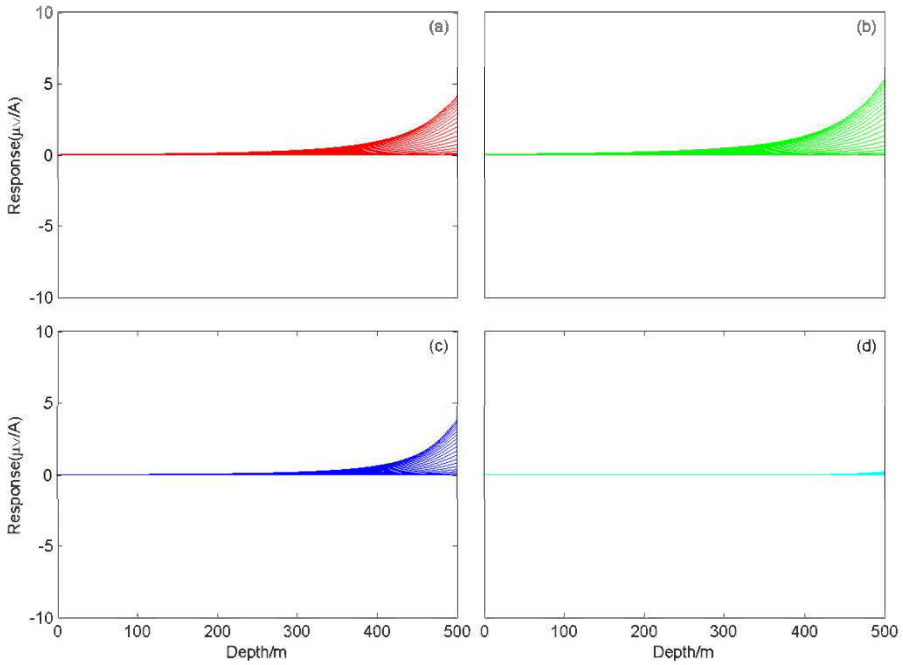

Figure 3.28 The results of component A of Model Series 3 when loop location is in the centre (a) horizontal, (b) dip 45° to west, (c) vertical, (d) dip 45° to east

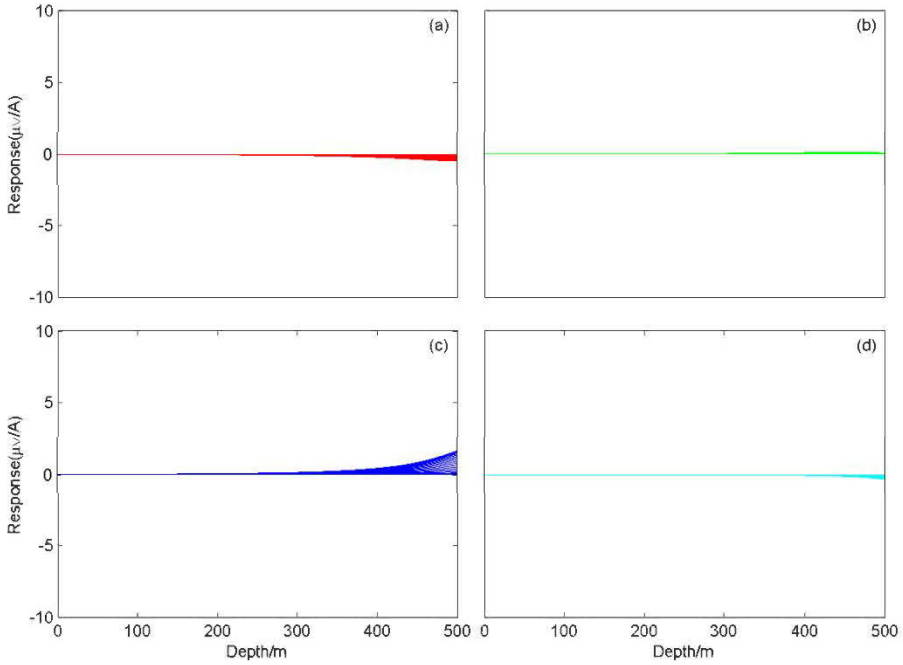

Figure 3.29 The results of component U of Model Series 3 when loop location is in the centre (a) horizontal, (b) dip 45° to west, (c) vertical, (d) dip 45° to east

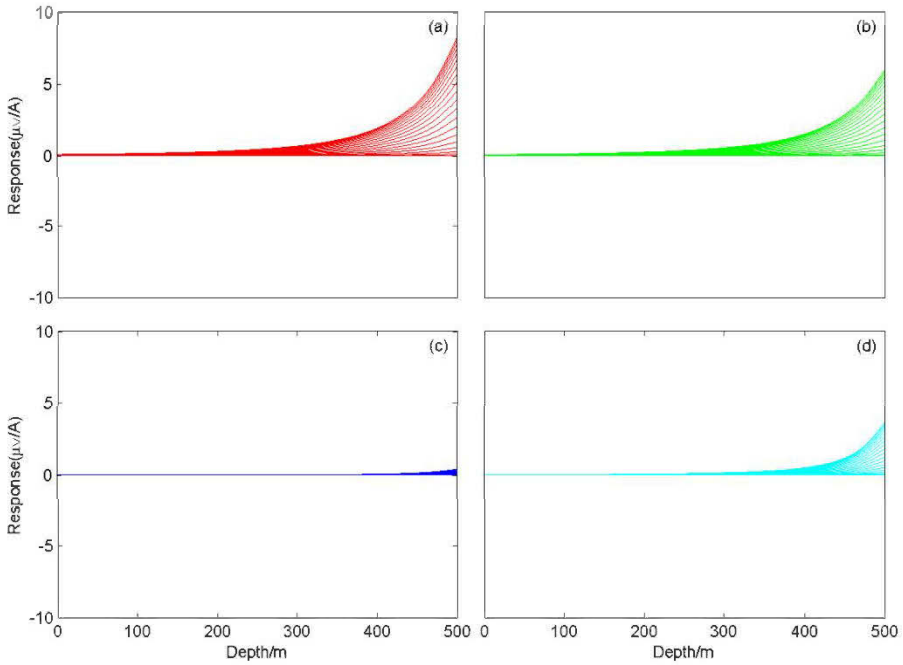

Figure 3.30 The results of component A of Model Series 3 when loop location is in the east of drill hole
(a) horizontal, (b) dip 45° to west, (c) vertical, (d) dip 45° to east

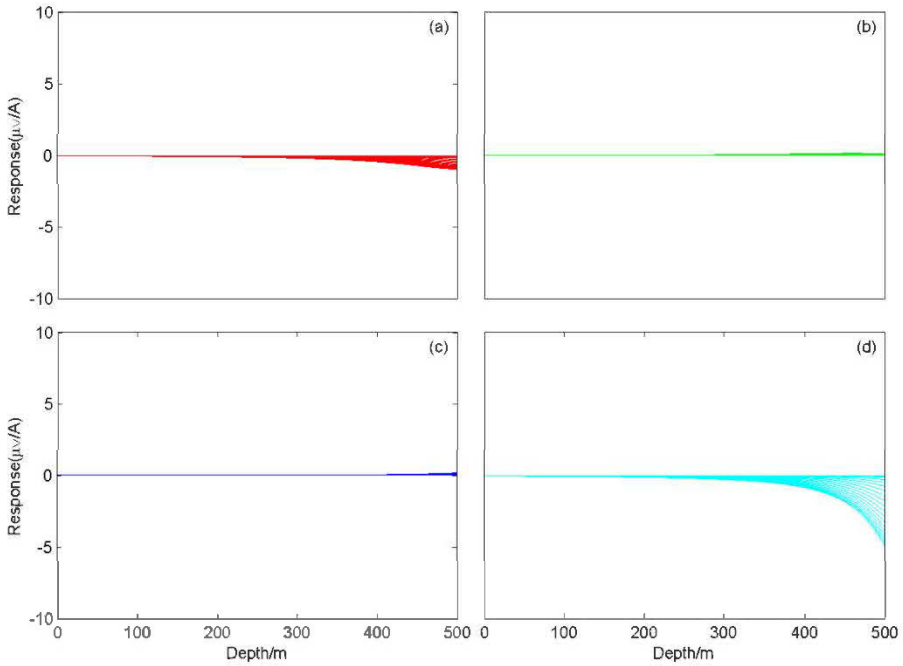

Figure 3.31 The results of component U of Model Series 3 when loop location is in the east of drill hole
(a) horizontal, (b) dip 45° to west, (c) vertical, (d) dip 45° to east

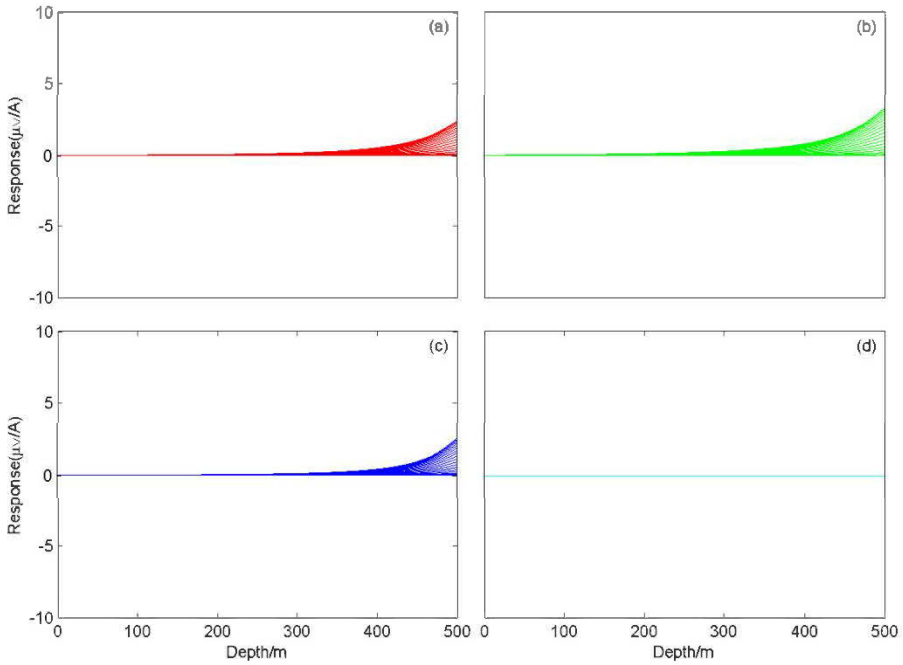

Figure 3.32 The results of component A of Model Series 3 when loop location is in the north of drill hole
(a) horizontal, (b) dip 45° to west, (c) vertical, (d) dip 45° to east

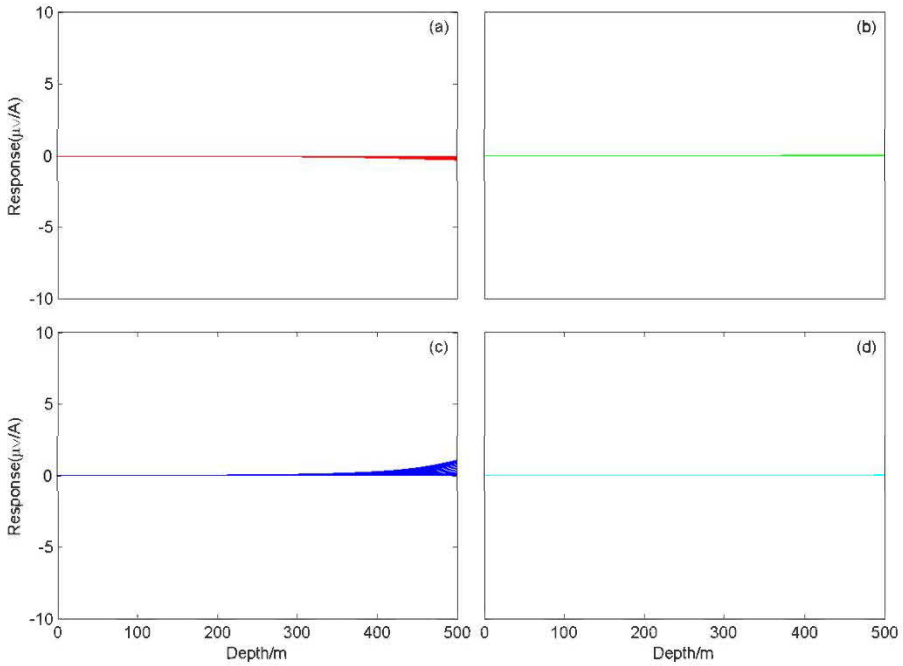

Figure 3.33 The results of component U of Model Series 3 when loop location is in the north of drill hole
(a) horizontal, (b) dip 45° to west, (c) vertical, (d) dip 45° to east

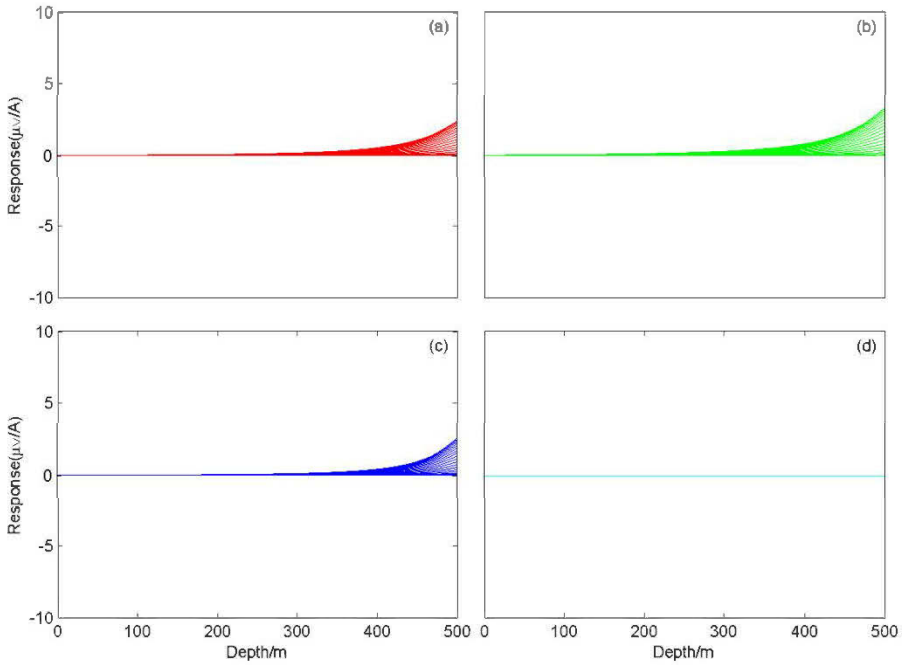

Figure 3.34 The results of component A of Model Series 3 when loop location is in the south of drill hole
(a) horizontal, (b) dip 45° to west, (c) vertical, (d) dip 45° to east

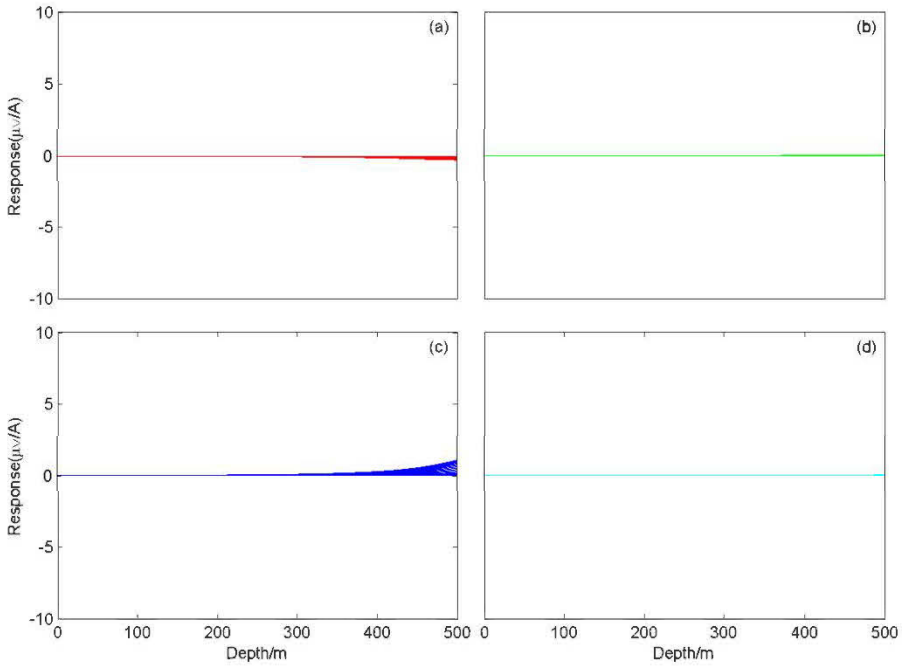

Figure 3.35 The results of component U of Model Series 3 when loop location is in the south of drill hole
(a) horizontal, (b) dip 45° to west, (c) vertical, (d) dip 45° to east

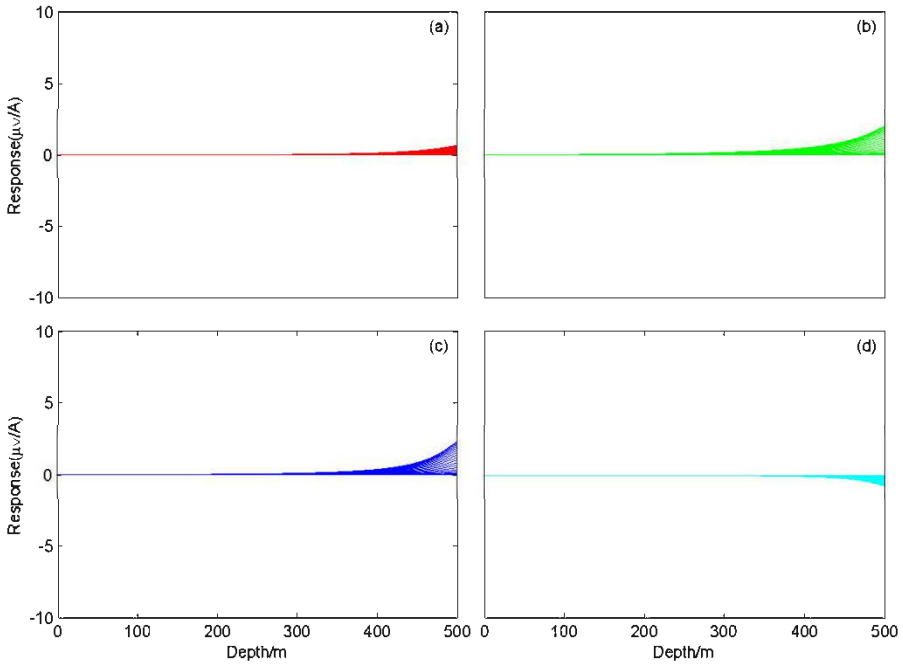

Figure 3.36 The results of component A of Model Series 3 when loop location is in the west of drill hole
(a) horizontal, (b) dip 45° to west, (c) vertical, (d) dip 45° to east

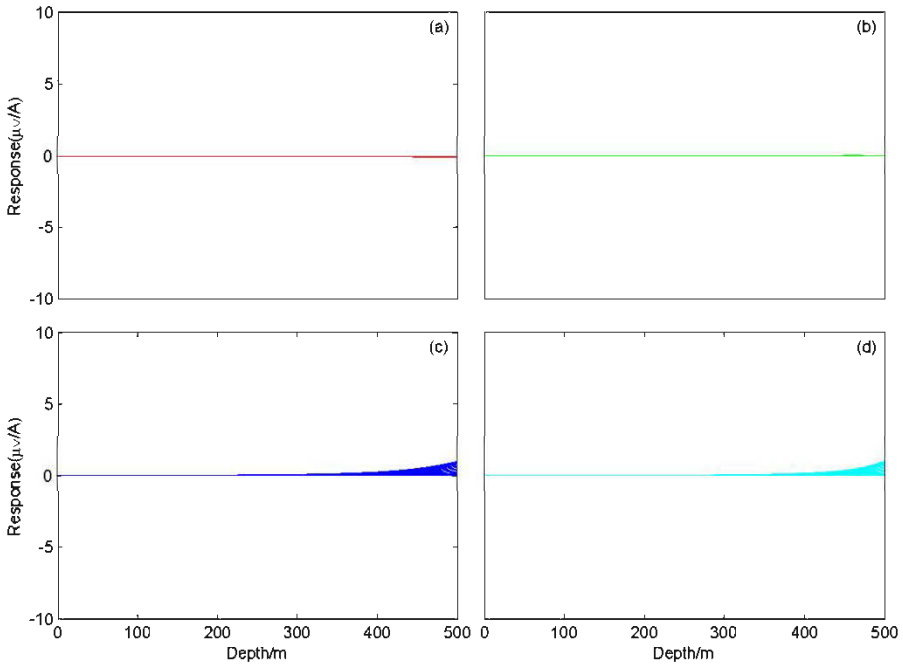

Figure 3.37 The results of component U of Model Series 3 when loop location is in the west of drill hole
(a) horizontal, (b) dip 45° to west, (c) vertical, (d) dip 45° to east

As we said before, nowadays, shallow deposits are rarer and rarer, and deep deposits will definitely become the main targets in the future. But methods

operated on surface of the earth or in the air can hardly reach that depth. Through the results of Model Series 3 we find that BHTEM can effectively discovery targets at deep location. In fact, the exploration range can be extended several hundred meters from the bottom of the hole.

Here are the features observed from figures above:

1. Generally, amplitude of component U is smaller than that of component A, except when the plate dips 45° to the east and the loop locates on the east side of the hole (Figure 3.30d and Figure3.31d).
2. For every plate, we got identical BHTEM signals when the transmitter loop locates at the north and south sides of the hole.
3. In this model case, when the plate dips 45° to west, values of U component are virtually zero (Figure 3.33b and Figure 3.35b), while values of A are not zero (Figure 3.32b and Figure 3.34b); when the plate dips 45° to the east, values of both U and A are zero (Figure 3.32d to Figure 3.35d).
4. For a vertical plate, largest amplitude is obtained when the transmitter loop is centred over the hole (Figure 3.28 and Figure 3.29). And for a non-vertical pate, when the transmitter loop is situated on the east side of the hole, we can get the most obviously abnormal (Figure 3.30 and Figure 3.31).

As discussed above, in order to get better measurement results, we should centre the loop over the hole for horizontal plates and for other plates the loop should be placed on the side of the drill hole dipping direction.

3.2.4 Model Series 4

The plate situates on south side of the drill hole; the depth of its centre point is 300 meters. The horizontal distance between the drill hole and the centre point of the plate is 200m. See Figure 3.38.

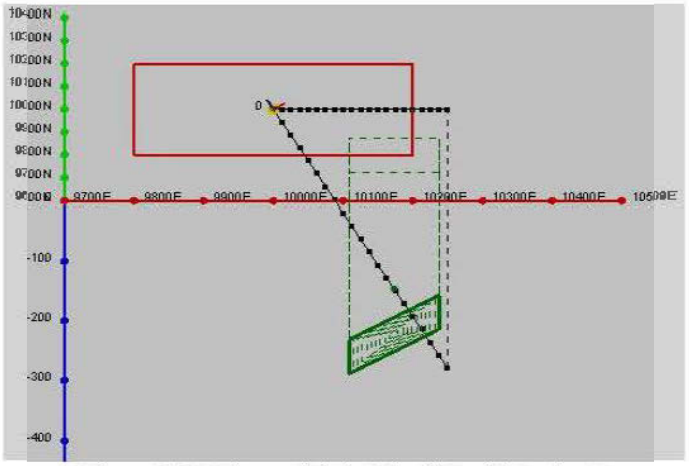

Figure 3.38 The model sketch of Model Series 4

In this case, values of three components A, U and V are not zero. Results are showed in following figures.

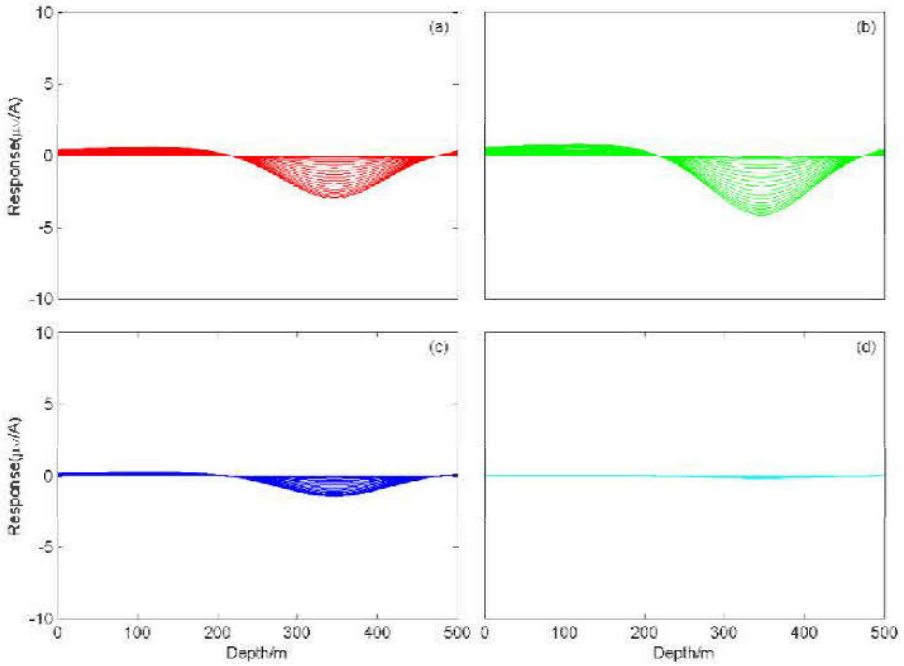

Figure 3.39 The results of component A of Model Series 4 when loop location is in the centre (a) horizontal, (b) dip 45° to west, (c) vertical, (d) dip 45° to east

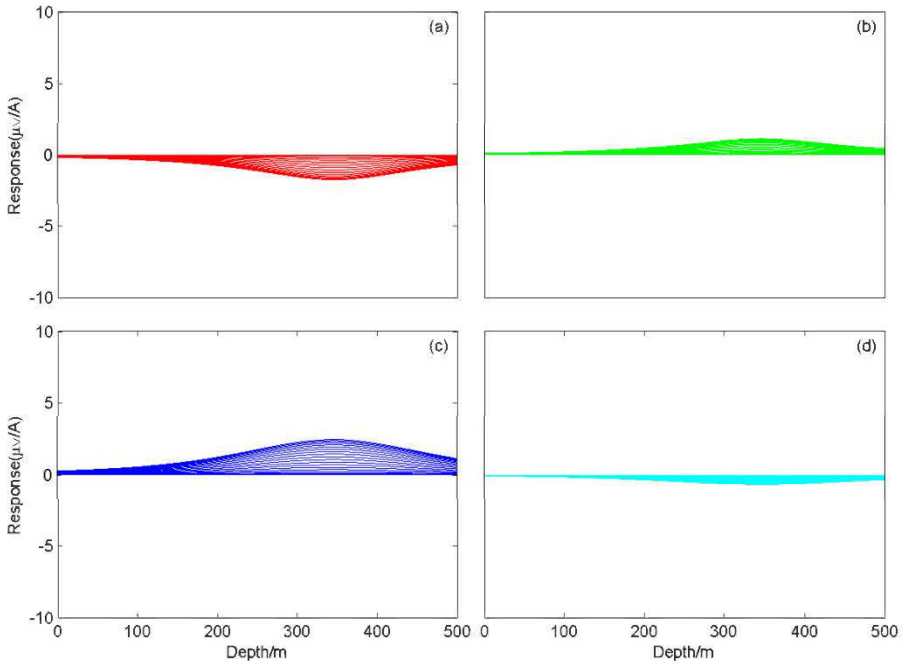

Figure 3.40 The results of component U of Model Series 4 when loop location is in the centre (a) horizontal, (b) dip 45° to west, (c) vertical, (d) dip 45° to east

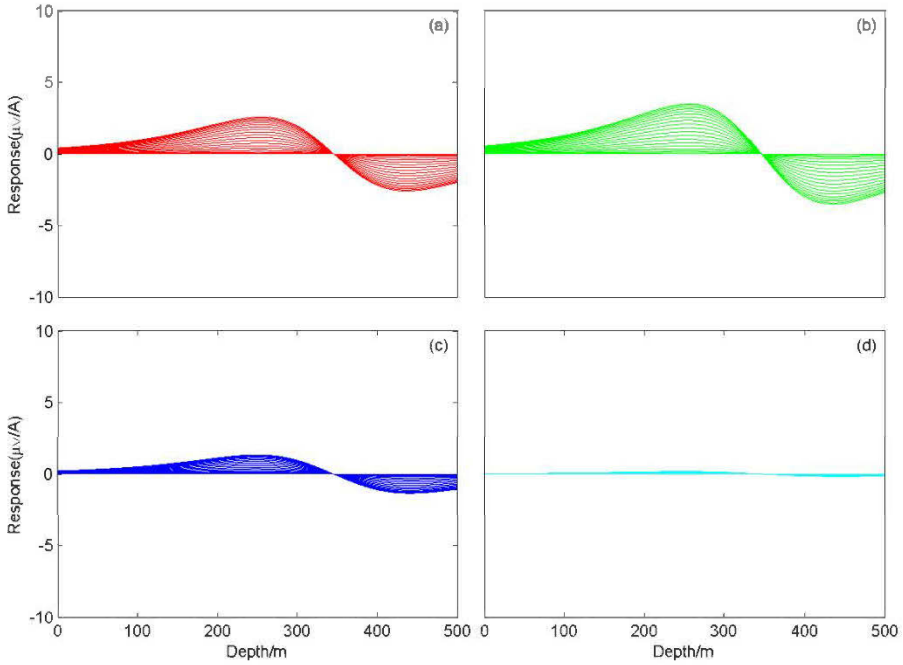

Figure 3.41 The results of component V of Model Series 4 when loop location is in the centre (a) horizontal, (b) dip 45° to west, (c) vertical, (d) dip 45° to east

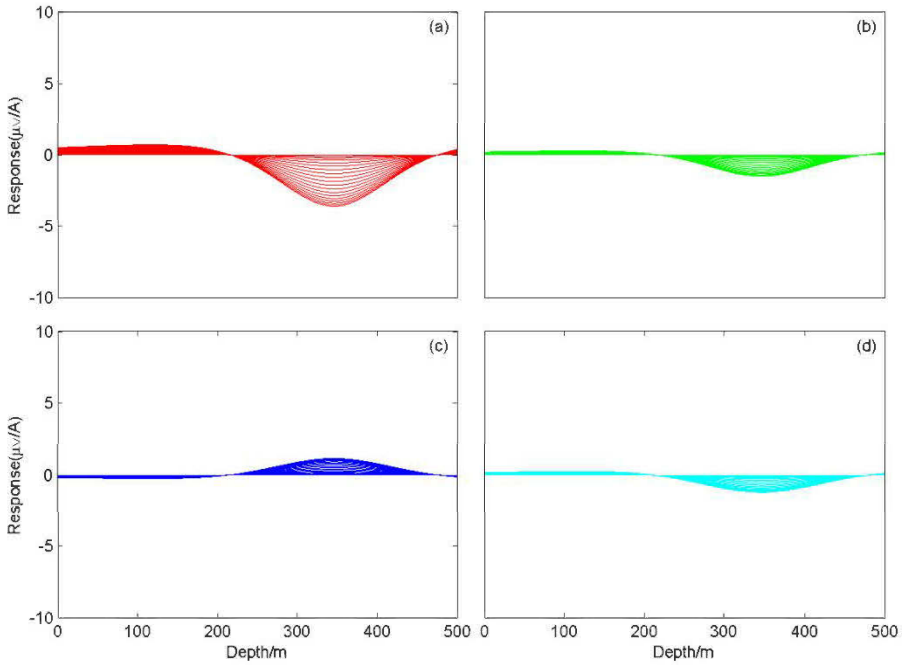

Figure 3.42 The results of component A of Model Series 4 when loop location is in the east of drill hole
(a) horizontal, (b) dip 45° to west, (c) vertical, (d) dip 45° to east

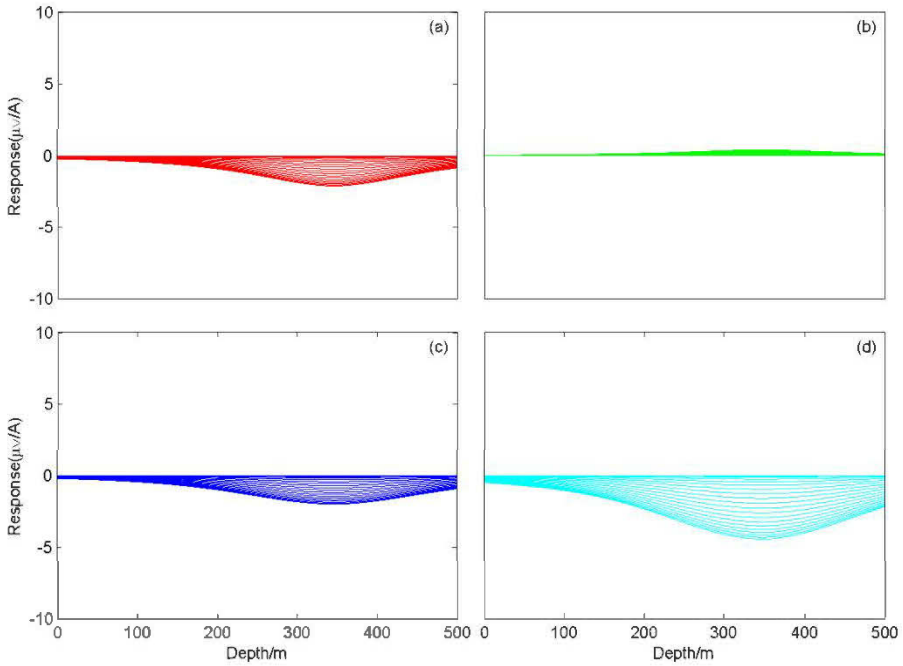

Figure 3.43 The results of component U of Model Series 4 when loop location is in the east of drill hole
(a) horizontal, (b) dip 45° to west, (c) vertical, (d) dip 45° to east

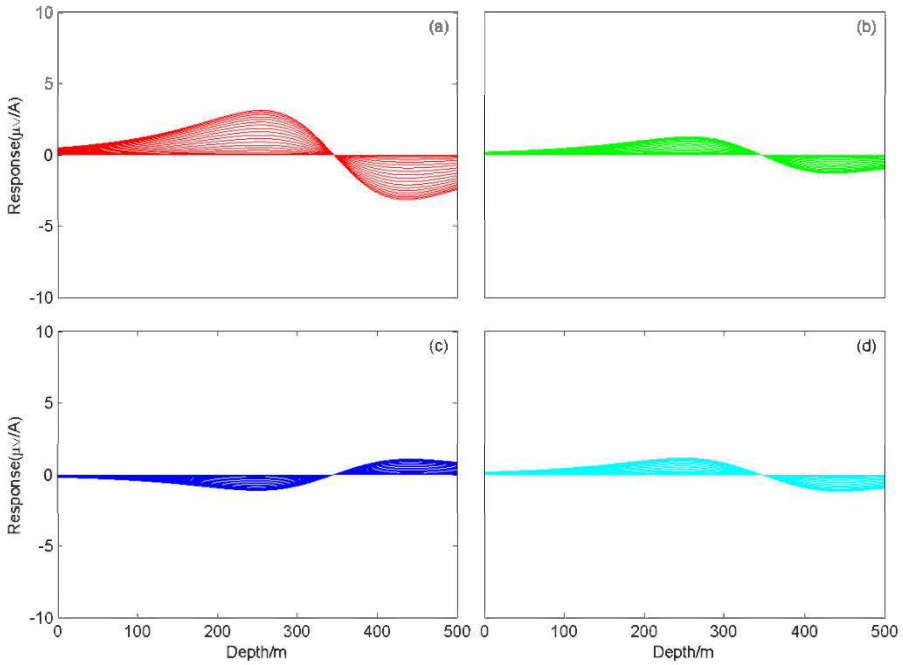

Figure 3.44 The results of component V of Model Series 4 when loop location is in the east of drill hole
(a) horizontal, (b) dip 45° to west, (c) vertical, (d) dip 45° to east

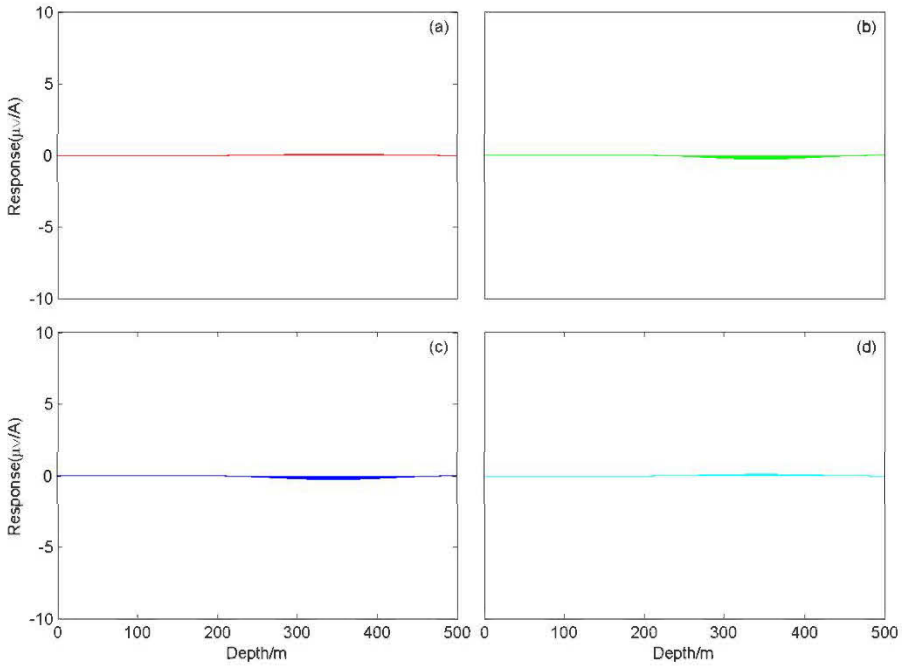

Figure 3.45 The results of component A of Model Series 4 when loop location is in the north of drill hole
(a) horizontal, (b) dip 45° to west, (c) vertical, (d) dip 45° to east

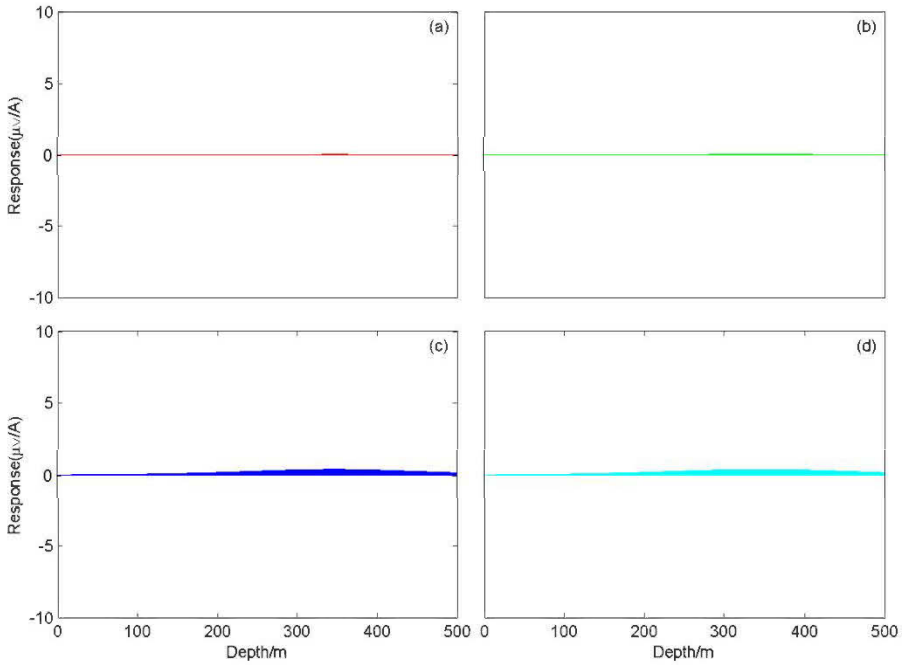

Figure 3.46 The results of component U of Model Series 4 when loop location is in the north of drill hole
(a) horizontal, (b) dip 45° to west, (c) vertical, (d) dip 45° to east

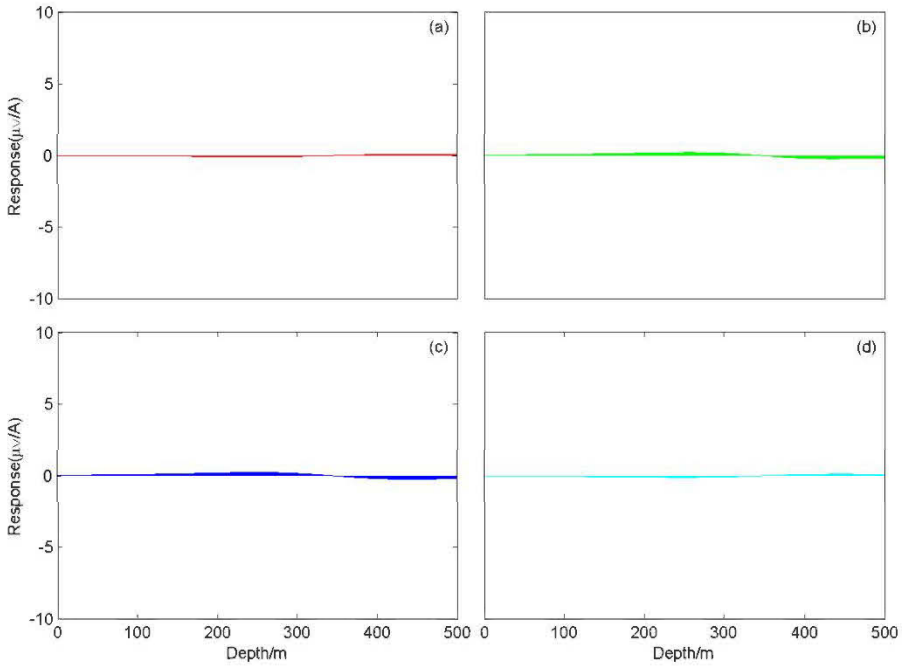

Figure 3.47 The results of component V of Model Series 4 when loop location is in the north of drill hole
(a) horizontal, (b) dip 45° to west, (c) vertical, (d) dip 45° to east

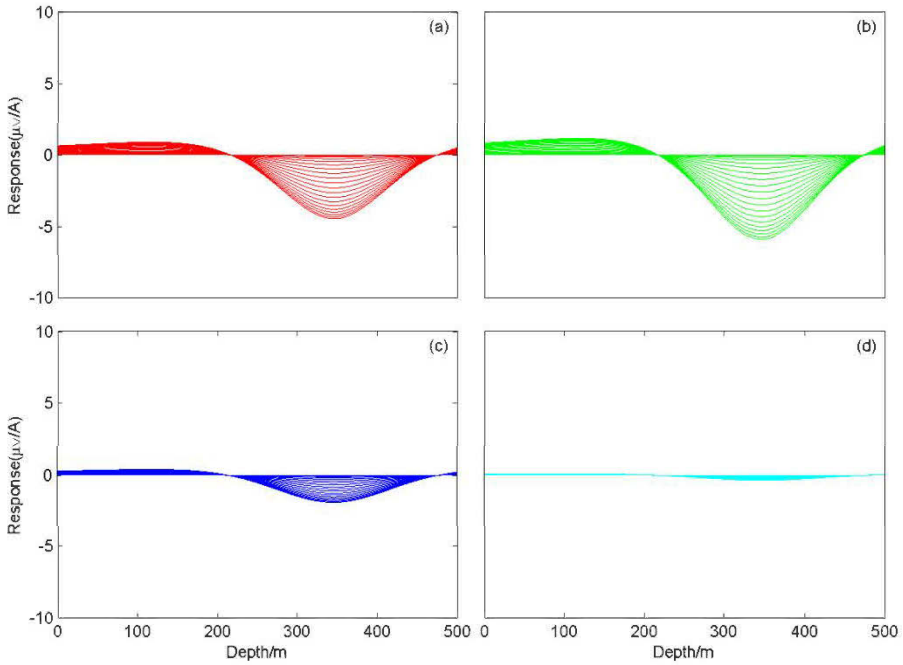

Figure 3.48 The results of component A of Model Series 4 when loop location is in the south of drill hole
(a) horizontal, (b) dip 45° to west, (c) vertical, (d) dip 45° to east

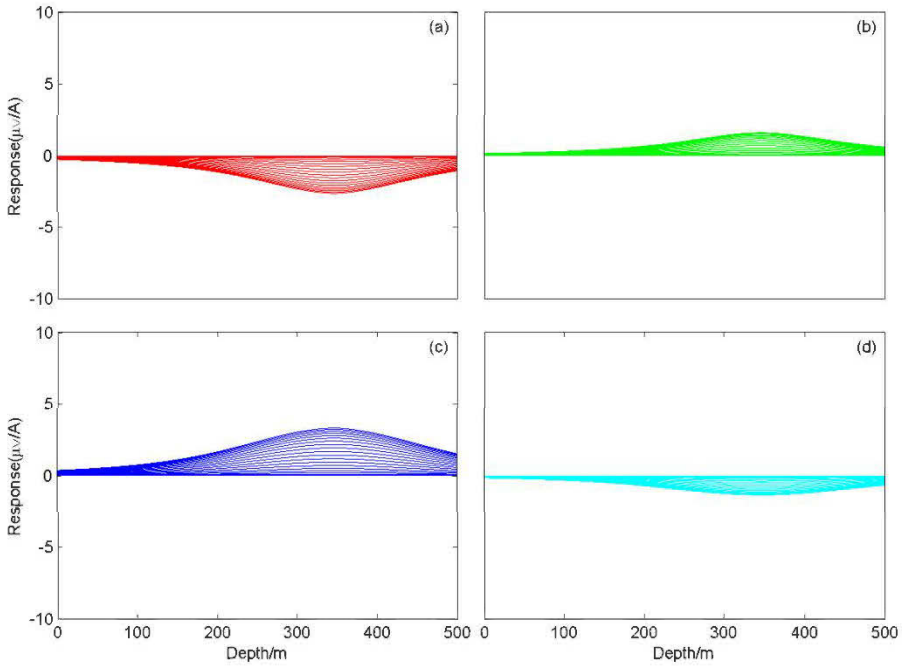

Figure 3.49 The results of component U of Model Series 4 when loop location is in the south of drill hole
(a) horizontal, (b) dip 45° to west, (c) vertical, (d) dip 45° to east

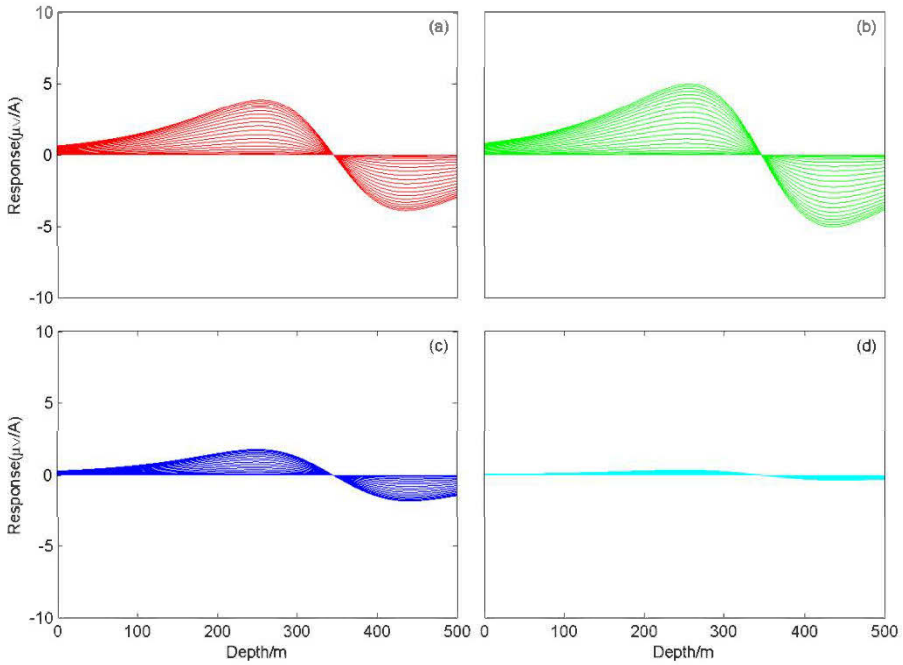

Figure 3.50 The results of component V of Model Series 4 when loop location is in the south of drill hole
(a) horizontal, (b) dip 45° to west, (c) vertical, (d) dip 45° to east

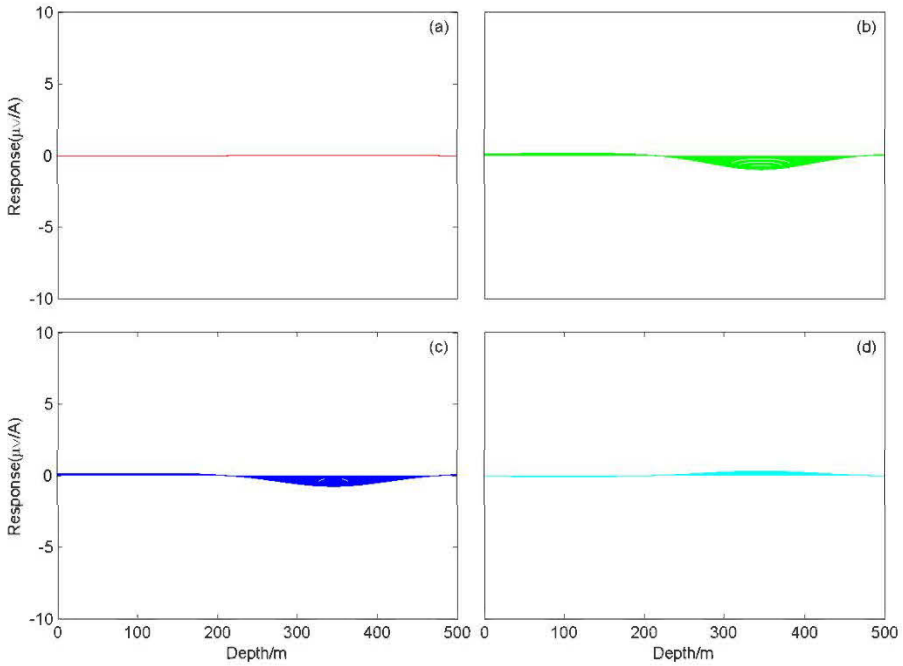

Figure 3.51 The results of component A of Model Series 4 when loop location is in the west of drill hole
(a) horizontal, (b) dip 45° to west, (c) vertical, (d) dip 45° to east

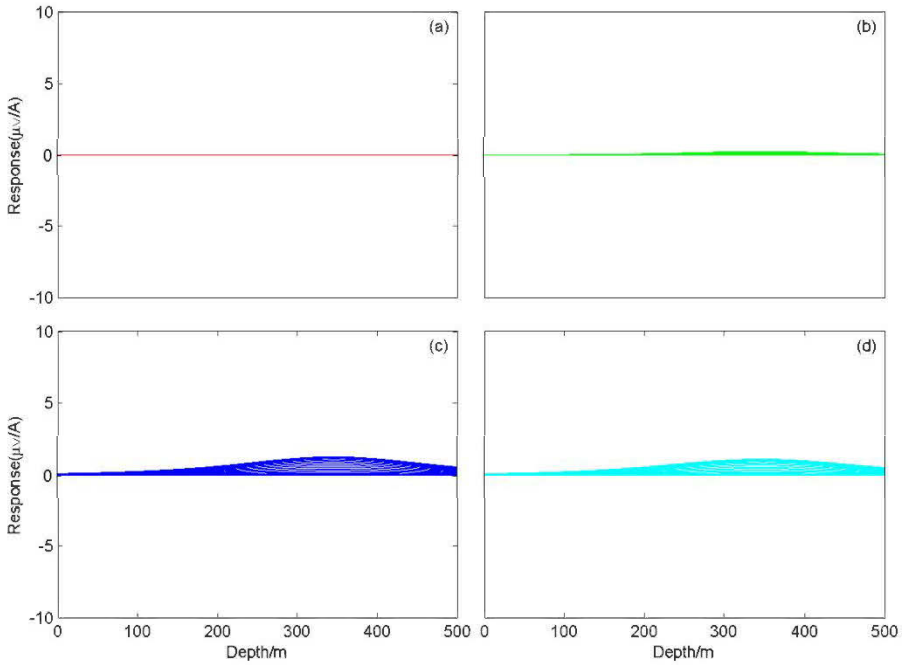

Figure 3.52 The results of component U of Model Series 4 when loop location is in the west of drill hole
(a) horizontal, (b) dip 45° to west, (c) vertical, (d) dip 45° to east

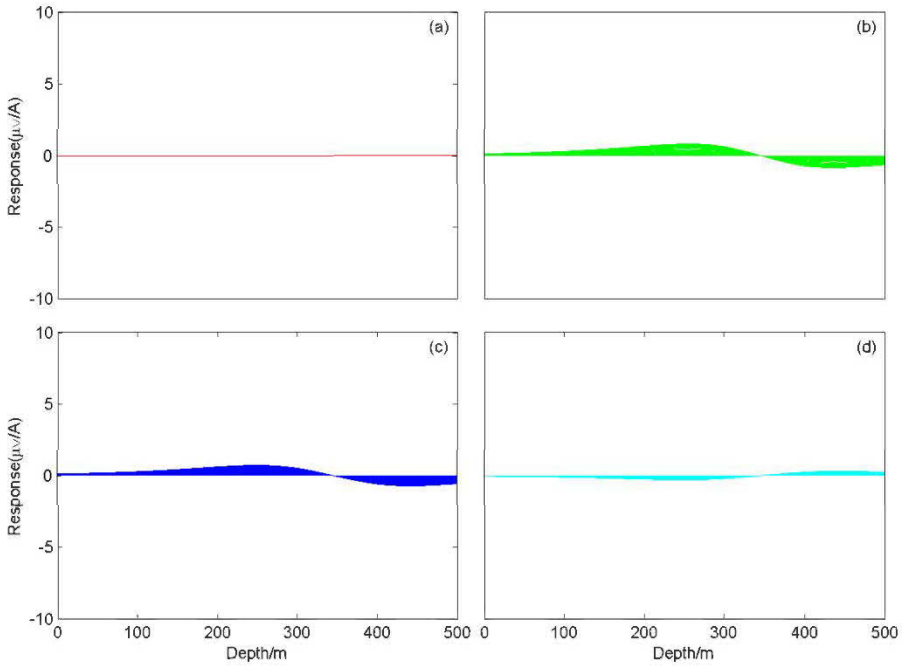

Figure 3.53 The results of component V of Model Series 4 when loop location is in the west of drill hole
(a) horizontal, (b) dip 45° to west, (c) vertical, (d) dip 45° to east

Following features are observed by analyzing the numerical simulation results of Model Series 4:

1. Unlike the former three model series, in this case the three components are not zero and BHTEM signal curves are distinct from loop to loop.
2. Curves of component U are very simple: values of each curve are either all positive, or all negative.
3. Generally, features of component A are: there is a negative main peak on two sides of which there are two secondary positive peaks (Figure 3.39, Figure 3.42 and Figure 3.48).
4. There is no apparent change in shape of signals of three components with the change of transmitter loop location. However, the amplitude varies a lot with the change of transmitter loop location. Relatively, when the loop placed on the east side, the response curves' shape of components A and V of vertical plate is reversed compared with other plates' (Figure 3.42 and Figure 3.44), and the shape of component U of the plate dipping 45° to the west differs from other plates' when the east loop is used (Figure 3.43).
5. Except the plate dipping 45° to the east for which we obtain the largest amplitude signal when the loop is placed on the east side (Figure 42 to Figure 44); otherwise, when the loop is placed on the south side we can get the largest abnormal amplitude (Figure 48 to Figure 50).

In conclusion, for the plate which is horizontal, dipping 45° to the west, or vertical, the transmitter loop should be placed on the south side of the hole; when the plate is dipping 45° to the east, the east side loop should be chosen.

3.2.5 Model Series 5

The drill hole penetrates through the centre point of the plate and the depth is 300m. See Figure 3.54.

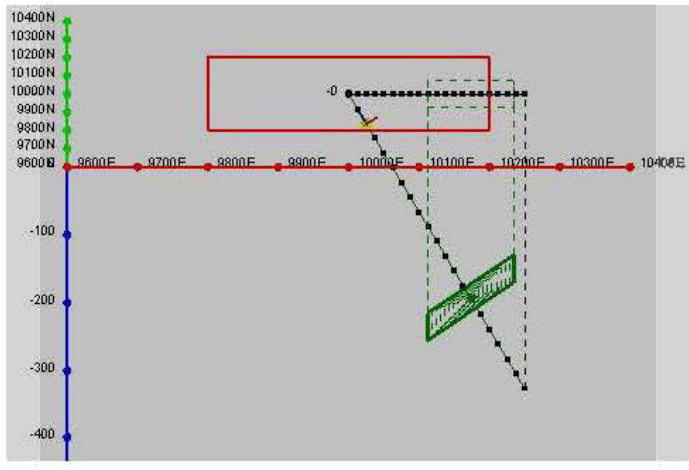

Figure 3.54 The model sketch of Model Series 5

In this series, values of component V are zero. Results are shown as follows:

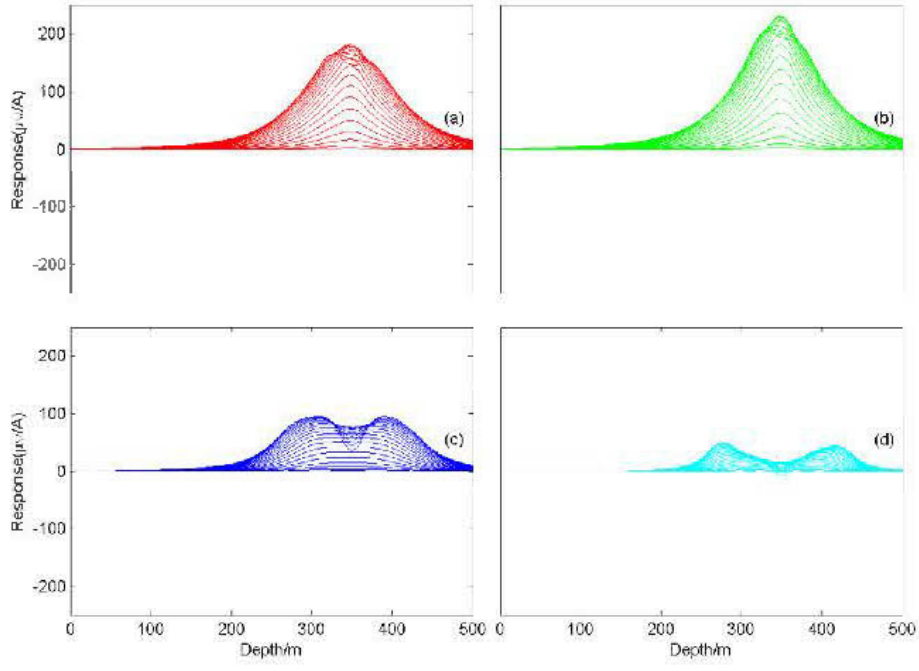

Figure 3.55 The results of component A of Model Series 5 when loop location is the in centre (a) horizontal, (b) dip 45° to west, (c) vertical, (d) dip 45° to east

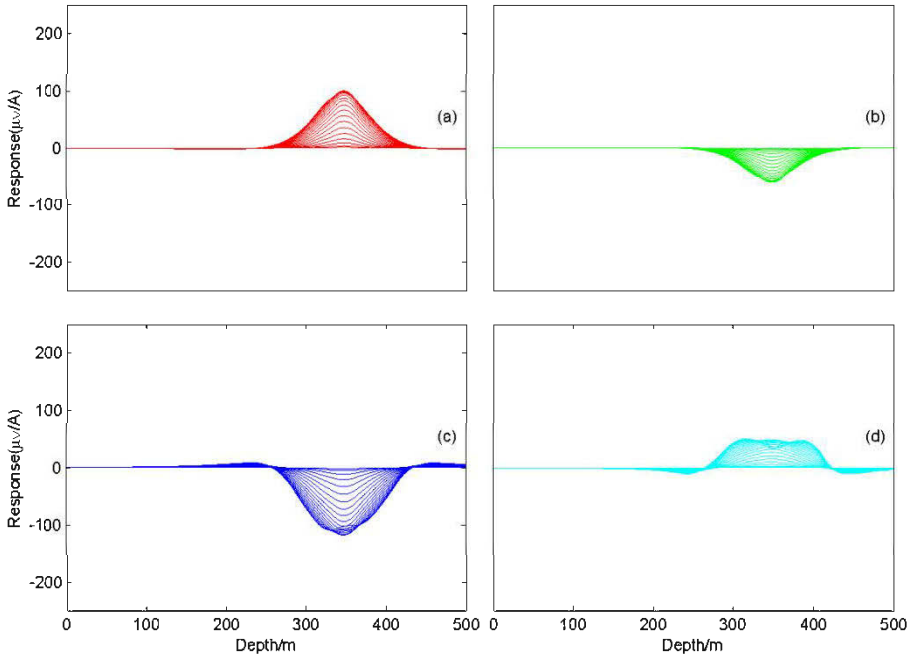

Figure 3.56 The results of component U of Model Series 5 when loop location is in the centre
(a) horizontal, (b) dip 45° to west, (c) vertical, (d) dip 45° to east

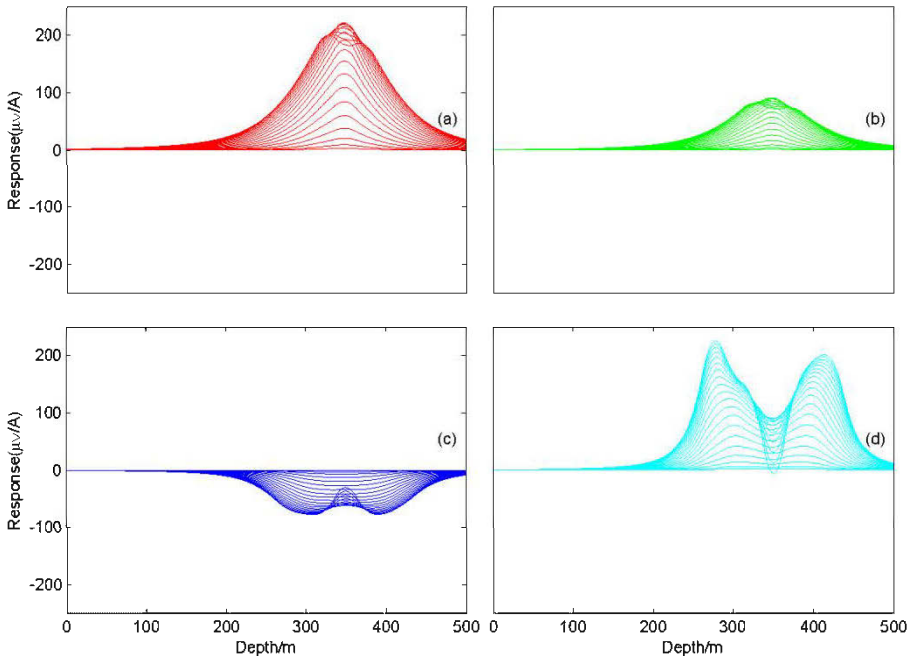

Figure 3.57 The results of component A of Model Series 5 when loop location is in the east of drill hole
(a) horizontal, (b) dip 45° to west, (c) vertical, (d) dip 45° to east

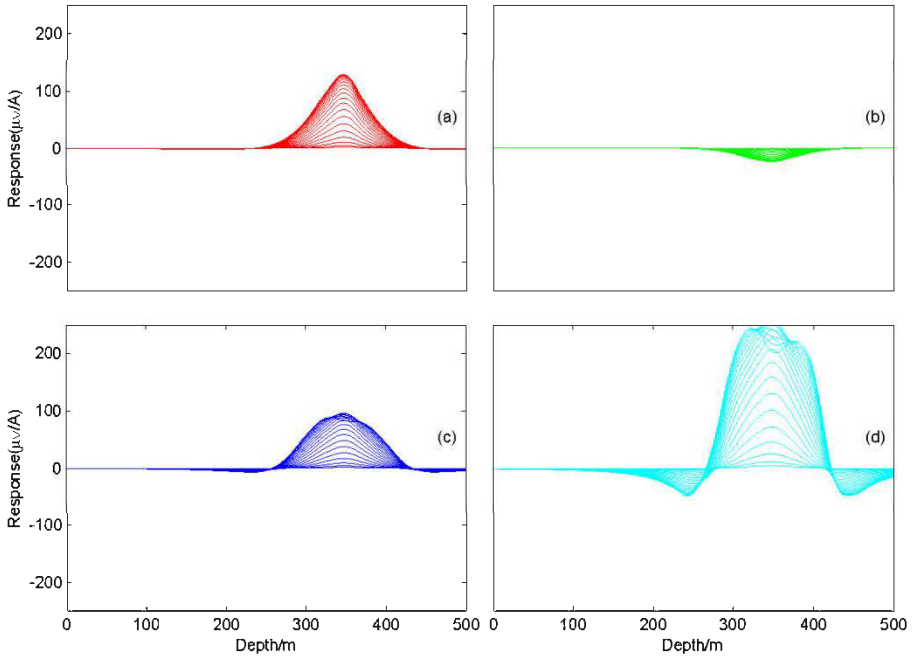

Figure 3.58 The results of component U of Model Series 5 when loop location is in the east of drill hole
(a) horizontal, (b) dip 45° to west, (c) vertical, (d) dip 45° to east

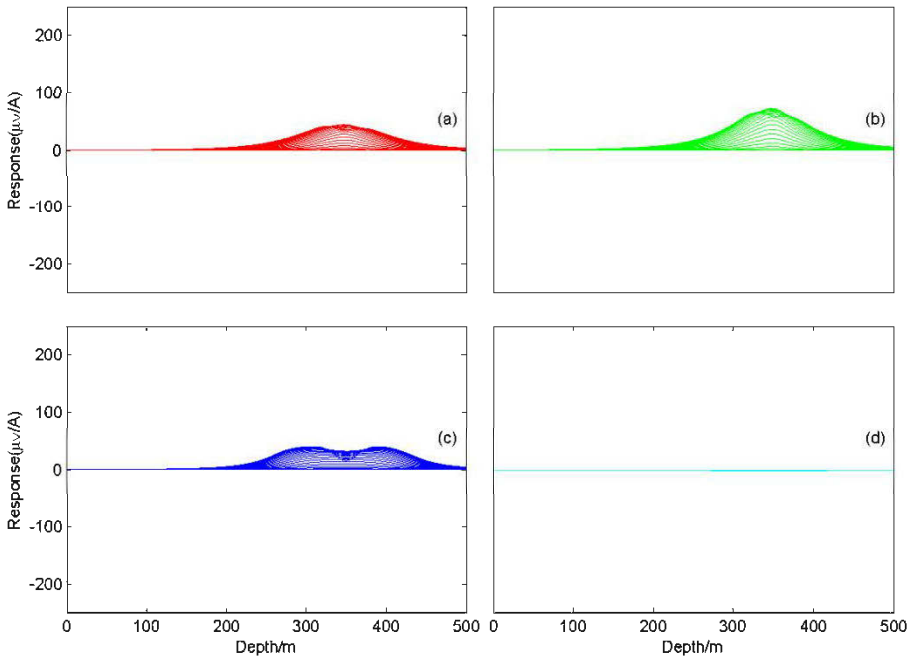

Figure 3.59 The results of component A of Model Series 5 when loop location is in the north of drill hole
(a) horizontal, (b) dip 45° to west, (c) vertical, (d) dip 45° to east

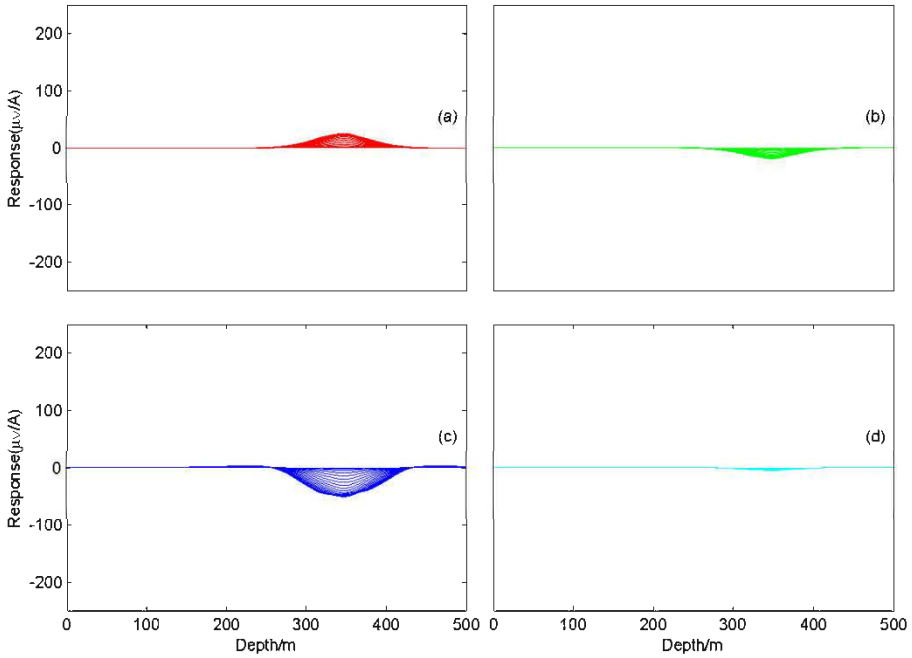

Figure 3.60 The results of component U of Model Series 5 when loop location is in the north of drill hole
(a) horizontal, (b) dip 45° to west, (c) vertical, (d) dip 45° to east

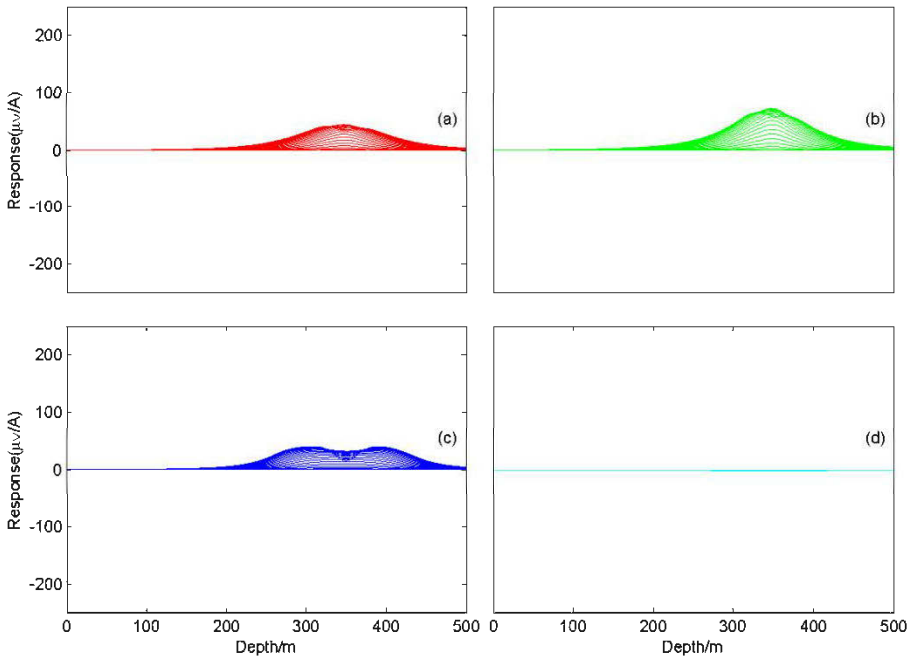

Figure 3.61 The results of component A of Model Series 5 when loop location is in the south of drill hole
(a) horizontal, (b) dip 45° to west, (c) vertical, (d) dip 45° to east

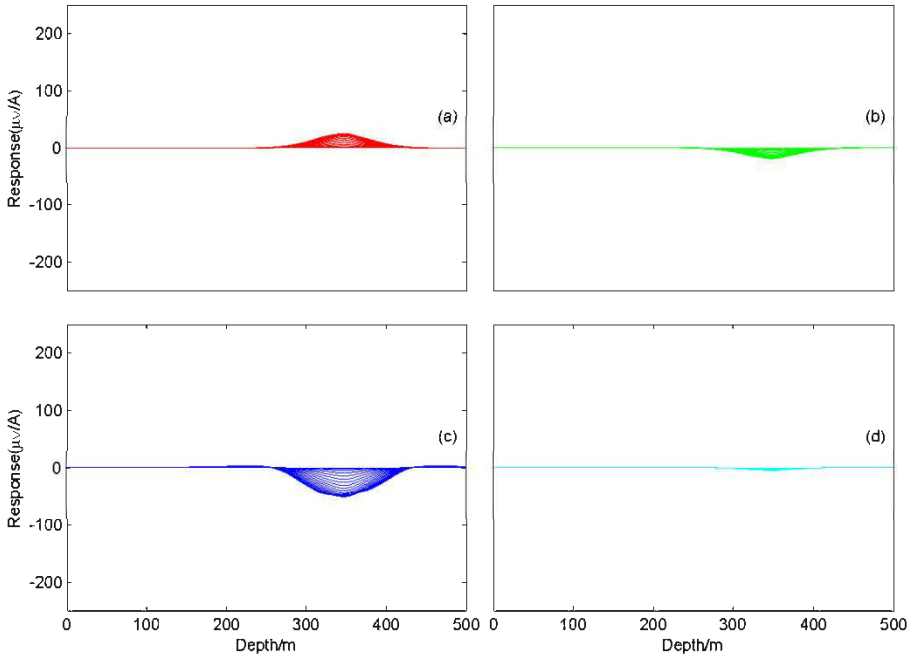

Figure 3.62 The results of component U of Model Series 5 when loop location is in the south of drill hole
(a) horizontal, (b) dip 45° to west, (c) vertical, (d) dip 45° to east

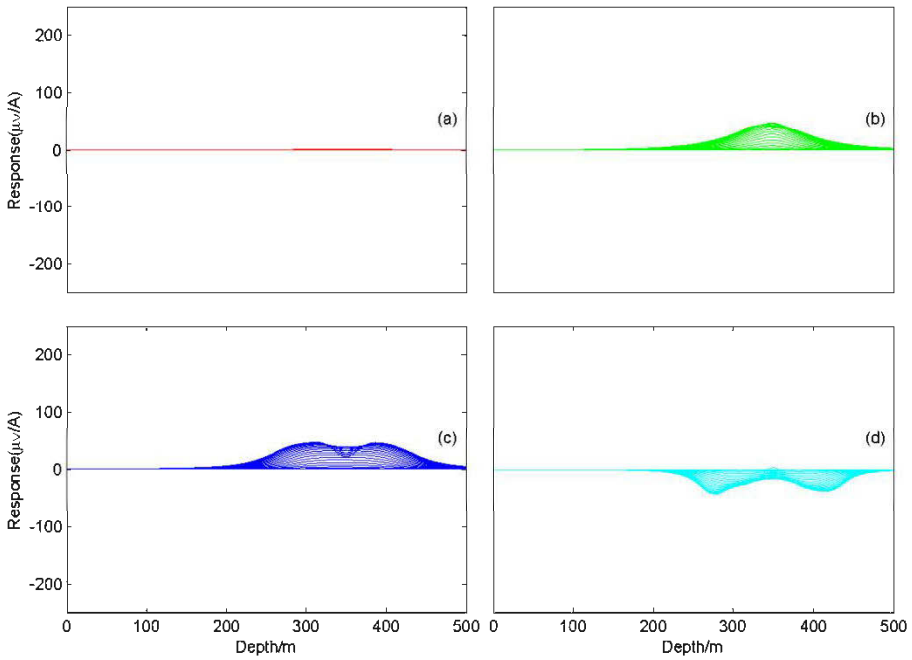

Figure 3.63 The results of component A of Model Series 5 when loop location is in the west of drill hole
(a) horizontal, (b) dip 45° to west, (c) vertical, (d) dip 45° to east

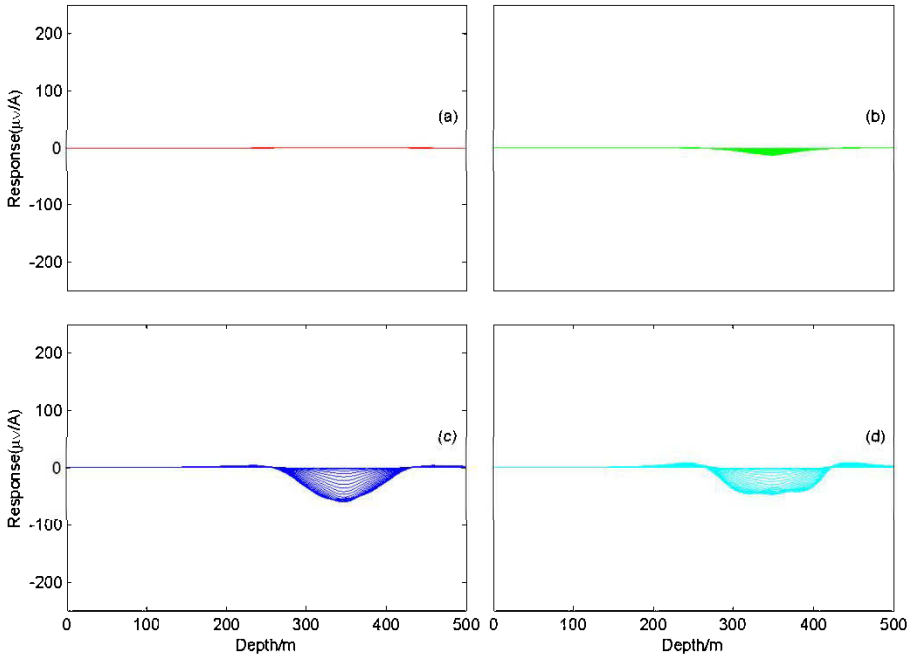

Figure 3.64 The results of component U of Model Series 5 when loop location is in the west of drill hole
(a) horizontal, (b) dip 45° to west, (c) vertical, (d) dip 45° to east

Following are features observed from numerical simulation results of Model Series 5:

1. Compared with the previous four model series, we can find that abnormal amplitude of this model series is much larger.
2. We got identical signals for each plate when the loop locates on the north and south sides (Figure 3.59 to Figure 3.62).
3. No matter the plate is horizontal, vertical or inclined; the abnormal curve is symmetrical.
4. Signals of component A are single-valued; while for component U, when the plat is vertical or dipping 45° to the east, there will be secondary peaks on two sides of the main peak and the sign of the secondary peak is opposite to that of the main peak (see Figure 3.56, Figure 3.58, Figure 3.60, Figure 3.62 and Figure 3.64).
5. When the plate is horizontal or dipping 45° to the east, we can get largest abnormal amplitude by using the east side transmitter loop location (Figure 3.57 and Figure 3.58); other cases, largest amplitude is obtained

when the loop is centred on the hole (Figure 3.55 and Figure 3.56).

Thus, in practical cases, we should use centre loop to detect vertical plate and those dipping 45° to the west. For horizontal plate and plate dipping 45° to the east, we should choose east loop configuration.

CHAPTER IV

ANALYSES OF THE NUMERICAL SIMULATION RESULTS

We have made a brief summary after each model series in Chapter 3. But they were more descriptive than analysis. In this chapter we will do a comprehensive analysis on the numerical simulation results to disclose effects of the variation of different parameters as listed in Table 3.1, and try to conclude essential regulations.

4.1 The distribution of electromagnetic field

Figure 4.1 shows map view of the primary magnetic field, emitted from a horizontal rectangular transmitter loop. If there is a conductor in this field, since the primary field varies with time, the time-varying eddy current will be induced in the conductor and it generates the second magnetic field inside and around the conductor. For a thin plate as in the following figure, when its plane direction perpendicular to the field lines we get maximum induction (such as plate 2 and 6 in Figure 4.1), which means the strongest response. As we see in Chapter 3 that the BHTEM signal varies with multiple factors, such as the conductor's occurrence, the spatial relationship between the conductor, borehole and transmitter loop, we will discuss their impact on BHTEM observations in following aspects.

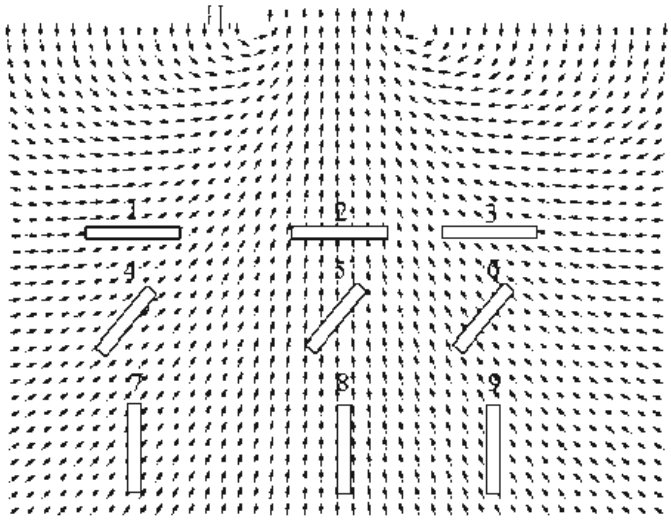

Figure 4.1 the section view of the primary magnetic field

4.2 Coupling effect

The signal we measured in the hole during the field work is the secondary magnetic field or its derivatives which is induced by the coupling between the primary field and the conductor. Thus, the coupling relationship between the loop (transmitting the primary field) and the conductor (plate) will definitely affect the recording results as we had seen in the previous chapters.

As we all know, the intensity of the secondary field is proportion to the change rate of the flux and the effective area. Under the circumstance of a provided primary field, the change rate of the flux is fixed, so the intensity of the secondary field is affected by the effective area, i.e., when the effective area is smaller, the secondary field is weak, and otherwise it is strong; and we might say that the signal we recorded is proportional to the effective area. When the plate is paralleled to the field line, the effective area is zero, so there is no secondary field induced and the signal recorded is null (see examples: Figure 3.6c and Figure3.7c); when the plate is perpendicular to the field line, we have the largest effective area and get more intensive secondary field, therefore the electromagnetic signal is more visible. We can see several examples from Figure 3.6a and Figure 3.7a.

4.3 BHTEM signal variations with plate's parameters

As we mentioned above, we can get the strongest induction if field lines of the primary field are perpendicular to the conductor. Therefore, the conductor's parameters, such as its dip angle and relative position, determine how it couples with the primary field.

4.3.1 Conductor not penetrated by the hole

From the results above, we know that when the plate is symmetrical to the hole, values of component V are zero. Like those simulated in Model Series 1 and Model Series 2. Shape of curves varies very little with the change of plate's location; however, changes in amplitude are apparent. Nearer the plate to the hole, larger the amplitude of the main peak is; and the secondary peak on the side which the plate slopes to is larger than the other.

Generally, when the distance from the transmitting loop to the plate is shorter, we can get larger amplitude. But we have special cases: for a vertical plate situating on the east side of the hole under the east loop excitation which is the nearest loop to the plate, but abnormal values are zero as shown in Figure 3.19c and 3.20c. This is caused by the coupling relationship between the plate and the transmitting loop; in this case, the plate is parallel to the primary field so that it cannot induce the secondary field, thus the abnormal field is zero. Another exception is that the plate dipping 45° to the east situating on the south side of the hole, we get the largest amplitude when the east loop, not the south loop which is the nearest one, is used (compare figures Figure 3.42d to Figure3.44d and Figure3.48d to Figure 3.50d).

4.3.2 Plate penetrated by the hole

Because the hole penetrated through the plate at the centre point, we got symmetrical curves. Curves of component A are very simple "single-valued" curves, i.e., values of one specific case are all positive or negative. In some cases, there are minimal values which occur at the intersection point of the hole and the plate at early phases (see figures from Figure 3.55 to Figure 3.64), and when the

acute angle formed by the hole and the plan of the plate is smaller this phenomenon is more apparent.

4.3.3 Plate under the hole

From the figure we can find that signal of component U is very week (see figures Figure 3.29, Figure 3.31, Figure 3.33, Figure3.35, and Figure 3.37). The curves possesses an open-mouth form, which means the value increases with the depth and reach the maximum value at the bottom of the hole.

4.4 Optimized transmitter loop location

4.4.1 Plate situating on west side of the hole

1. Horizontal plate: Largest amplitude is obtained when centred transmitting loop is used. For other four loop locations we obtained identical curves.
2. Vertical plate: Amplitude is zero when we use centred, south or north loop location. For east and west locations, we obtained symmetrical curves with same amplitude.
3. Plate dipping 45° to the west: Largest amplitude is obtained when centred transmitting loop is used. When we used east transmitting loop, we obtained abnormal curves with positive main peaks on each side of which there exists a negative secondary peak. For other loop locations, we obtained abnormal curves with negative main peaks on each side of which there exists a positive secondary peaks.
4. Plate dipping 45° to the east: Largest amplitude is obtained when centred transmitting loop is used. The sign of values obtained by using east loop is reversed compared with those obtained by using other loops.

4.4.2 Plate situating on east side of the hole

1. Horizontal plate: Largest amplitude is obtained when east transmitting loop is used. Abnormal signals for north, south and west loop locations

are very week.

2. Vertical plate: Amplitude is zero when we use east loop location. Strongest abnormal signal is observed when under centred loop excitation. And values of component U are all negative.

3. Plate dipping 45° to the west: Results are very similar to those of horizontal plate. The difference between them is the location of the larger secondary peak which appears on the side to which the plate is inclined with respect to the drill hole.

4. Plate dipping 45° to the east: When the east loop is used the amplitude is the largest. Amplitude for other loop locations are the same, but signs of values obtained in centred loop case are reversed compared to those values obtained in other cases.

4.4.3 Plate situating on south side of the hole

1. Horizontal plate: Largest amplitude is obtained when south transmitting loop is used. Abnormal signals for north and west loop locations are almost zero. And values of component U are all negative.

2. Vertical plate: Largest amplitude is obtained when south transmitting loop is used. Signs of values obtained in east loop case are reversed compared to those of values obtained in other cases.

3. Plate dipping 45° to the west: Regulations of components A and V are same as horizontal plate, but component U are all positive.

4. Plate dipping 45° to the east: Signals of components A and V are too week to analyse. Only consider U, positive values are obtained using north and west loop, otherwise are negative values; and strongest abnormal signals are observed when we use east loop.

4.4.4 Plate penetrated by the hole

1. Horizontal plate: Largest amplitude is obtained when east transmitting

loop is used and if west loop is used amplitude obtained is almost zero. And all values of components A and U are positive.

2. Vertical plate: Largest amplitude is obtained when centred transmitting loop is used. Signs of component A are contrary to that of component U for each loop location.

3. Plate dipping 45° to the west: Same as horizontal plate, except that values of component A are all positive but values of component U are all negative.

4. Plate dipping 45° to the east: Largest amplitude is obtained when east transmitting loop is used. When loop is located on south and north sides abnormal values are almost zero.

CHAPTER V

CONCLUSIONS

In the frame of this Master degree study, we performed 100 numerical models to characterize the response features of borehole electromagnetic method (BHTEM). Based on these results, we have seen in Chapter 3, the centred loop is extremely effective in prospecting horizontal plates under the loop, but for vertical plates under the loop, the response will be zero if the centred loop is used. So it is very important to set measurement configuration appropriately in a practical field work.

A quick field survey by setting transmitting loop in four directions around the drill-hole can help to estimate the quadrant potentially to find a conductor. Taking the drill-hole dipping direction plane as x-z plane, the most visible response indicates that the conductor is perpendicular or sub-perpendicular to this plane (the central loop Figure 6; the east loop in Figure 7; the east loop in Figure 8; the south loop in Figure 9). As soon as the third component (V) appears, the conductor is probably situated in the plane which is perpendicular to the drilling path plane.

It is important to notice that we need to take the drill-hole dipping direction plane as x-z plane to apply above rules in the field. Indeed, it is justified by the fact that the drill-hole is only given information in the field, therefore we serve it as the reference for the model space, and we can generalize above rules to any field measurement no matter the dip direction of the drill-hole.

Since BHTEM responses mainly depend upon the coupling between the primary magnetic field and the conductor, we guess that there is no essential difference between BHTEM response and surface TEM system response except the system configuration is different. The main concern is to finding optimized measurement system configuration to get maximum induction from targets.

BHTEM is a new prospecting method and several measurement systems are in development over the world. There are still many studies to be done; for example, mineralized bodies are often massive or lenticular who have certain thickness. It is valuable to do modeling with a prism or other volumetric models instead of thin plate. Doing so, more components will be observed (three components instead of two), we will have more constraints on the BHTEM interpretation and consequently we have a higher spatial resolution about the occurrence of the model. This work will be done in near future.

After my master degree, my PhD study will focus on the 3D forward modeling and inversion algorithms development for BHTEM system, especially for hole to hole data interpretation.

REFERENCES

Annan, A.P. (1974). The equivalent source method for electromagnetic scattering analysis and its geophysical application: [doctoral dissertation]. Canada: Memorial University of Newfoundland.

Brakni, E. M. (2011). Réseaux de neurones artificiels appliqués à la méthode électromagnétique transitoire InfiniTEM: [master dissertation]. Canada : Université du Québec à Chicoutimi.

Cao, H., Wang, X. B., He, Z. X., Mao, L. F. and Lv, D. W. (2012). Calculation of borehole-to-surface electromagnetic response on horizontal stratified earth medium. Oil Geophysical Prospecting, 47(2): 338-343.

Claprood Maxime, (2005). Classification automatique d'anomalies megatem de type plaque mince : [master dissertation]. Canada: Université de Montréal.

Guo, T. and Liu, G. Q., (2002). A new algorithm for borehole electromagnetic measurements employing Lambert W function. Mathematical Geology, Vol. 34, 529-542.

Hanneson, J.E. and West, G.F. (1984). The horizontal loop electromagnetic response of a thin plate in a conductive earth: Part 1—Computational method. Geophysics, Vol. 49, 411-420.

He, Z. X., (2006). Research to Borehole-surface Electromagnetic Technique-A New Way of Mapping Reservoir Boundary: [Doctor dissertation]. Sichuan: Chengdu University of Technology.

Jing, L., He, Z. X., Wang, X. B., Jiang, Y. L. and Luo, Y. X. (2010). Research on quick simulation 1D EM forward of borehole-surface electromagnetic method in frequency domain. Chinese Journal of Engineering Geophysics, 7(5), 579-583.

Killeen, P.G. (1997). Borehole geophysics: exploring the third dimension. In: A.G. Gubins, eds. Proceedings of Exploration 97: Fourth Decennial International Conference on Mineral Exploration, 31-42.

Lajoie, J. J. and West, G. F. (1976). The electromagnetic response of a conductive inhomogeneity in a layered earth. Geophysics, Vol. 41, 1133-1156.

Lamontagne, Y. (2007). Deep exploration with EM in boreholes. Advances in Ground and Borehole Geophysics, 401-415.

Lamontagne, Y. and West, G.F. (1971). EM response of a rectangular thin plate. Geophysics, Vol. 36, 1204-1222.

Li, J. H. and He, Z. X. (2012). 3D electrical response characteristics modeling for surface-to-borehole vertical electromagnetic walkaway profile. Oil Geophysical Prospecting, 47(4): 653-664.

Li, X. T., (2009). Research on network well-earth electrical method Muti-parameters detection system: [Master dissertation]. Jilin: Jilin University.

Lv, Y. Z., Ruan, B. Y. and Peng, S. P. (2012). A study on anomaly of surface-borehole direction induced polarization survey. Progress in Geophysics, Vol. 27(1), 0201-0206.

Malmqvist, L., Pantze, R., Kristensson, G. and Karlsson, A. (1990). Electromagnetic fields in boreholes – measurements and theory in three dimensions. Lund Institute of Technology, Sweden.

Pardo, D., T. V. Carlos (Ian) and Zhang, Z. L (2008). Sensitivity study of borehole-to-surface and crosswell electromagnetic measurements acquired with energized steel casing to water displacement in hydrocarbon-bearing layers. Geophysics, Vol. 73, F261-F268

Sasaki, Y., Matsuo, K. and Yokoi, K. (1994). Resistivity reversion of cross-hole and borehole-to-surface EM data using axially symmetric models. Geophysical Prospecting, Vol. 42, 745-754.

Scrivens, S. (2005). A comparison between helicopter and fixed-wing time-domain electromagnetic systems: [bachelor dissertation]. Canada: Carleton University.

Song, X. J., Dang R. R. and Dong, Z. (2010). Modelling and Simulation of the Cross-well Electromagnetic Logging Responses. Nuclear Electronics & Detection Technology, 30(9), 1173-1176.

Song, Y., Kim, H. J. and Lee, K. H. (2002). An integral equation representation of wide-band electromagnetic scattering by thin sheets. Geophysics, Vol. 67, 746-754.

SPIES, B. R. (1996). Electrical and electromagnetic borehole measurements: a review. Surveys in Geophysics, Vol. 17, 517-556.

Su, Y. J. (2010). New improved formulas for calculating gravity and magnetic anomalies based on a cylinder model: [master dissertation]. Canada: Université de Montréal.

Walker, P.W. and West, G.F. (1991). A robust integral equation solution for electromagnetic scattering by a thin plate in conductive media. Geophysics, Vol.

56, 1140-1152.

Wang, Z. G., He, Z. X. and Wei W. B. (2007). 3D modelling and Born approximation inversion for the borehole surface electromagnetic method. Applied Geophysics, Vol. 4, 84-88.

Wang, Z. G., He, Z. X., Wei W. B. and Deng M. (2005). 3D physical experiments of well-to-ground electrical survey. Oil Geophysical Prospecting, Vol. 40(5), 594-597.

Wang, Z. X. and Wang, X. G. (2012). Study on Anomalies of Wells in Hujianian Area in Anhui Province. Land & Resources of Shandong Province, 28(3), 32-34.

Wilt, M. J., Morrison, H. F., Becker, A. and Lee, K. H. (1991). Cross-borehole and surface-to-borehole electromagnetic induction for reservoir characterization. U. S. Department of Energy.

Zhang, J. F. (2005). A study on using hole-to-surface electrical resistivity method to determine the range of oil and gas reservoir:[Master Dissertation]. Shanxi: Chang'an University.

Zhang, R. F. and Wen, P. L. (1999). Sensitivity analysis of the well-surface electromagnetic imaging. Computing Techniques for Geophysical and Geochemical Exploration, Vol. 21(1), 54-58.

APPENDIX I

SYNTHESIS OF THE DISSERTATION

1. Résumé

La méthode électromagnétique transitoire dans le trou de forage (EMTF) est un outil d'exploration prometteur pour la recherche des dépôts profonds. Pour augmenter l'efficacité du travail sur le terrain, l'objectif de cette recherche est d'étudier les principales caractéristiques de réponses EMTF et de quantifier la variation dans les réponses EMTF en fonction de la variation des paramètres du conducteur. En définissant un conducteur dans diverses situations, nous avons systématiquement étudié les variations de réponse EMTF avec différentes occurrences du conducteur. Nous avons observé que l'intensité du champ magnétique secondaire est proportionnelle à la surface effective. Lorsque cette surface est perpendiculaire à la ligne du champ magnétique primaire, nous avons la plus grande surface effective donc nous obtenons une réponse de EMTF forte. Au contraire, lorsque la surface effective est parallèle à la ligne du champ magnétique primaire, il n'y a pas de champ magnétique secondaire induit en raison de l'absence de couplage entre le champ primaire et le conducteur. Les résultats de ces simulations sont entièrement compatibles avec les interprétations de données électromagnétiques aéroportés et au sol qui sont toutes basées sur le même principe du champ électromagnétique. Les résultats de cette étude seront utiles pour faire des interprétations rapides sur le terrain pour sélectionner la configuration optimale du système de mesure selon l'interprétation en temps réel. Cela permettra d'améliorer l'efficacité du travail de terrain ainsi réduire les coûts d'exploration.

2. Introduction

Les ressources minérales jouent un rôle très important dans le développement de notre société. Nous sommes confrontés au défi de trouver de nouvelles ressources

à la profondeur. Les méthodes géophysiques sont largement utilisées dans l'exploration minérale en raison de l'avantage de pénétration profonde et la capacité d'investiguer la structure interne de la Terre. Parmi nombre de méthodes géophysiques, les méthodes électromagnétiques sont particulièrement utiles dans l'exploration des métaux de base. La ceinture des roches vertes d'Abitibi est bien connu riche en or et métaux de base. Afin d'augmenter la capacité d'exploration en profondeur de la méthode électromagnétique transitoire, deux techniques en forage sont développées et utilisées dans l'exploration minière. Ce sont l'EMTF dans deux trous de forage ou dans un seul trou. L'étude de sensibilité démontre que la technique utilisée dans deux trous espacés de 100 mètres peut détecter une couche conductrice mince d'un mètre d'épaisseur (Wilt *et al.,* 1991). Dans le cadre de cette maîtrise, nous nous concentrons sur la technique de l'EMTF appliqué à un seul trou de forage, car elle représente la condition générale du terrain. La couche des roches sédimentaires à la surface (mort-terrain) est un obstacle dans un levé électromagnétique au sol ou en avion. L'EMTF pourrait surmonter une partie de ce problème en approchant des conducteurs enfouis profondément.

Un système de l'EMTF en forage est composé d'une boucle de courant à la surface et à proximité du trou de forage dans lequel le récepteur enregistre le champ électromagnétique induit en descendant vers la profondeur (Figure 1). La position typique de la boucle émettrice est dans quatre directions, illustrée par la figure 2, qui peut être à l'est, au nord, au sud ou à l'ouest du forage, et aussi être directement au-dessus du trou de forage (centre).

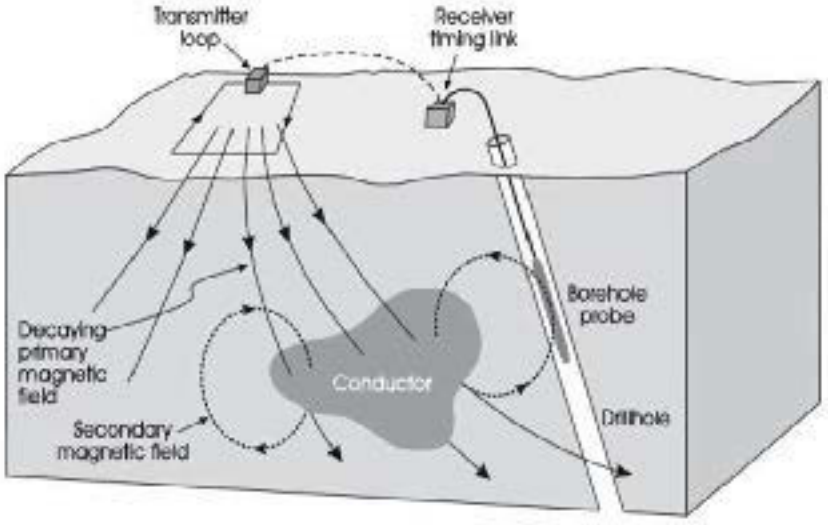

Figure A- 1 le concept d'un système électromagnétique en forage (Killeen, P.G., 1997)

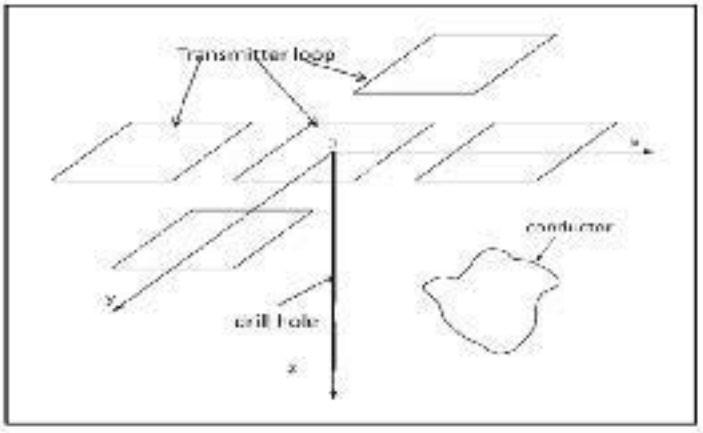

Figure A- 2 Cinq emplacements typiques de boucle émettrice mesure BHTEM

Dans le passé, de nombreuses recherches ont été effectués pour simuler le champ électromagnétique. Lajoie et West (1976) ont calculé le champ électromagnétique en trois dimensions au voisinage d'une mince plaque conductrice dans un environnement stratifiée horizontalement et conductible. Dans leur développement, les variables sont représentés par une paire de potentiels scalaires qui signifient la divergence nulle et sans courant circule dans la plaque et dont les valeurs du potentiel sont connues au niveau des noeuds d'une grille rectangulaire. L'équation intégrale de base est constituée d'un ensemble d'équations linéaires qui peuvent être résolues numériquement. Hanneson et West (1984) ont présenté un algorithme de simulation pour la réponse électromagnétique dans le domaine fréquentiel d'un conducteur mince, tabulaire et vertical, situé dans une terre à deux

couches. Par la suite, Walker et West (1991) ont développé une solution plus générale pour la modélisation d'une plaque mince qui peut être située dans un milieu résistant ou conductible. Cette solution nous permet de modéliser la réponse électromagnétique des conducteurs de faible conductivité à forte conductivité. Wang *et al.*, (2007) a présenté une approche 3D pour la modélisation numérique de l'électromagnétique forage-à-surface méthode (BSEM) et réalisé l'inversion en 3D de données BSEM contribué à la délimitation du réservoir. Lv, Ruan et Peng (2012) ont étudié les caractéristiques anormales de réponses de BHTEM sur certains modèles simplifiés, tels que les corps cubiques anormaux et les plaques.

L'importance de la méthode électromagnétique en forage est de détecter les variations de la conductivité dans trois dimensions. La méthode a, entre autres capacités, à détecter les gisements de sulfures massifs volcanogène (SMV) dans la profondeur. S'il y a plus d'un forage autour d'un gisement de SMV, basée sur des mesures en forage, nous serons pouvoir estimer leur tonnage plus précisément. Afin d'aider au développement des nouveaux systèmes de mesure, nous utilisons la méthode de simulation numérique pour étudier la complexité du champ électromagnétique en tenant compte de plusieurs facteurs qui peuvent avoir un impact significatif à l'observation. Par conséquent, les études de cette thèse visent à : 1) maîtriser la base théorique de la simulation numérique des données EM en forage ; 2) trouver les facteurs les plus significatifs qui font impacts sur la réponse d'EMTF ; 3) trouver la configuration optimale du système de mesure d'aider à la planification de l'enquête d'EMTF.

Les travaux de modélisation dans ce mémoire sont effectués en utilisant le logiciel *Maxwell* qui est développé par EMIT (ElectroMagnetic Imaging Technology Pty Ltd., Australie). Ce logiciel nous permet de changer les paramètres de l'émetteur (l'intensité de courant, la forme d'onde, la fenêtre de temps, etc.) ; la configuration du système de mesure (position spatiale) peut également être prise en compte lors de la modélisation. La réponse d'EMTF calculée est obtenue presque simultanément après que les paramètres du modèle sont définis. Donc, nous

pouvons facilement voir les principaux changements en réponse d'EMTF avec les modifications de paramètres du modèle.

3. Les théories de base

3.1 Calcul du champ EM d'une plaque mince

Le principe de la mesure d'EMTF est : un transmetteur à la surface émet un courant alternatif ou transitoire dans une boucle fermée, qui représente le champ électrique primaire et qui génère un champ magnétique primaire perpendiculaire au plan de la boucle. Lorsque ce champ magnétique primaire interagit avec un conducteur, selon la théorie de Maxwell, un champ électrique secondaire (courant de Foucault) sera générée dans le conducteur; puisque ce champ électrique secondaire varie dans le temps qu'il génère un champ magnétique secondaire qui sera finalement enregistré par le récepteur dans le forage.

On utilise une plaque mince pour représenter le conducteur dans un espace libre. La plaque est tellement mince que son épaisseur est négligeable par rapport aux dimensions latérales de la plaque ou à la distance entre elle et le point d'observation (Lamontagne, 1971).

A partir des équations de Maxwell, il y a:

$$\nabla \times \mathbf{H} = \mathbf{J} + \frac{\partial \mathbf{D}}{\partial t} \tag{A-1}$$

$$\nabla \times \mathbf{E} = -\frac{\partial \mathbf{B}}{\partial t} \tag{A-2}$$

Pour le problème d'induction, le déplacement de courant à l'intérieur de conducteur est beaucoup plus faible que le courant d'émetteur. Donc, le terme $\partial \mathbf{D}/\partial t$ peut être ignoré :

$$\nabla \times \mathbf{H} = \mathbf{J} \tag{A-3}$$

Les relations empiriques qui lient les propriétés physiques au champ électromagnétique sont :

$$\mathbf{B} = \mu \mathbf{H} \tag{A-4}$$

$$\mathbf{J} = \sigma \mathbf{E} \tag{A-5}$$

En utilisant une identité $\nabla \cdot (\nabla \times F) \equiv 0$, c'est-à-dire, la divergence du rotationnel de une quelconque fonction est zéro. L'équation (A-3) devient :

$$\nabla \bullet \mathbf{J} = 0 \tag{A-6}$$

Substituer **B** de l'équation (A-4) et, **E** de l'équation (A-5) dans l'équation(A-2), pour une source sinusoïdale avec la fréquence angulaire ω et dans un milieu homogène, on obtient :

$$\nabla \times \mathbf{J} = -i\sigma\mu\omega \mathbf{H} \tag{A-7}$$

Remplacer **H** par l'équation (A-3) dans l'équation(A-7) :

$$\nabla \times \mathbf{J}(\mathbf{r}_0) = -i\sigma\mu\omega \int_V \frac{\mathbf{J}(\mathbf{r}) \times (\mathbf{r} - \mathbf{r}_0)}{4\pi |\mathbf{r} - \mathbf{r}_0|^3} d^3\mathbf{r} \tag{A-8}$$

V indique l'espace entier où le courant s'écoule.

On peut diviser ensuite le terme intégral de l'équation (A-8) en deux parties : une partie liée au champ primaire ; l'autre partie liée au champ secondaire. La fonction $\mathbf{P}(\mathbf{r}_0)$ représente une fonction du courant d'émetteur, alors :

$$\nabla \times \mathbf{J}(\mathbf{r}_0) = -i\sigma\mu\omega \bullet \left\{ \mathbf{P}(\mathbf{r}_0) + \int_C \frac{\mathbf{J}(\mathbf{r}) \times (\mathbf{r} - \mathbf{r}_0)}{4\pi |\mathbf{r} - \mathbf{r}_0|^3} d^3\mathbf{r} \right\} \tag{A-9}$$

Où c indique l'espace occupée par le conducteur.

Supposons que la plaque est suffisamment mince, la densité de courant peut être considérée comme constante à travers l'épaisseur. En conséquence, la densité volumique peut être remplacée par la densité de surface. La densité de surface est définie comme :

$$\mathbf{K} = \int_{-t/2}^{t/2} \mathbf{J} dx = \mathbf{J} t$$

Substituer cette densité dans l'équation (A-9) :

$$\nabla\times\mathbf{K}(\mathbf{r}_0)=-i\sigma\mu\omega t\bullet\left\{\mathbf{P}(\mathbf{r}_0)+\int_S\frac{\mathbf{K}(\mathbf{r})\times(\mathbf{r}-\mathbf{r}_0)}{4\pi|\mathbf{r}-\mathbf{r}_0|^3}d^2\mathbf{r}\right\} \quad \text{(A-10)}$$

Où S représente la surface de la plaque mince. Cette équation est obtenue en supposant que t est géométriquement petit de telle sorte que $\left\{(\mathbf{r}-\mathbf{r}_0)/|\mathbf{r}-\mathbf{r}_0|^3\right\}$ ne varie pas à travers l'épaisseur. Afin de résoudre l'équation ci-dessus, on définit un vecteur potentiel U qui satisfait à l'équation : $\nabla\times\mathbf{U}=\mathbf{K}$ et $\nabla\bullet\mathbf{U}=0$. Intégrer ces deux équations dans l'équation (A-10) et utiliser l'identité $\nabla\times\nabla\times\equiv(\nabla\nabla\bullet)-(\nabla^2)$:

$$\nabla^2\mathbf{U}(\mathbf{r}_0)=i\sigma\mu\omega t\bullet\left\{\mathbf{P}(\mathbf{r}_0)+\int_S\frac{[\nabla\times\mathbf{U}(\mathbf{r})]\times(\mathbf{r}-\mathbf{r}_0)}{4\pi|\mathbf{r}-\mathbf{r}_0|^3}d^2\mathbf{r}\right\} \quad \text{(A-11)}$$

Dans le système de coordonnées cartésien (Figure 3), il y a seul composant non-nulle du potentiel U est le composant-x. Du fait que le courant Eddy circuit parallèle au plan de plaque, l'équation (A-11) est devenue :

$$\nabla^2U(y,z)=i\sigma\mu\omega t\bullet\left\{P(y,z)+\int_S\frac{\nabla U(y,z)\bullet(\mathbf{r}-\mathbf{r}_0)}{4\pi|\mathbf{r}-\mathbf{r}_0|^3}d^2r\right\} \quad \text{(A-12)}$$

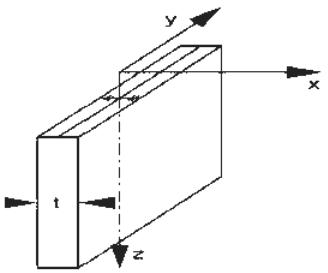

Figure A- 3 Le système de coordonnées qui est attaché au conducteur (Source: Yves Lamontagne and G.F. West, 1971)

Pour résoudre l'équation (A-12), nous avons besoin de conditions aux limites ou conditions initiales. Dans le problème décrit ci-dessus, on suppose que $U = 0$ sur le bord de la plaque.

$$\begin{cases} \nabla^2 U(y,z) = i\sigma\mu\omega t \bullet \left\{ P(y,z) + \int_S \frac{\nabla U(y,z) \bullet (\mathbf{r} - \mathbf{r}_0)}{4\pi |\mathbf{r} - \mathbf{r}_0|^3} d^2 r \right\} \\ U|_\Gamma = 0 \end{cases} \tag{A-13}$$

Où Γ représente le bord de la plaque mince. L'équation (A-13) peut être résolue par des méthodes numériques.

3.2 Simulation numérique

Pour simuler la réponse électromagnétique d'une plaque mince, nous utilisons le logiciel commercial *Maxwell*, qui est basé sur la théorie des circuits. La plaque est divisée en plusieurs éléments de rubans conducteurs (équivalent à un circuit). En conséquence, le courant est contraint de circuler à l'intérieur de la voie assignée par le ruban. La simulation de la réponse EMTF de plaques différentes peut être réalisée par varier la largeur des éléments de ruban. Les inductances mutuelles équivalentes incluent :

1. entre deux éléments de rubans.
2. entre un élément de ruban et l'émetteur ou le récepteur.
3. entre l'émetteur et le récepteur.

Pour un élément quelconque j , si la fréquence angulaire est ω , l'équation de voltage est :

$$i\omega \sum_{l=1}^{n} \mathbf{X}_{jl} \mathbf{A}_l + \frac{\mathbf{A}_j}{\mathbf{S}_j} = i\omega \mathbf{T}_j C \tag{A-14}$$

A_j dénote le courant s'écoulant dans l'élément j. $\mathbf{X}$ est la matrice d'inductance mutuelle entre deux quelconques rubans. $\mathbf{T}$ est le vecteur d'inductance mutuelle entre le transmetteur et un ruban. C est le curant de transmetteur. Résoudre cette équation pour A_j, on a la réponse électromagnétique de plaque mince :

$$Y = i\omega \mathbf{R} \bullet \mathbf{A} \tag{A-15}$$

La méthode numérique utilisée par *Maxwell* est similaire à celle d'Annan (1974).

En déterminant les valeurs propres (λ_k) de la matrice $\mathbf{X}$ et les vecteurs propres (V_k) du système des équations linéaires, nous pouvons obtenir une autre forme de l'équation (A-14):

$$i\omega\lambda_k a_k + a_k = i\omega t_k c \tag{A-16}$$

Où $t_k = \mathbf{T} \bullet \mathbf{V}_k$ et $\mathbf{A} = \sum_k d_k a_k \mathbf{V}_k$, d_k est un facteur d'amortissement entre zéro et un dépendant de vecteur propre. L'équation (A-15) devient

$$y_k = i\omega a_k r_k \tag{A-17}$$

La solution complète est donc :

$$Y = \sum_k d_k r_k t_k \left(\frac{(i\omega)^2 C}{1 + i\omega\lambda_k} \right) \tag{A-18}$$

Dans le domaine du temps, il est:

$$y(t) = \sum_k d_k r_k t_k E_k(t) \tag{A-19}$$

Où $E_k(t) = \left(\frac{d}{dt} e^{t/\lambda_k} \right) * \left(\frac{d}{dt} C(t) \right)$. Pour une simple excitation de l'impulsion, $\frac{d}{dt} C(t)$ est la fonction $\delta(t)$. Ainsi, $E_k(t) = \delta(t) - \frac{e^{t/\lambda_k}}{\lambda_k}$. La réponse dans le domaine du temps peut être normalisée par le facteur de normalisation Q. Le facteur de normalisation peut être calculé dans l'une des trois façons :

1. En utilisant le pic absolu de l'EMF primaire : $Q = |C(t)|_{\max} |\mathbf{P}|$
2. En utilisant le moyen de la racine de carré de l'EMF primaire : $Q = \sqrt{\frac{1}{T} \int_0^T [C(t)]^2 dt} |\mathbf{P}|$
3. En utilisant la valeur absolue moyenne de l'EMF : $Q = \frac{1}{T} \int_0^T |C(t)| dt |\mathbf{P}|$

4. Simulation des réponses d'EMTF

4.1 Paramètres utilisés

Il y a multiples facteurs qui peuvent influencer le résultat de la mesure sur un levé

d'EMTF. Nous supposons d'abord que la boucle d'émetteur a une taille de 400m×400m, horizontal (Figure 4). Un courant de xxx ampère circuit dans la boucle à une fréquence de 25 Hz avec une forme d'onde sinusoïde. Un récepteur se déplace dans un forage incliné de 60° degrés et l'angle d'azimut du forage est de 90° (vers l'est). Un conducteur du type de plaque mince, qui a une dimension de 150m×150m, orienté nord-sud et possédant une conductivité de $100S \cdot m^{-1}$, se situe à une profondeur de 300 m (distance verticale par rapport à la surface). Considérer 5 positions de la boucle d'émetteur (est, ouest, nord, sud et centre), plus les variations de l'inclinaison de la plaque mince, nous divisons les modèles en cinq séries (Tableau 1). Dans chacune série, nous fixons la position de la plaque et changeons la position de la boucle par rapport au forage ainsi que l'angle d'inclinaison de la plaque. Les résultats sont présentés série par série.

Tableau A- 1 Les valeurs des paramètres de modèle considérés dans la simulation numérique

Dip angle/° of the conductor	location of the conductor	Loop location related to the drill-hole
0 (horizontal)	In the west of the hole (west plate)	Centre
45 (inclined)	In the East of the hole (east plate)	East
90 (vertical)	Penetrated by hole	North
135 (inclined but opposite to 45)	In the South of the hole (south plate)	South
	below the hole	West

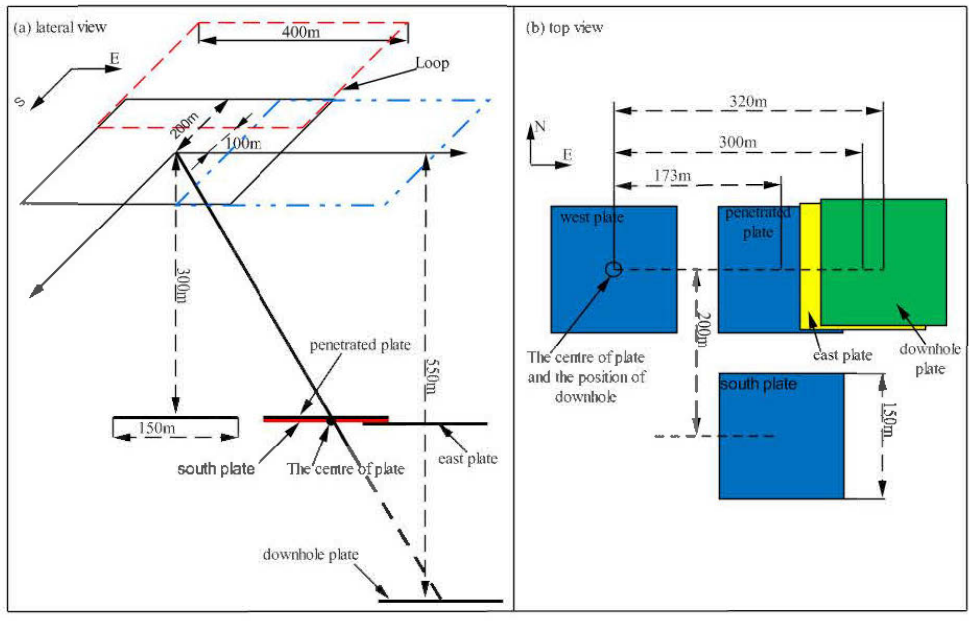

Figure A- 4 L'esquisse des positions de la boucle et de la plaque

Les spécifications techniques pour les systèmes de mesure sont : nous utilisons Protem 25Hz comme « the standard EM instrument times » ; la surface effective des trois composants est de 100. La réponse électromagnétique calculée est exprimée en trois composants : A, U et V. A représente composant axial, c'est-à-dire le long du trou de forage, positif vers le haut ; les composants U et V sont dans le plan perpendiculaire à A et ils se sont orthogonaux (Figure 5).

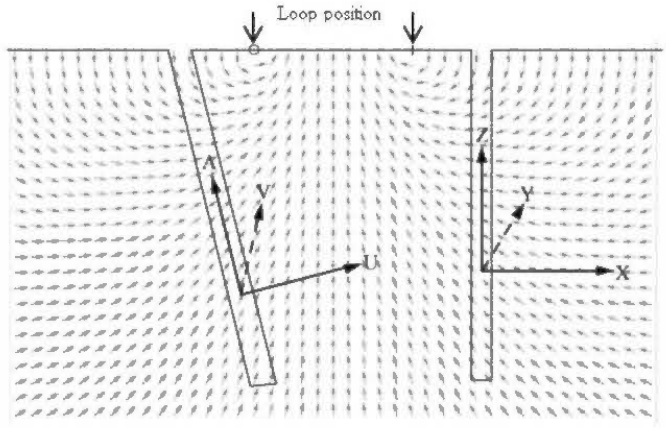

Figure A- 5 Trois composants du champ électromagnétique calculé A, U, V (correspondent à Z, X, Y respectivement)

4.2 Les résultats de simulation numérique

4.2.1 Série 1

Dans cette série, la plaque mince orientée N-S est située à l'ouest du forage. Les résultats sont montrés dans Figure 6.

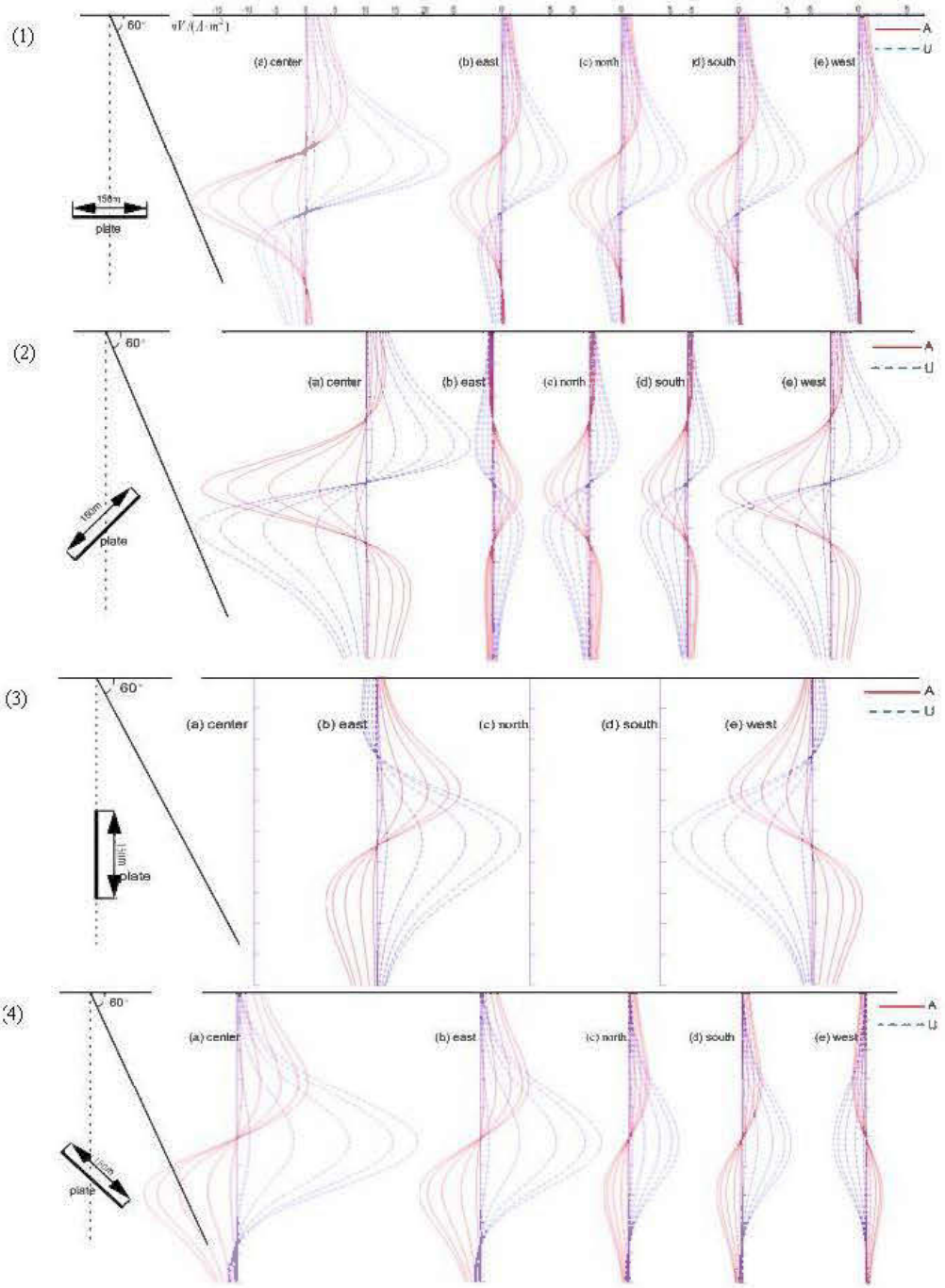

Figure A- 6 Les résultats de simulation de la Série 1 : (1) plaque horizontale (2) plaque inclinée 45° vers l'ouest (3) plaque verticale (4) plaque inclinée45°vers l'est

Un bref résumé pour Série 1 :

1. Il y a deux composants non nulles (Composant A et U) dans cette série.
2. Pour la plaque horizontale sous la tête de puits, on a quatre séries de réponse identique (E, O, N, S); la réponse de la boucle centrale est maximum.
3. L'excitation de la boucle à l'ouest, elle valorise la réponse de la plaque qui s'incline 45 degrés vers l'ouest; la boucle à l'est favorise la réponse de la plaque qui est inclinée 45 degrés vers l'est.
4. Pour une plaque verticale: la réponse de la plaque lorsque la boucle est à l'ouest du forage est une image miroir de celle obtenue en utilisant la boucle à l'est. Et pour les autres positions de boucle, la réponse est nulle.

4.2.2 Série 2

Dans cette série, la plaque se trouve à l'est du forage. Les résultats sont comme suites.

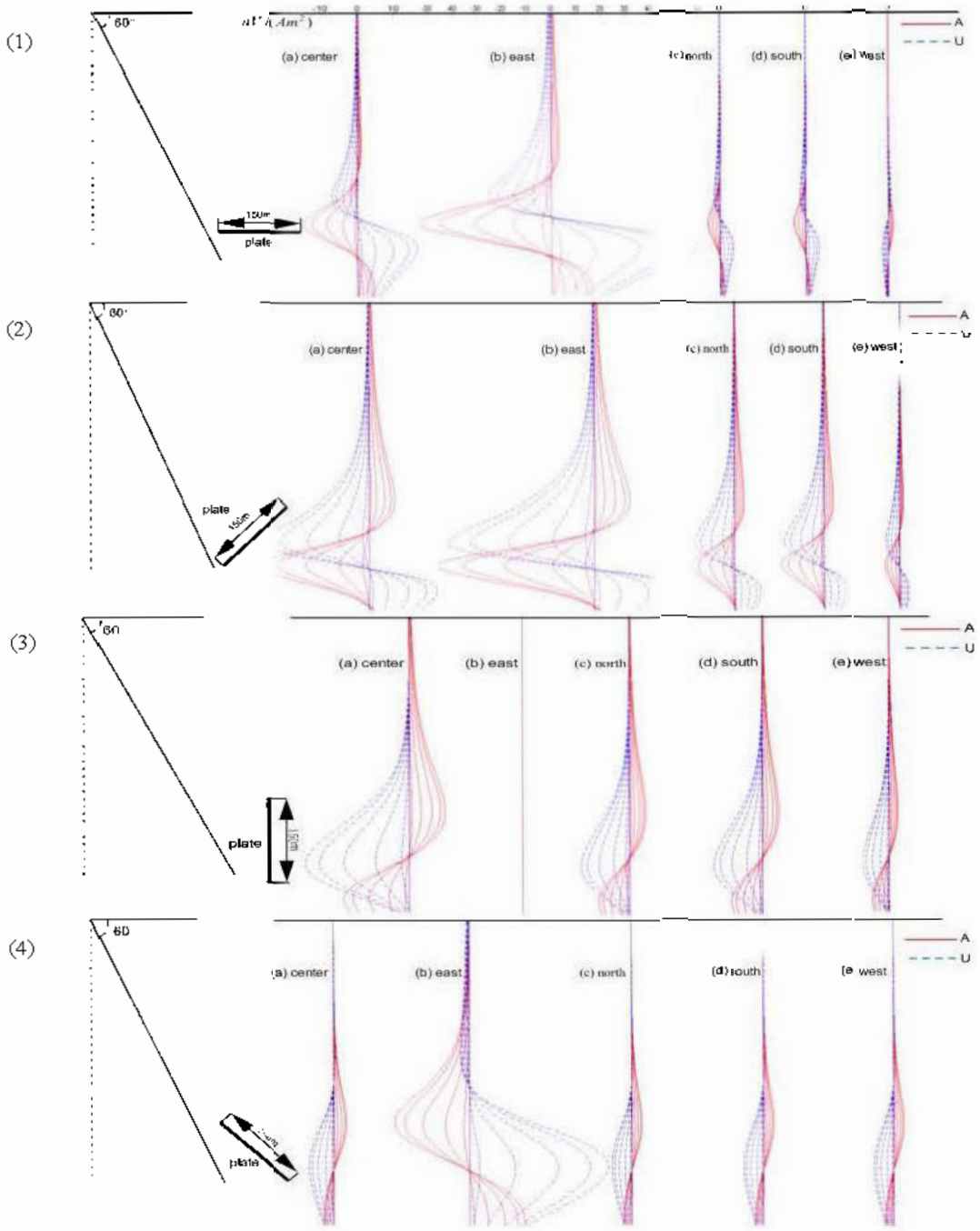

Figure A- 7 Les résultats de simulation de la Série 2

(1) plaque horizontale (2) plaque inclinée 45° vers l'ouest (3) plaque verticale (4) plaque inclinée45°vers l'est

Les faits observés de cette série sont :

1. Il y a aussi seulement deux composants non nulles (A et U). La réponse obtenue sous l'excitation de la boucle à l'est est le plus grande, sauf la plaque verticale, pour elle, l'amplitude est zéro.
2. Pour la plaque horizontale: le maximum négatif du composant A correspond au point zéro du composant U qui est une réponse sinusoïde inverse. Quant à la plaque verticale, le maximum négatif du composant U correspond au point zéro du composant A qui est une réponse sinusoïde.
3. Pour la plaque s'incline de 45 degrés vers l'ouest: la réponse des deux composants est négative, mais déphasée l'une de l'autre.
4. Lorsque la plaque s'incline de 45 degrés vers l'est: le signe de la réponse de boucle à l'est est opposé à celui des autres boucles.

4.2.3 Série 3

Dans cette série, le forage pénètre le point central de la plaque. Les résultats sont :

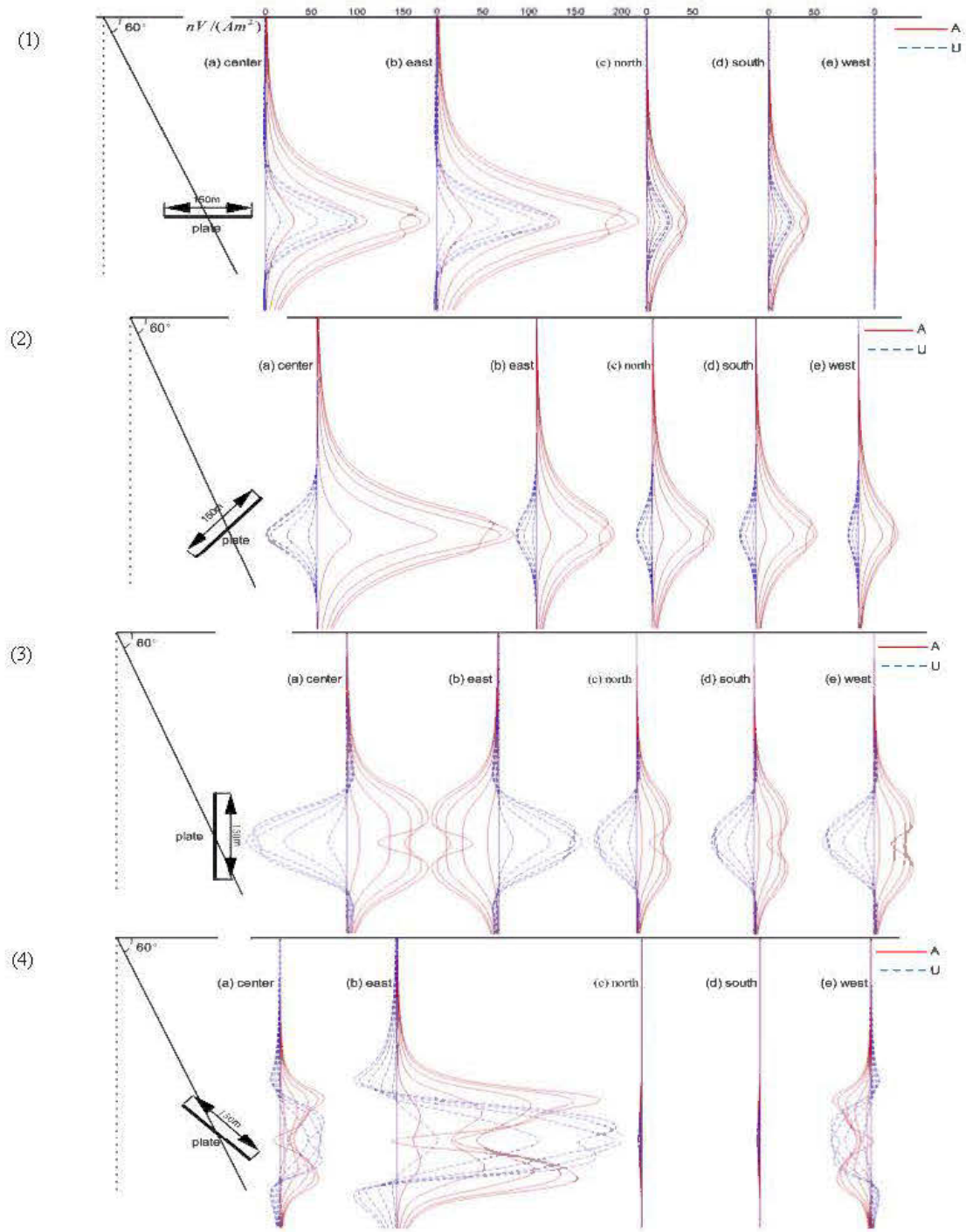

Figure A- 8 Les résultats de simulation de la Série 3

(1) plaque horizontale (2) plaque inclinée 45° vers l'ouest (3) plaque verticale (4) plaque inclinée45°vers l'est

Les caractéristiques des réponses de cette série sont :

1. Il y a aussi seulement deux composants A et U, cependant il y a de la perturbation dans les fenêtres du temps tôt.
2. Pour la plaque horizontale: les valeurs des deux composants sont positives, et nous obtenons la plus grande réponse lorsque nous utilisons la boucle à l'est.
3. Pour la plaque s'incline de 45 degrés vers l'ouest: les valeurs du composant A sont positives, mais celles du composant U sont négatives; et nous obtenons la plus forte réponse lorsque nous utilisons la boucle centrale.
4. Pour la plaque s'incline de 45 degrés vers l'est: composants A et U possèdent le même signe; nous obtenons la plus grande réponse quand nous utilisons la boucle à l'est, mais les signaux sont presque nulles lorsque la boucle au sud ou au nord est utilisée.
5. Pour la plaque verticale: les deux composants possèdent signes contraires.

4.2.4 Série 4

La plaque se situe sur le côté sud du trou de forage.

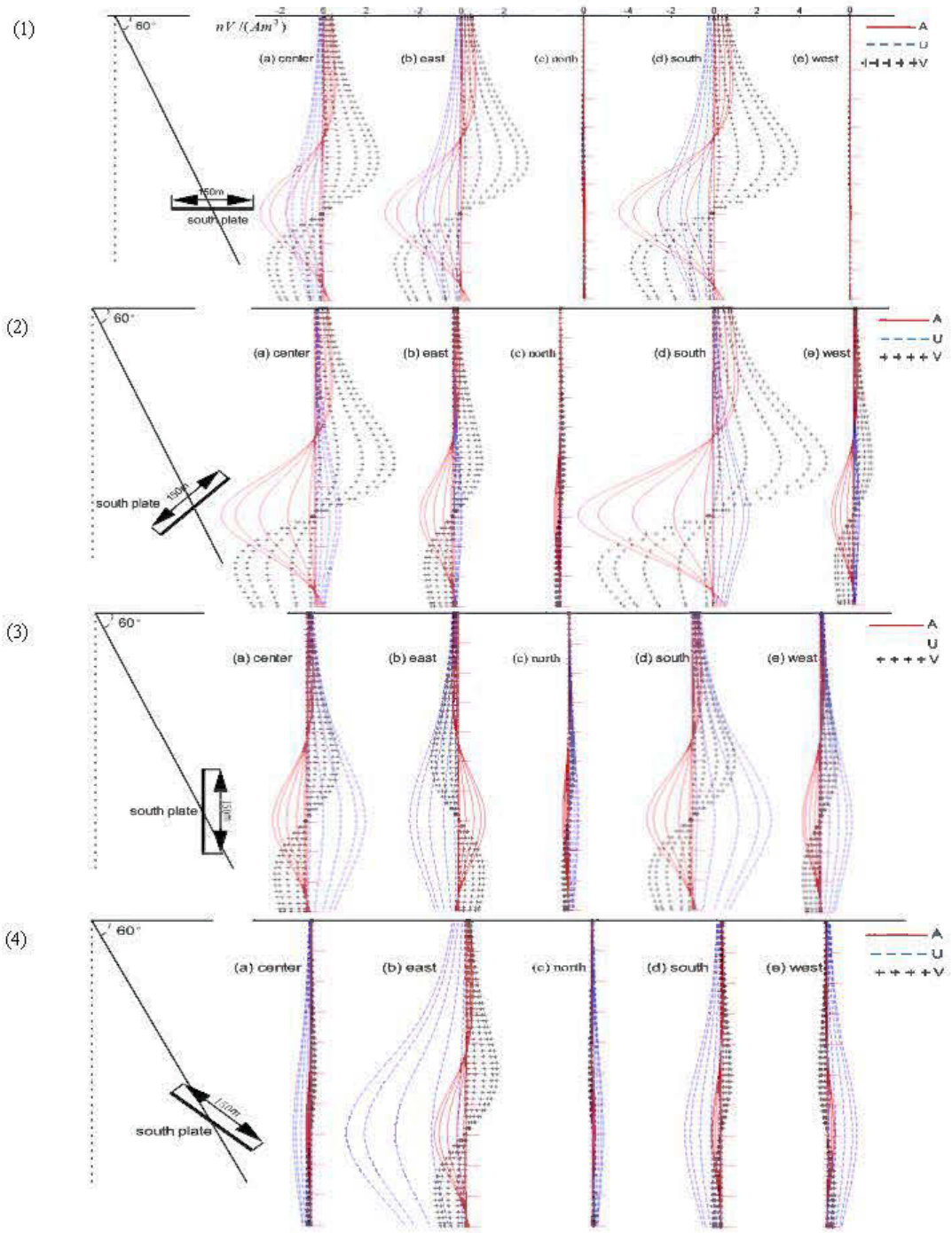

Figure A- 9 Les résultats de simulation de la Série 4

(1) plaque horizontale (2) plaque inclinée 45° vers l'ouest (3) plaque verticale (4) plaque inclinée45°vers l'est

Le résumé pour Série 4 :

1. Nous avons trois composants non-nuls. Généralement, la réponse est plus grande sous l'excitation de la boucle au sud; sauf la plaque inclinée de 45 degrés vers l'est c'est la boucle à l'est qui est optimale. Le signal de V est sinusoïde.
2. La réponse est très petite lorsque la boucle au nord est utilisée pour toutes les inclinaisons de plaque mince.
3. Les réponses des composants A et U ont un seul pic pour la plaque horizontale et celle qui s'incline vers l'est. Le signe du composant A est opposite de celui du composant U pour la plaque horizontale ainsi que verticale; mais pour la plaque inclinée vers l'est, ils possèdent le même signe.
4. Pour la plaque verticale les signes des trois composants de la boucle à l'est sont contraires aux autres.

4.2.5 Série 5

La plaque est située à la profondeur de 550 mètres, et le forage s'arrête à 433 mètres.

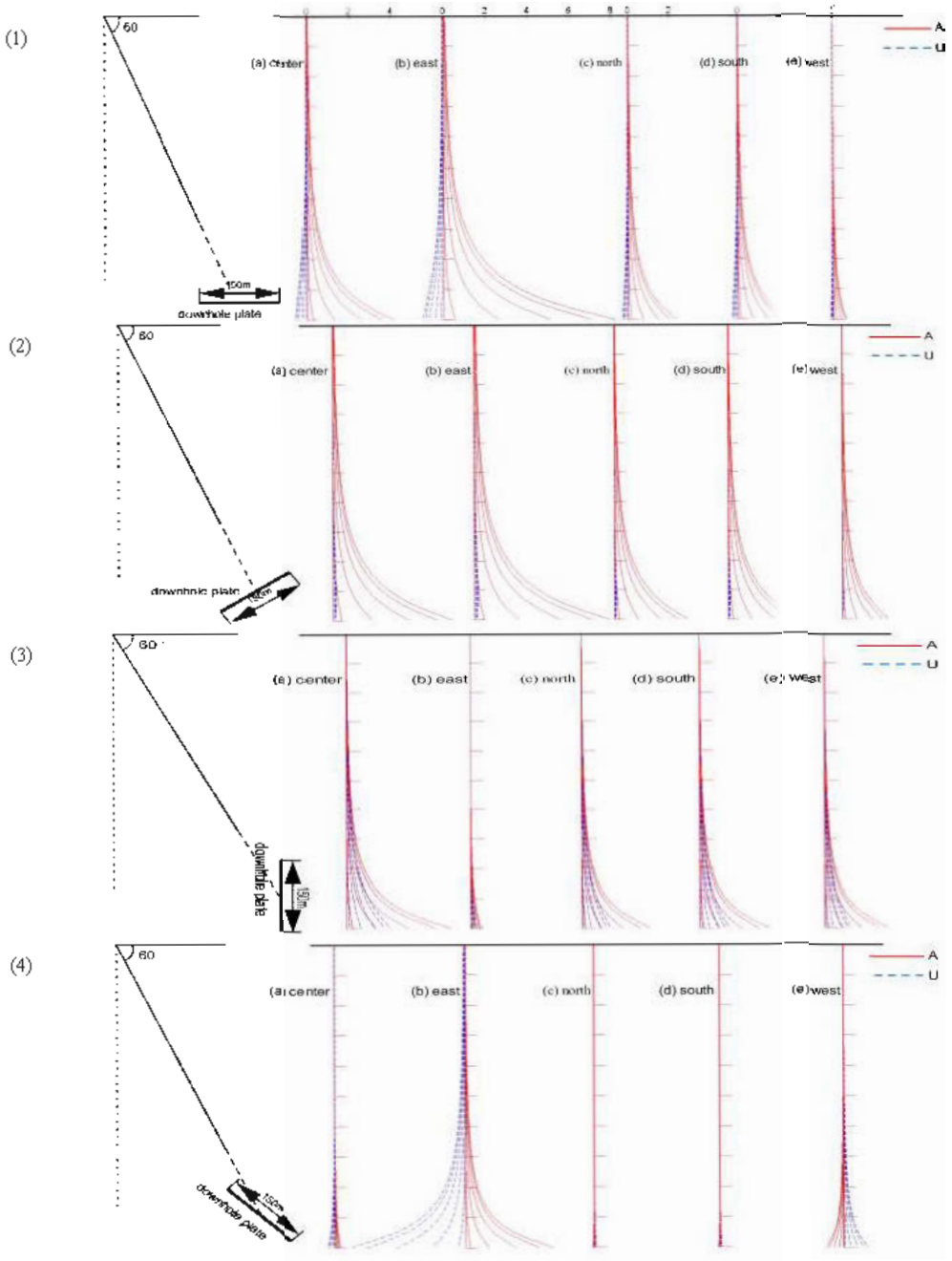

Figure A- 10 Les résultats de simulation de la Série 5

(1) plaque horizontale (2) plaque inclinée 45° vers l'ouest (3) plaque verticale (4) plaque inclinée 45°vers l'est

Gisements profonds sont des cibles principales de l'exploration minière dans l'avenir. Par les résultats de Série 5, nous montrons qu'un système EMTF peut détecter efficacement les cibles profondes:

1. Il y a toujours deux composants non nuls (A et U), qui sont caractérisés par des courbes « ouvertes » dans toutes les situations.
2. Généralement, l'amplitude de la réponse du composant A est plus grande que celle du composant U; et la boucle à l'est favorise davantage l'excitation, sauf pour la plaque verticale qui a une réponse quasi nulle.
3. Composant A possède un signe contraire de celui du composant U pour la plaque horizontale et la plaque inclinée de 45 degrés vers l'ouest.

5. Analyse des résultats

Le signal enregistré dans une mesure d'électromagnétique transitoire en forage est la dérivée du champ magnétique secondaire qui est induit par le champ électromagnétique primaire. Il résulte du couplage entre le champ électromagnétique primaire et le conducteur. Pour mieux comprendre l'interaction entre le champ électromagnétique induit et le conducteur, nous montrons une distribution schématique du champ magnétique primaire généré par une boucle rectangulaire ci-dessous (Figure 11).

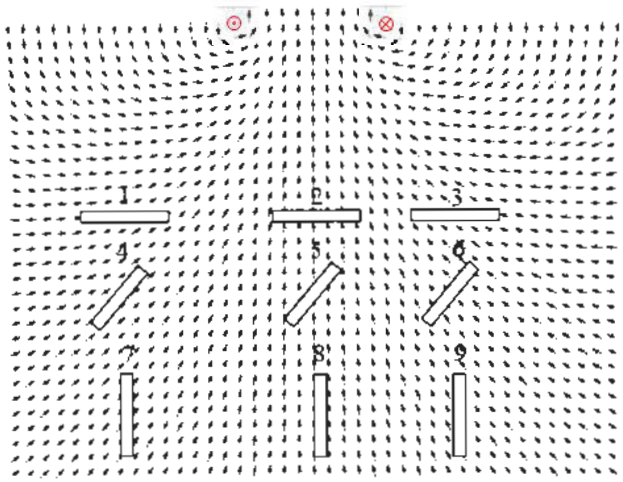

Figure A- 11 La vue en coupe du champ magnétique primaire

Les rectangulaires représentent l'occurrence d'une plaque mince perpendiculaire an plan

L'intensité du champ magnétique secondaire est proportionnelle à la vitesse de variation du flux à travers la surface effective. Pour un champ primaire donné, le taux de variation du flux est fixé, alors l'intensité du champ secondaire est affectée par la surface effective où les flux magnétiques traversent. Donc, nous pouvons dire que l'intensité du champ magnétique secondaire est proportionnelle à la surface effective. Lorsque la plaque est perpendiculaire à la ligne de champ (plaques 2 et 6 dans Figure 11), nous avons la plus grande surface efficace et obtenons une forte réponse en champ secondaire. C'est ce que nous avons observé pour la plaque horizontale dans Série 1 (Figure 6) lorsque la boucle centrale est utilisée. Au contraire, lorsque la plaque est parallèle à la ligne de champ (plaque 4 et la plaque 8 dans Figure 11), la surface effective est nulle, il n'y a pas de champ secondaire induit, à cause de l'absence de couplage entre le champ et le conducteur, donc la réponse est nulle. Nous pouvons trouver le même résultat dans la Série 1 pour la plaque verticale sous l'excitation de la boucle centrale (cas 3 dans Figure 6), et la plaque verticale sous l'excitation de la boucle à l'est dans la Série 2 (cas 3 dans Figure 7).

Comme ce que nous avons observé dans les résultats de simulation, il y a deux composants non nuls (composants A et U) et un composant zéro (composant V) pour la plupart de modèles (Séries 1, 2, 3 et 5). La raison est que l'épaisseur de la plaque est si petite qui est négligeable par rapport aux dimensions latérales de la plaque et par rapport à la distance entre le conducteur et le point où le champ magnétique secondaire est calculé. Par conséquent, le courant de Foucault induit est forcé de s'écouler sur la surface de la plaque, comme illustré à Figure 12. Selon la règle de droite, le champ magnétique secondaire est perpendiculaire à la surface de la plaque et rayonne dans toutes les directions. Dans les circonstances de ces séries de modèle, du fait que la plaque est orientée nord-sud, la ligne de champ et le forage incliné sont tous dans le plan ouest-est, par conséquent, nous ne pouvons que recevoir la réponse des composants A et U.

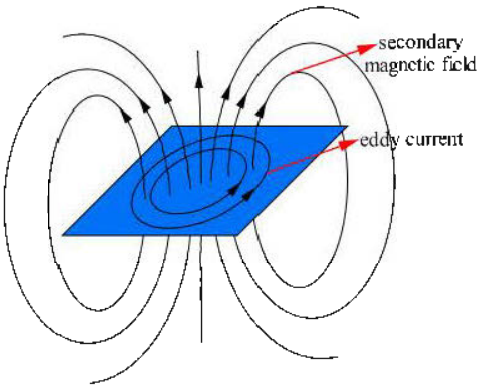

Figure A- 12 L'esquisse du champ magnétique secondaire et du courant de Foucault

6. Conclusion

En basant sur les résultats de la simulation numérique et l'analyse ci-dessus, nous résumons quelques régularités générales pour caractériser les variations de réponse d'EMTF.

1. Évidemment, nous pouvons obtenir la réponse la plus forte si le conducteur est sous la boucle émettrice; donc une enquête de terrain rapide par la mise en boucle émettrice dans quatre directions autour du trou de forage, il peut aider à cibler le quadrant potentiel de trouver un conducteur.
2. Prenant le plan qui contient le forage en tant que plan x-z, la réponse la plus visible indique que le conducteur est perpendiculaire ou sub-perpendiculaire à ce plan (la boucle centrale dans Figure 6; la boucle à l'est dans Figure 7; la boucle à l'est dans Figure 8; la boucle au sud dans Figure 9).
3. Si la boucle émettrice sud est utilisée et la réponse est quasi nulle, cela implique qu'il y a un conducteur orienté nord-sud, et situé dans le nord du trou de forage. Vice-versa, pour la boucle émettrice située au nord.
4. Si le signe de deux composantes orthogonales (ex. A et U dans ce cas), quand la boucle à l'est est utilisée, est inversé à celui des composants sous l'excitation de la boucle à l'ouest, il y a probablement un conducteur vertical dans la direction opposée de l'inclinaison du forage (cas 3 dans la

Figure 6) ; si le signe n'est pas inversé, le conducteur vertical est situé sous la boucle (cas 3 dans la Figure 7).

5. Si deux composants orthogonaux (ex. A et U dans le cas présent) ont même signe, mais se sont déphasés, le plan du conducteur est probablement sub-perpendiculaire ou perpendiculaire à la trajectoire de forage.
6. Pour conducteur profond (plus profond que le forage), en mettant la boucle émettrice dans quatre directions, nous pouvons trouver rapidement le quadrant favorable en utilisant le composant A. Si le composant A est positif et sa réponse est visible dans les quatre directions, ceci implique qu'il y a un conducteur dans la direction de l'extension du forage (cas 1, 2 et 3 de la Figure 10).
7. Dès que le troisième composant (V) apparaît, le conducteur est probablement situé dans le plan qui est perpendiculaire au plan de la trajectoire de forage.

Il est important de noter que la définition du plan X-Z est essentielle afin d'appliquer les règles de cette étude. Ce choix est justifié par le fait que le trou de forage est la seule information connue sur le terrain. Nous prenons le plan qui contient la trajectoire du forage comme le plan X-Z, de cette façon nous pouvons généraliser les régularités observés ci-dessus, peu importe que le forage s'incline vers quelle direction ou l'orientation de conducteur. C'est une notion relative donc plus flexible à la pratique.

L'EMTF est une nouvelle technique de prospection et plusieurs systèmes de mesure sont en développement dans le monde. Il y a encore beaucoup d'études à faire, par exemple, les corps minéralisés sont souvent massives ou lenticulaire qui ont certaine épaisseur. Il est utile de faire de la modélisation avec un prisme ou d'autres modèles volumétriques au lieu de plaque mince. Ce faisant, plus de composants seront être observés (trois composantes au lieu de deux), nous aurons plus de contraintes sur l'interprétation des données EMTF et par conséquent, nous avons une plus haute résolution spatiale sur

l'occurrence du modèle. Ce travail se fera dans le futur proche.

Après mes études de maîtrise, je vais me concentrer sur la modélisation 3D et le développement d'un nouvel algorithme d'inversion pour l'EMTF, en particulier pour l'interprétation des données trou-à-trou.